Analysis of activity-induced changes in the subcellular distribution of the postsynaptic scaffold protein gephyrin in cultured hippocampal neurons from *Mus musculus* (Linnaeus, 1784)

Dissertation

zur Erlangung des Doktorgrades
am Department Biologie der Fakultät für Mathematik, Informatik und Naturwissenschaften der Universität Hamburg

vorgelegt von

Louisa Rathgeber
aus Hamburg

Hamburg
Mai 2013

Genehmigt vom Fachbereich Biologie
der Fakultät für Mathematik, Informatik und Naturwissenschaften
an der Universität Hamburg
auf Antrag von Professor Dr. M. KNEUSSEL
Weiterer Gutachter der Dissertation:
Professor Dr. C. LOHR
Tag der Disputation: 05. April 2013

Hamburg, den 21. März 2013

Professor Dr. C. Lohr
Vorsitzender des
Fach-Promotionsausschusses Biologie

Zusammenfassung

Gerichteter intrazellulärer Proteintransport in Neuronen bildet die Grundlage zur Entwicklung und Aufrechterhaltung neuronaler Morphologie und Polarität. Die meisten Proteine werden im Zellsoma synthetisiert und anschließend in das somato-dendritische oder das axonal Kompartiment transportiert. Der Verteilung neusynthetisierter Proteine liegen dabei zwei Prozesse zu Grunde: Proteinsortierung und Proteintransport. Während der Proteinsortierung wird die Zusammensetzung einzelner Transportvesikel bestimmt und eine Unterteilung der Transportkomplexe nach ihrem Bestimmungsort im somato-dendritischen oder axonalen Kompartiment vorgenommen. Der Sortierung folgt der Proteintransport, welcher die aktive Bewegung von Motorproteinen und ihren Transportgütern entlang des Zytoskeletts beinhaltet. Der Langstreckentransport auf Mikrotubuli kann durch mehrere Mechanismen reguliert werden. Beispielsweise können Adapterproteine, die Motoren mit Frachtgütern verbinden, Motorproteine beeinflussen, indem sie ihre Prozessivität regulieren oder in das richtige Kompartiment lenken. Dess Weiteren tragen auch die „Schienen“, auf denen der intrazelluläre Transport stattfindet, zu dessen Regulierung bei. So gibt es verschiedene posttranslationale Modifikationen von α- und β-Tubulin, welche die Affinität und Prozessivität von Motorproteinen beeinflussen und richtungsweisende Signale setzen können.

Im Rahmen dieser Arbeit wurden Mechanismen untersucht, die die Verteilung von Fluoreszenz-markiertem Gephyrin (tomato-Gephyrin) in hippokampalen Neuronen regulieren. Gephyrin ist ein Teil des postsynaptischen Gerüsts an inhibitorischen Synapsen, wo es für die Verankerung von $GABA_A$- und Glyzin-Rezeptoren in der postsynaptischen Membran verantwortlich ist. Es ist außerdem am Transport des Glyzin-Rezeptors beteiligt, da es die Bindung der Motoren KIF5 und Dynein zum Rezeptor vermittelt. In dieser Arbeit wurde erforscht, wie sich die subzelluläre Verteilung von Gephyrin in Folge einer Aktivierung von ionotropen AMPA Rezeptoren verändert. Eine vorangehende Arbeit hatte zeigen können, dass die Verteilung von Gephyrin nach Strychnin-induzierter Glyzin-Rezeptor Blockade aufgrund vermehrter Tubulin-Polyglutamlylierung – einer posttranslationalen Modifikation des Zytoskeletts – verändert war. Diesen Ergebnissen von Maas et al. (2009) entsprechend konnte in

der jetzigen Arbeit gezeigt werden, dass sich die Zahl der tomato-Gephyrin Aggregate in den Neuriten von kultivierten hippokampalen Neuronen signifikant reduziert, nachdem AMPA-Rezeptoren aktiviert wurden. Des Weiteren wurde eine Veränderung von zwei Arten von posttranslationalen Modifikationen an Tubulin nach AMPA-Rezeptor-Aktivierung entdeckt. Polyglutamylierung, eine Veränderung die das Anfügungen von Glutamylresten an die C-Termini von α- und β-Tubulin beeinhaltet, war nach AMPA-Rezeptor-Aktivierung im Vergleich zu Kontrollen signifikant erhöht. Tubulin Tyrosinierung hingegen, also das Anfügungen eines zuvor entfernten Tyrosinrestes an die C-Termini von α- und β-Tubulin, war im Vergleich zu Kontrollen signifikant reduziert. Diese Veränderungen weisen auf eine entscheidende Funktion der Tubulin Modifikationen in der Regulation von intrazellulären Transportprozessen hin. Es konnte zusätzlich gezeigt werden, dass die Aktivierung von AMPA-Rezeptoren für einen signifikanten Anstieg der intrazellulären Kalzium-Konzentration und für eine Aktivierung der Calcium/Calmodulin abhängigen Protein Kinase II (CaMKII) sorgt. Nachfolgende Experimente untersuchten die Rolle verschiedener intrazellulärer Signalkaskaden nach AMPA-Rezeptor-Aktivierung. Hierbei gezeigt werden, dass die Inhibierung der Glykogen Synthase Kinase 3β (GSK3β) – welche Gephyrin phosphoryliert – die Verteilung von tomato-Gephyrin in die Zellperipherie in ähnlicher Weise beeinflusst wie die AMPA-Rezeptor-Aktivierung.

Ein zweiter Teil dieser Arbeit befasste sich mit der Identifizierung und Charakterisierung weiterer Folgen von AMPA-Rezeptor-Aktivierung in Bezug auf die Aggregat-Bildung und Verteilung von tomato-Gephyrin. Es wurde beobachtet, dass eine vermehrte Umverteilung von tomato-Gephyrin ins Axon als Folge von AMPA-Rezeptor-Aktivierung auftritt. Eine Umverteilung ins Axon konnte ferner für weitere Komponenten inhibitorischer Synapsen, wie Glyzin-Rezeptoren und das Zelladhesionsmolekül Neuroligin-2 gezeigt werden, während PSD95, welches an exzitatorischen Synapsen vorkommt, nicht umverteilt wurde.

Zusammenfassend konnte diese Arbeit einen Beitrag zur Aufklärung von Mechanismen leisten, die den intrazellulären Proteintransport nach Aktivierung von Neurotransmitter-Rezeptoren regulieren, indem spezifische posttranslationale Tubulin-Modifikationen und eine mögliche Rolle von Adaptorprotein-Phosphorylierung identifiziert werden konnten. Außerdem wurde eine Umverteilung von Komponenten der inhibitorischen Synapse in Axone kultivierter hippokampaler Neurone als Folge von AMPA-Rezeptor-Aktivierung entdeckt. Weiterführende Arbeiten sind notwendig, um

die Rolle von Tubulin-Modifikationen und der GSK3β-vermittelten Phosphorylierung von Gephyrin als Regulatoren des Transportes zu untermauern. Zudem sind weitere Experimente erforderlich, um die Umverteilung inhibitorischer synaptischer Komponenten ins Axon genauer zu beschreiben und physiologische Gründe – wie zum Beispiel homöostatische Regulation – dafür zu bestimmen.

Summary

Directed intracellular transport in neuronal cells is essential for the establishment and maintenance of neuronal morphology and polarity. Most proteins are synthesized within the cell soma and subsequently transported into the somato-dendritic or the axonal compartment towards their final destination. Two processes are involved in the distribution of newly-synthesized proteins: sorting and transport.
Protein sorting determines the composition of individual transport vesicles and establishes the seperation of transport complexes designated for either the somato-dendritic or the axonal compartment. Protein transport is the processes following sorting and involves the active movement of motor proteins and their cargoes along cytoskeletal tracks. The long-distance intracellular transport along microtubules from the soma to the periphery can be regulated by several mechanisms. For instance, motor-cargo-adaptors are capable of influencing motor proteins by regulating their processivity or by directing them towards a specific cellular compartment. Also, the molecular tracks underlying intracellular transport can contribute to its regulation. Several posttranslational modifications of α- and β-tubulin can influence motor protein affinity and processivity or provide directional cues.

In this study, mechanisms underlying the targeted distribution of fluorescently-labelled gephyrin (tomato-gephyrin) in cultured hippocampal neurons were investigated. Gephyrin is part of the postsynaptic scaffold at inhibitory synapses, anchoring $GABA_A$ and glycine receptors within the postsynaptic membrane. It is furthermore involved in the transport of glycine receptors to and from the synapse by mediating the binding to the molecular motors KIF5 and cytoplasmic dynein, respectively. In the current study, it was investigated how the subcellular distribution of tomato-gephyrin is altered upon activation of the AMPA-type of ionotropic glutamate receptors. A previous study had revealed that gephyrin targeting is changed upon strychnine-induced glycine receptor blockade due to an increase of tubulin polyglutamylation, a posttranslational modification of the microtubular cytoskeleton. In line with these results, it could be shown in this study that the number of tomato-gephyrin clusters within the neurites of cultured hippocampal neurons was significantly reduced upon AMPA receptor activation when compared to control neurons. Furthermore, it was discovered that

two types of tubulin posttranslational modifications were significantly changed in AMPA-treated neurons when compared to controls. Polyglutamylation of tubulin, a modification that involves the attachment of several glutamyl residues to the C-termini of α- and β-tubulin, was strongly increased upon AMPA receptor activation, while tubulin tyrosination, i.e. the re-attachment of a previously removed tyrosine residue to the C-terminus of α- and β-tubulin, was decreased compared to controls. It could also be shown that AMPA receptor activation caused a significant increase of intracellular calcium concentrations and led to the activation of calcium/Calmodulin-dependent protein kinase II (CaMKII). Further experiments investigated the role of several signaling cascades following AMPA receptor activation and it could be shown that inhibition of glycogen synthase kinase 3β (GSK3β), which is known to phosphorylate gephyrin, influences the targeting of tomato-gephyrin to the cell periphery in a similar manner as AMPA receptor stimulation.

A second part of this study dealt with the identification and description of additional effects of AMPA receptor activation on the clustering and distribution of tomato-gephyrin. It was observed that tomato-gephyrin clusters are increasingly distributed into the axon of hippocampal neurons upon AMPA receptor activation. A redistribution into the axonal compartment could moreover be shown for further components of inhibitory synapses, such as glycine receptors and the cell adhesion molecule neuroligin-2, while PSD95, a part of excitatory synapses, was not redistributed into the axon.

Summarizing, this study shed light on the mechanisms involved in the regulation of intracellular protein transport after activation of neurotransmitter receptors by identifying specific changes in posttranslational modifications of tubulin and a possible role of adaptor protein phosphorylation. Furthermore, this study revealed a redistribution of inhibitory synapse components into the axons of hippocampal neurons as a result of AMPA receptor activation. Future investigations will be necessary to confirm the specific roles of tubulin modifications and gephyrin-phosphorylation by GSK3β as critical regulators of gephyrin targeting. Also, the redistribution of inhibitory synapse constituents into the axon upon AMPA receptor activation needs to be investigated in more detail in order to determine the physiological reasons – possibly homeostatic regulation – for this effect.

1 Introduction

1.1 THE MAMMALIAN NERVOUS SYSTEM

The mammalian nervous system is a highly complex organ that enables an organism to interact with its environment by perception and processing of external and internal stimuli and by triggering of adequate physiological responses. A differentiation is made between the central nervous system (CNS) and the peripheral nervous system (PNS). The CNS comprises the brain and spinal cord, while the PNS includes the multitude of nerve cells innervating the periphery of the body. The PNS is responsible for the perception of external and internal stimuli, their conduction towards the CNS and the subsequent execution of behaviours generated in response to such stimuli. The integration of the multitude of incoming signals and the generation of appropriate responses, however, take place in the CNS (Trepel, 2004).

1.1.1 Neurons

The fundamental units of the central nervous system are individual cells that can be classified into two distinct types: neurons and glial cells. Glial cells were initially considered to fulfil a mere supportive function (Brodal, 2004), but recent research underlined their essential role in a multitude of physiological processes such as neuronal guidance during development and regulation of synaptic neurotransmitter release (Smith, 2010).

The actual task of information transfer in the nervous system is carried out by neurons. These cells posses the ability to receive information from external sources or other nerve cells and propagate this information over considerable distances towards target cells. Within neuronal networks, information is transferred intracellularly from one part of the cell to the other as well as intercellularly between individual cells. The points of contact between neurons and their target cells where intercellular communication takes place are called synapses (Levitan & Kaczmarek, 1997).

1.1.1.1 Neuronal morphology

Much of the unique function of neurons and their ability to perform information transfer is owed to the special morphology of this cell type. Like cells from other tissues, neurons have a cell body with a nucleus surrounded by cytoplasm, which is referred to as the cell soma (Brodal, 2004). Long processes called neurites extend from the soma, which can be divided into axons and dendrites.

The several dendrites that arise from the soma are oftentimes highly branched resulting in a complex network that is called the dendritic tree (Levitan & Kaczmarek, 1997). Dendrites are the sites where information is received from external sources or other neurons and thousands of synaptic contacts can be formed within the extensively branched dendritic tree. The information received accumulates in the cell soma from where it can be passed on along the axon.

Most neurons possess a single axon which is a tube-like process that can vary in length from a few millimeters to more than one meter (Levitan & Kaczmarek, 1997). Its function is to rapidly propagate signals from the cell soma to the axon terminals, where the stimulus is conveyed to target cells at synapes.

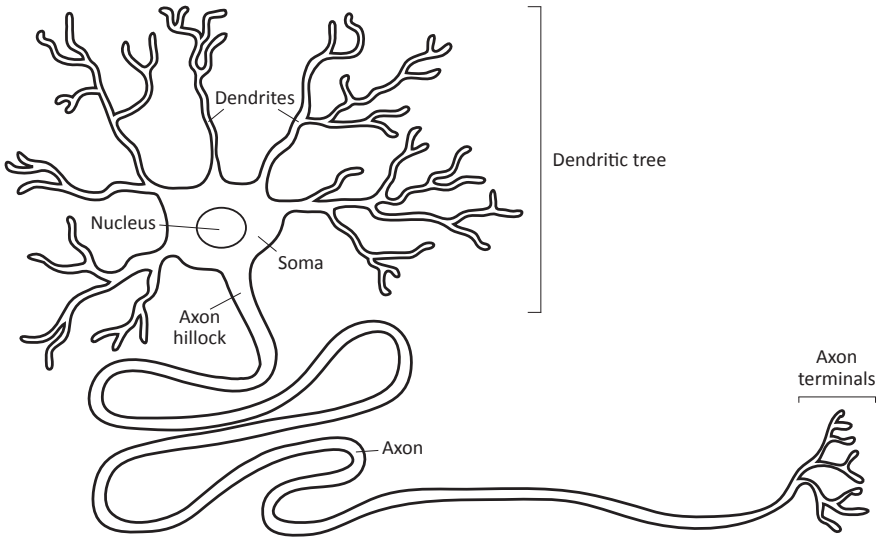

Figure 1.1: The Neuron
Several processes – or neurites – arise from the cell soma: dendrites and an axon. While the dendrites form a highly branched network, the axon can reach great length. Information transmission on an intracellular level happens when signals are received at synapses in the dendrites, integrated within the cell body and subsequently conveyed onto target cells along the axon.

Because of its strong polarity a neuron is functionally divided into the axonal and the somato-dendritic compartment. This classification not only underlines the differences in function, but also points out the importance to maintain neuronal polarity needed for the successful transmission of information. The general structure of a neuron and its compartments can be seen in Figure 1.1.

1.1.1.2 Neuronal excitability

Besides their unique morphology, it is the electrical excitability that qualifies neurons to function as information carriers. Fast signal conductance within the neuron is achieved through electrical discharges. The neuronal cell membrane creates a barrier seperating the intracellular and extracellular fluid. Ion composition between the two fluids differs in that there are more negatively charged ions in the intracellular fluid than in the extracellular fluid – a state that is maintained by selective ion channels in the neuronal membrane (Ruby, 2008). The resulting negative potential across the membrane is termed membrane potential and ranges from -50 mV to -80 mV in resting neurons. Upon activation and opening of ion channels at synapses positively charged ions enter the cell and lead to local depolarization of the membrane within the dendrites. Accumulation of depolarization in the cell soma can trigger the generation of so-called action potentials within the axon hillock (Figure 1.1) once a certain threshold is reached (Armstrong & Hille, 1998; Brodal, 2004). Action potentials are generated in an all-or-nothing fashion and then rapidly conducted along the axon towards the terminal where they provoke the release of neurotransmitter from synaptic vesicles (Rudy, 2008).

1.1.2 The chemical synapse

At synapses, an electrical signal conducted along the axon of a neuron is converted into a chemical signal in the form of so-called neurotransmitters that diffuse across the synaptic cleft and bind to neurotransmitter receptors within the membrane of the target cell. The bouton at the sending axon terminal is termed presynapse, while the receiving structure at the dendrite or the soma of the target cell is called postsynaptic site or postsynapse (Brodal, 2004; Rudy, 2008). At the postsynaptic cell, binding of

neurotransmitter can lead to depolarization of the membrane, thereby converting the chemical signal into an electrical one. The temporary conversion of electrical into chemical signals creates a time lag in the speed of information transmission, yet it permits better regulation of transmission rather than all-or-nothing responses. Depending on the type of neurotransmitter released at the presynapse and the kind of neurotransmitter receptor present at the postsynapse, synapses can be of excitatory or inhibitory nature. At inhibitory synapses, the activation of anion channels causes an influx of negatively charged ions, lowering the membrane potential in a process called hyperpolarization. At excitatory synapses, cation channels are activated which leads to a depolarization of the postsynaptic membrane. Since both, inhibitory and excitatory synapses can be activated simultaneously on the same neuron, only the summation of several signals – spacially and temporarily – determines if an action potential is generated in the axon hillock (Kandel *et al.*, 2000).

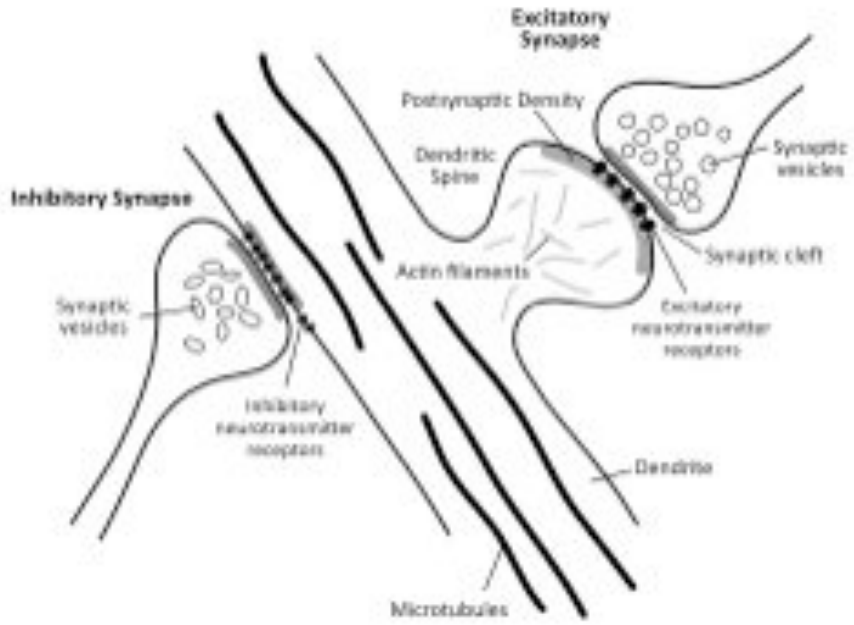

Figure 1.2: Chemical synapses
Along dendrites of neurons, signals from other neurons are received at chemical synapses. Synapses can be of excitatory or inhibitory nature. Excitatory synapses are often located at the tips of dendritic spines, while inhibitory synapses are located on the dendritic shaft.

1.1.2.1 Excitatory synapses

Electron microscopy identified notable differences in structure between the pre- and postsynaptic sites of excitatory synapses, which is why they are also termed asymmetrical synapses (Gray, 1969). While the presynaptic bouton is filled with synaptic vesicles containing neurotransmitter molecules that are released into the synaptic cleft when an action potential reaches the terminal (Kandel *et al.*, 2000), the postsynaptic site is marked by a large electron-dense protein network below the plasma membrane called the postsynaptic density (PSD). Furthermore, excitatory postsynapses are often located on small membrane processes forming a thin neck and a bulbous head called dendritic spines (Boyer *et al.*, 1998). Dendritic spines are approximately 1-1.5 µm in length (Boyer *et al.*, 1998) and the assumed function of these special compartments is the containment of activity-induced changes in intracellular Ca^{2+} concentration (Yuste & Majewska, 2001).

The most abundant excitatory neurotransmitter in the CNS is the amino acid glutamate and glutamate receptors (GluRs) in the postsynaptic membrane mediate the vast majority of excitatory transmission (Ozawa *et al.*, 1998). Depending on their mode of action, glutamate receptors are classified as ionotropic or metabotropic receptors. Ionotropic glutamate receptors (iGluRs) are ligand-gated ion channels termed AMPA (α-amino-3-hydroxy-5-methyl-4-isoxazole propionate), NMDA (N-methyl-D-aspartate) or kainate receptors, according to their synthetic agonists (Ozawa *et al.*, 1998). All three types of iGluRs are tetrameric proteins encoded by 18 different genes, many of which undergo alternative splicing and RNA editing (Hollmann & Heinemann, 1994). Differences in splicing and subunit composition can determine the exact localization and functional regulation of the receptor (Derkach et al., 2007). The four subunits of each receptor form a central pore which is cation-selective and permeable for Na^+ and K^+ ions as well as for Ca^{2+} (Traynelis *et al.*, 2010; MacDermott *et al.*, 1986; Mayer & Westbrook, 1987). One of the most prominent features of ionotropic glutamate receptors is their diversity in gating kinetics which defines the time course of synaptic currents (Traynelis *et al.*, 2010; Lester *et al.*, 1990). Once glutamate is bound, AMPA receptors display fast activation (opening) and deactivation (closing) rates, paired with rapid and strong desensitization, which is defined as a reduction in response in the presence of a sustained stimulus (Traynelis *et al.*, 2010). AMPA receptors desensitize within approximately 10 ms depending on the respective subunit composition, causing

a decrease of approximately 90% in current amplitudes (Quirk *et al.*, 2004; Swanson *et al.*, 1997). NMDA receptors in contrast, show much slower gating kinetics with activation in the millisecond range and deactivation following after seconds. Also, NMDA receptors display only weak or no desensitization at all (Vicini *et al.*, 1998). The slower kinetics observed in NMDA receptors are mainly due to a Mg^{2+} ion occupying the receptor pore in its resting state (Mayer *et al.*, 1984; Dingledine *et al.*, 1999). This block exhibits strong voltage-dependence in that NMDA receptors become activated only if a previous postsynaptic depolarization removes the Mg^{2+} ion from the pore.
The kainate type of iGluRs is similar to AMPA receptors in its fast gating kinetics but is more versatile than the other receptor types in that it can also signal via G-protein-coupled second-messengers causing signaling cascades to downstream effectors (Traynelis *et al.*, 2010; Rodriguez-Moreno & Lerma, 1998).
The metabotropic glutamate receptors (mGluRs) are G-protein-coupled receptors meaning that they transduce intracellular signals via the interaction with G-proteins (Niswender & Conn, 2010). They are grouped into three classes based on sequence homology and ligand selectivity. The synaptic transmission mediated by this type of receptor is relatively slow since it requires the modulation of synaptic ion channels and intracellular protein kinases via second messengers (Niswender & Conn, 2010).

Anchoring of neurotransmitter receptors in the postsynaptic membrane to ensure a localization opposite the presynaptic bouton is conveyed by a tightly packed protein complex below the plasma membrane called postsynaptic density (PSD). The PSD forms a disc of cytoskeletal, scaffolding and regulatory proteins with a total mass of approximately 1 gigadalton (Chen *et al.*, 2005). Besides its function in anchoring neurotransmitter receptors at membrane specializations, the PSD also maintains close spacial proximity of protein kinases and phosphatases to cater for fast transmission of synaptic signals. Consisting of more than 400 different proteins, roughly 6% are scaffolding proteins that function to anchor the receptors, support signaling constituents and connect the network to the actin cytoskeleton (Sheng & Hoogenraad, 2007). One of the most abundant scaffold proteins is postsynaptic density-95 (PSD-95) which directly interacts with the NMDA receptor NR2 subunit and indirectly also connects to the AMPA receptor (Kornau *et al.*, 1995; Kornau *et al.*, 1997). Approximately 20% of the PSD proteins are kinases, phosphatases, GTPases and regulatory proteins, responsible for fast and efficient transmission of synaptic signals

(Sheng & Hoogenraad, 2007). The two most numerous ones are the synaptic GTPase-activating protein (SynGAP) and the Ca^{2+}/Calmodulin-dependent protein kinase II (CaMKII), the latter of which is especially involved in activity-dependent signaling as it becomes activated upon local increases in Ca^{2+} concentration (Sheng & Hoogenraad, 2007).

1.1.2.2 Signal transduction at excitatory synapses

Activation of postsynaptic glutamate receptors due to presynaptic neurotransmitter release leads to depolarization of the postsynaptic membrane by an influx of Na^{+} ions through AMPA receptors and – if the presynaptic signal was sufficiently strong – Ca^{2+} influx through NMDA receptors. Free intracellular Ca^{2+} binds to calmodulin which causes activation of CaMKII and its binding to NMDA receptors at the plasma membrane. Also, other kinases such as protein kinase C (PKC), protein kinase A (PKA) and SRC (cellular sarcoma) family tyrosine kinases become activated amplifying the initial signal (Lisman *et al.*, 2012; Soderling & Derkach, 2000; Traynelis *et al.*, 2010). Active CaMKII at the plasma membrane phosphorylates AMPA receptors, thereby increasing receptor conductance and membrane depolarization (Lisman *et al.*, 2012; Soderling & Derkach, 2000). Besides activation of CaMKII, Ca^{2+}-bound calmodulin also enhances production of cyclic adenosine monophosphate (cAMP) by activating the adenylate cyclase and increases in cAMP concentration activate PKA. PKA can phosphorylate voltage-gated calcium channels (VGCCs), thereby increasing the Ca^{2+} influx and amplifying Ca^{2+} signaling (Cohen & Greenberg, 2008). Metabotropic glutamate receptors that bind glutamate lead to the activation of intracellular G-proteins, which stimulate phospholipase C (PLC) to cleave PIP_2 (phosphatidylinositol-4,5-bisphosphate) into DAG (diacyl glycerol) and IP_3 (inositol-1,4,5-trisphosphate). IP_3 triggers the release of Ca^{2+} from internal stores such as the endoplasmatic reticulum (ER) and DAG can – in combination with Ca^{2+} – activate PKC (Amadio *et al.*, 2006). PKC is responsible for the induction of a multitude of downstream processes, including receptor modulation, cytoskeletal remodelling, local translation activation and nuclear signaling (Amadio *et al.*, 2006). Another important signaling pathway that is initiated by activity-induced increases in local Ca^{2+} concentrations is the mitogen-activated protein kinase (MAPK) cascade, which propagates synaptic signals towards the nucleus, confering changes in gene transcription (Wiegert & Bading, 2010). Ca^{2+}/calmodulin

complexes activate the small G-protein Ras which causes phosphorylation of extracelluar signal-regulated kinases 1 and 2 (ERK1/2), belonging to the MAPK family. ERK1/2 elicit their function by transmitting signals into the cell nucleus either indirectly by phosphorylating downstream kinases or by direct translocation into the nucleus, where gene transcription is induced (Wiegert & Bading, 2010).
The examples above illustrate the complexity of cellular signaling following synaptic activation, its amplification potential and the numerous implications on cellular processes like cytoskeletal remodelling, protein trafficking and gene transcription.

1.1.2.3 Inhibitory synapses

In contrast to excitatory synapses, electron micrographs of inhibitory synapses did not reveal notable structural differences between the pre- and postsynaptic site – hence inhibitory synapses are also termed symmetric synapses (Gray, 1969). Another difference to excitatory synapses lies in the subcellular localisation of inhibitory synapses, as it is mainly restricted to dendritic shafts and the cell soma rather than dendritic spines (Qian & Sejnowski, 1990). Inhibitory synaptic transmission in the CNS is mediated by two different neurotransmitters, the amino acids GABA (γ-aminobutyric acid) and glycine. These transmitters activate distinct but homologous classes of Cl^--permeable ion channels termed GABA receptors (GABARs) and glycine receptors (GlyRs), respectively (Moss & Smart, 2001). Both, GABARs and GlyRs mediate fast inhibitory transmission due to an influx of Cl^- ions upon ligand binding to the ion channels. The negatively charged Cl^- ions cause a postsynaptic hyperpolarization, thereby lowering the membrane potential and decreasing the probability of depolarization.
Most of the inhibitory transmission in the brain is mediated by GABA receptors and several types of GABARs can be differentiated according to their mode of action: the metabotropic $GABA_B$ receptor and the ionotropic $GABA_A$ and $GABA_C$ receptors. Furthermore, GABAergic transmission is divided into an early phasic inhibition that is mediated by synaptically localized receptors and a later tonic inhibition mediated by extrasynaptic GABA receptors (Farrant & Nusser, 2005).
All GABA receptors are pentameric assemblies of subunit classes that form a central ion channel. In case of the $GABA_A$ receptor seven different subunits that occur in a total of 19 distinct isoforms can assemble a large variety of receptors that are

distributed differentially among brain region, neuronal populations and during development (Farrant & Nusser, 2005). Subunit composition of individual receptors also influences physiological and pharmacological aspects, as well as the synaptic or extrasynaptic localization of the receptors (Farrant & Nusser, 2005; Belleli *et al.*, 2009). $GABA_C$ receptors are less diverse in their subunit composition, only three different subunit types are arranged into pentameric channels that differ from $GABA_A$ receptors in their pharmacological properties in that they are unaffected by several chemicals used for the successful blockade of $GABA_A$ receptors (Chebib & Johnston, 1999).
$GABA_B$ receptors are metabotropic G-protein-coupled receptors that activate second messenger cascades and influence Na^+ and K^+ channels, similar to metabotropic glutamate receptors (Chebib and Johnston, 1999).
Like GABARs, glycine receptors are pentameric anion channels composed of different subunits. Four genes encode different α subunits (GLRA1-4), while only one β subunit-encoding gene has been identified (GLRB) (Dresbach *et al.*, 2008; Laube *et al.*, 2002; Lynch, 2004). α and β subunits assemble into channels with a fixed stochiometric ratio of two α to three β subunits (Kirsch, 2006). Although GlyRs are widely expressed in the spinal cord and brain stem and were originally thought to be absent from other areas in the CNS, it is now established that they are also present in brain structures such as the hippocampus (Danglot *et al.*, 2004). Glycinergic transmission fulfils a role in the processing of motor and sensory information that controls movement, vision and audition (Kirsch, 2006; Lopez-Corcuera *et al.*, 2001) and is highly sensitive to the alkaloid strychnine which acts as a competitive antagonist of the receptor.

In a similar way to excitatory synapses, inhibitory synapses are also supported intracellularly by a multitude of scaffolding and regulatory proteins, forming a postsynaptic density (PSD). The inhibitory PSD is not as complex as the one at excitatory synapses and its main component is the 93 kDa scaffolding protein gephyrin (Tyagarajan & Fritschy, 2010; Fritschy *et al.*, 2008). By oligomerization gephyrin forms a hexagonal lattice that anchors GABARs and GlyRs and interacts with the cytoskeleton (Kneussel & Betz, 2000; Sola *et al.*, 2004). Because of its relevance for this study the characteristics of the scaffold protein gephyrin will be discussed in more detail in the following chapter (see Chapter 1.1.3).

1.1.3 The postsynaptic scaffold protein gephyrin

When the glycine receptor was first purified by SDS-PAGE, not only the α- and β-subunits could be detected, but also a heterogeneous band of 93 kDa in size. This protein could be dissociated from the plasma membrane by elution with basic pH, leading to the assumption that a peripheral membrane protein was discovered (Schmitt *et al.*, 1987). Further studies revealed that the 93 kDa protein binds tubulin with a similar stochiometry as MAP2 which led to the hypothesis that this protein could form a bridge between the GlyR and the underlying microtubular cytoskeleton (Kirsch *et al.*, 1991; Prior *et al.*, 1992; Dresbach *et al.*, 2008). Due to this assumption the newly described protein was named gephyrin (εφυρα; Greek: bridge) (Prior *et al.*, 1992).

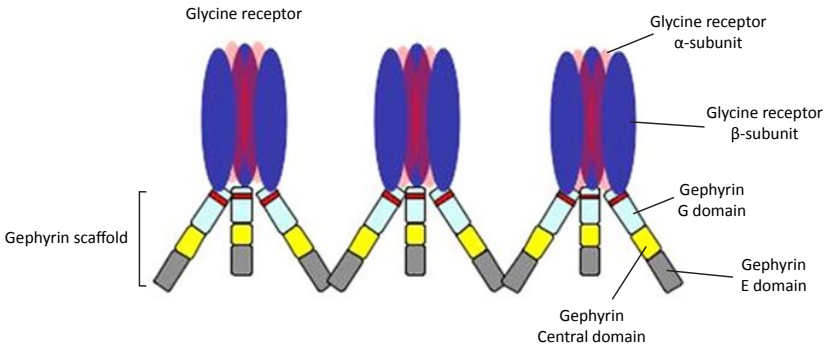

Figure 1.3: The postsynaptic scaffold protein gephyrin in complex with the glycine receptor
Gephyrin anchors inhibitory neurotranmitter receptors in the postsynaptic membrane of inhibitory synapses. It binds the β-subunit of the glycine receptor with its G domain. G domains can form trimers with other gephyrin G domains, while the E domain can for homomeric dimers. This leads to the formation of a hexagonal lattice below the postsynaptic membrane. Modified after Dresbach *et al.* (2008).

It was soon discovered, that an 18 amino acid (aa) long sequence in the cytoplasmic loop of GlyR β-subunits mediates the interaction between the glycine receptor and gephyrin (Kirsch e*t al.*, 1995; Kneussel *et al.*, 1999; Meyer *et al.*, 1995). Incorporation of this sequence into NMDA receptor subunits led to the targeting of the receptors to gephyrin-rich domains, indicating that this short binding sequence is the decisive motif responsible for accumulation of receptors at postsynaptic sites (Kins *et al.*, 1999; Dresbach *et al.*, 2008). A similar, 10 aa long sequence was identified in $GABA_A$ α_2 receptor subunits, equally sufficient for the targeting of receptor proteins to inhibitory synapses (Tretter *et al*., 2008). These findings raised the notion that synaptic

accumulation of GlyRs and $GABA_A$ receptors depends on their ability to bind gephyrin and therefore, research interest focused on the molecular and cellular mechanisms underlying gephyrin cluster formation (Dresbach *et al.*, 2008).

Although expressed in many tissues, gephyrin is abundant in the brain and spinal cord. Within the brain, co-localization studies revealed that gephyrin colocalizes with both, the GlyR and $GABA_A$ receptors containing α_2 and/or γ_2 subunits (Kirsch & Betz, 1993; Sassoe-Pognetto *et al.*, 1995).

Analysis of a gephyrin knockout mouse revealed that neuronal gephyrin expression is indispensable for the formation of most inhibitory postsynaptic membrane specializations. The few remaining $GABA_A$ receptor clusters that could be identified in the brain of gephyrin deficient mice were those containing α_1 and α_5 subunits, but the numbers of α_2, α_3, $\beta_{2/3}$ and γ_2 subunit-containing $GABA_A$ receptors was significantly reduced (Fischer *et al.*, 2000; Kneussel *et al.*, 1999). Furthermore, gephyrin knockout mice die within one day after birth, they do not suckle and exhibit a rigid, hyperextendend posture upon mild tactile stimuli (Feng et al., 1998). The lethality is most likely due to the loss of postsynaptic inhibitory neurotransmitter receptor clusters in the brain (Grosskreutz *et al.*, 2003; Dresbach *et al.*, 2008).

An important aspect for the cluster formation at membrane specializations, is the fact that the N-terminal G-domain of gephyrin can form trimers with other G-domains, while the C-terminal E-domain is able to form dimers (Sola *et al.*, 2001; Sola *et al.*, 2004). It is therefore believed that gephyrin forms a hexagonal lattice *in vivo* and that such hexagonal structures can arrange to build higher order scaffolds underlying inhibitory postsynaptic membranes (Dresbach *et al.*, 2008). A serine residue within the central domain of gephyrin (S270) has been shown to be a target for phosphorylation by glycogen synthase 3β (GSK3β) and cyclin-dependent kinase (CDK) 1, 2 and 5 (Tyagarajan *et al.*, 2010; Kuhse *et al.*, 2012). Experiments using the phosphorylation-deficient gephyrin mutant S270A revealed an increase in the number of gephyrin clusters and increased amplitude of GABAergic currents (Tyagarajan *et al.*, 2011).

The presence of gephyrin at nearly all inhibitory postsynaptic membrane specializations has led to the extensive use of fluorescently-labelled gephyrin as a marker for inhibitory postsynaptic sites.

1.1.4 Synaptic plasticity in hippocampus-related learning and memory

It is believed that synapses are the fundamental unit for complex neuronal functions such as learning and memory and a reason for this assumption is that synapses can be modified in strength by experience (Rudy, 2008). The property to increase or decrease synaptic strength among groups of neurons is known as synaptic plasticity and mechanisms that support changes in synaptic strength have therefore been subject of investigation for more than 30 years (Rudy, 2008). Synaptic strength is described as the amplitude of the change in postsynaptic membrane potential following a presynaptic stimulus (Ruby, 2008, Kandel *et al.*, 2000). One example of how synaptic strength can be modified as a result of stimulation is provided by the concept of long-term potentiation (LTP). It was discovered that a single weak stimulus applied to a presynaptic cell evoked synaptic activity in the target cell. If a stronger stimulus was presented, the postsynaptic response was increased significantly and repeated weak stimuli afterwards evoked a strong response similar to that induced by the strong stimulus (Bliss & Lomo, 1973). This long-lasting increase in synaptic strength following a strong stimulus is termed LTP.

Importantly, synaptic plasticity is a bidirectional process and the polar opposite of LTP is long-term depression (LTD) a concept that describes the weakening of synaptic contacts in size and efficacy. LTD can be induced at synapses by applying low-frequency stimulation over several minutes to neuronal networks (Dudek & Bear, 1992). Both processes, LTP and LTD are dependent on NMDA receptors, as it is possible to block the induction of either of the processes by inhibiting NMDA receptors with the selective antagonist APV (Malenka & Bear, 2004). The important contribution of the NMDA receptors to LTP and LTD underlines the significance of changes in Ca^{2+} concentration at synapses and the consequences these changes induce.

On the synaptic level, LTP and LTD are characterized by structural changes in postsynaptic membrane composition and the activation of regulatory proteins (see Chapter 1.1.2.2). In the absence of neuronal activity, AMPA receptors at excitatory synapses are constantly inserted into and removed from the postsynaptic membrane. Upon removal, the receptors are sorted into recycling endosomes for reinsertion into the membrane or into late endosomes for subsequent degradation (Derkach *et al.*, 2007; Citri & Malenka, 2008). Upon induction of LTP, exocytosis of AMPA receptors from recycling pools is enhanced, leading to the insertion of receptors at perisynaptic

sites and the subsequent lateral diffusion to the postsynapse followed by anchoring in the PSD (Park *et al.*, 2004; Derkach *et al.*, 2007). Furthermore, phosphorylation of postsynaptic AMPARs during LTP can increase receptor conductance (Soderling & Derkach, 2000; Derkach *et al.*, 2007). Both processes, enhanced AMPA receptor exocytosis and receptor phosphorylation to increase ion conductance are essential during the early phase of LTP induction. For the establishment of long-lasting increases in synaptic strength additional processes such as gene expression, protein synthesis and targeted protein transport are necessary (Citri & Malenka, 2008).

LTD induction at exitatory synapses leads to the Ca^{2+}-mediated activation of protein phosphatases such as calcineurin and PP1 (protein phosphatase 1). Substrates that are phosphorylated by PKA or PKC during LTP are dephosphorylated by LTD-induced calineurin and PP1 activation (Citri & Malenka, 2008; Lee *et al.*, 2000). Subsequently, protein dephosphorylation causes the endocytosis of synaptic AMPA receptors, lowering synaptic transmission (Collingridge *et al.*, 2004; Derkach *et al.*, 2007; Malenka & Bear, 2004). Late phases of LTP are accompanied by shrinkage in the size of dendritic spines and dependent on gene transcription and protein translation (Nägerl *et al.*, 2004; Pfeiffer and Huber, 2006).

Although LTP and LTD are concepts that aim to explain the molecular basis of memory and learning at a synaptic level, much effort has also been made to identify higher brain structures involved in the aquisition and storage of memories. Many of the facts known about memory-related brain systems were gained from human patients with partial brain damage that exhibited difficulties in the aquisition and retrieval of memories (Rudy, 2008). Several studies identified the hippocampus – a part of the medial temporal lobe – as a central structure since damage to this region resulted in both anterograde and retrograde amnesia as well as severe learning deficits (Rudy, 2008; Milner, 1970; Cipolotti *et al.*, 2001; Zola-Morgan *et al.*, 1986). Because of its apparent relevance to memory and learning and due to its clear anatomical organization the hippocampus or cultures of hippocampal neurons have been used extensively to investigate the molecular mechanisms underlying processes such as LTP and LTD.

1.2 INTRACELLULAR PROTEIN TRANSPORT

The complex morphology of neurons, meaning the many extended neurites, together with constant structural changes due to plasticity requires a fast and efficient way to transport cellular components to their sites of action. The majority of protein synthesis machinery is located in the cell soma bringing about the necessity to (1) sort newly synthezised proteins into the compartment they are needed in (axonal vs. somato-dendritic) and (2) cater for the targeted transport towards the correct location of the cargoes. A variety of components is essential to achieve these two objectives.

1.2.1 The cytoskeleton

The fundamental structure accounting for the complex morphology of neurons and at the same time allowing protein transport over considerable distances is the cytoskeleton. On the one hand, the cytoskeleton provides the mechanical basis for the maintenance of neuronal morphology while on the other hand, parts of the cytoskeleton act as travel routes for cellular components.

Three main types of filaments with distinct mechanical properties, dynamics and biological functions work synergistically to fulfil the diverse functions of the cytoskeleton: Intermediate filaments (IFs), microtubules (MTs) and actin filaments (Alberts *et al.*, 2008). While intermediate filaments provide mechanical strength, microtubules determine the position of organelles and direct intracellular transport, and actin filaments determine and maintain the shape of the cell surface. All types of filaments are assembled from individual protein subunits, allowing the rapid reorganization of fibers in case of changing requirements (Alberts *et al.*, 2008).

Microtubules are hollow cylindrical structures – approximately 25 nm in diameter – consisting of 13 parallel protofilaments that are composed of individual α- and β-tubulin subunits (Alberts *et al.*, 2008). Heterodimers of α-tubulin and β-tubulin molecules are tightly bound together by noncovalent bonds (Ludueña, 1998). Both, α- and β-tubulin are small globular proteins that exist in numerous isoforms encoded by different genes and that can additionally undergo a variety of posttranslational modifications (Ludueña, 1998). Within a microtubule, the subunits comprising a protofilament are all oriented in the same direction giving the structure a distinct

polarity. The growing end, where β-tubulin molecules are exposed is termed plus end, while the other side terminating with α-tubulins is more stable and called minus end (Alberts *et al.*, 2008).

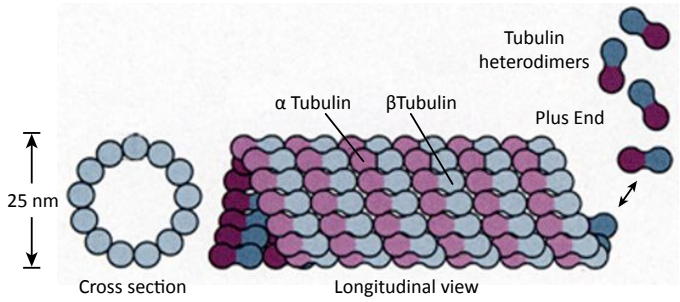

Figure 1.4: Structure of a microtubule
Heterodimers of α- and β-tubulin assemble to 25 nm wide cylindrical structures called microtubules. All α- and β-tubulin dimers are thereby oriented in the same direction. The fast-growing end, at which β-tubulin is exposed is called the plus end, while the other side is termed minus end. Within cells, microtubules determine the position of cellular organelles and serve as tracks for intracellular protein transport.

Actin filaments are assembled of two protofilaments containing individual globular subunits, that twist around each other forming a right-handed helix of roughly 5-9 nm in diameter. Compared to microtubules, actin filaments are relatively flexible structures that are generally shorter but crosslinked by accessory proteins to form malleable networks. In neurons, actin filaments are highly abundant in dynamic structures such as neurite tips (growth cones) and dendritic spines (Dent & Gertler, 2003; Tada & Sheng, 2006).
Intermediate filaments are ropelike fibers with a diameter of about 10 nm and one of their tasks is to line the inside of the nuclear envelope for mechanical support. In neurons they are usually termed neurofilaments and fulfil the important role to establish and maintain stability of the axon (Perrot *et al.*, 2008).

1.2.2 Molecular motors

While cytoskeletal structures such as microtubules provide a network of tracks throughout the cell, molecular motors or motor proteins are the vehicles utilizing these tracks for directed movement. Motor proteins from the kinesin, dynein and

myosin superfamily have been identified to perform transport processes within the cell, targeting the axon, the dendrites and dendritic spines (Hirokawa *et al.*, 2010).
The mechanism of movement is ATP-dependent and similar for the three types of motor proteins. ATP hydrolysis causes conformational changes in the motor domain that are conferred to neck regions, amplifying these changes (Schliwa & Woehlke, 2003). Firstly, this leads to the dissociation of the motor domain from the cytoskeletal filament and secondly, to a swing of one motor domain around and in front of the other. Continuous repetition of ATP hydrolysis cycles therefore induces movement of the motor protein in a so-called *hand-over-hand* mechanism (Schliwa & Woehlke, 2003). The motion generated by molecular motors can either lead away from the cell soma, in which case it is termed anterograde movement or towards the soma, a process called retrograde movement.

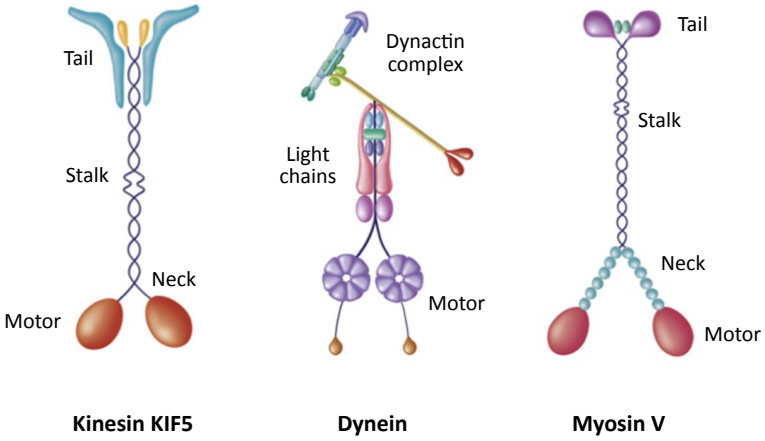

Figure 1.5: Molecular motors
Motors proteins from the kinesin family such as KIF5 transport cargoes along microtubules. Cytoplasmic dynein also uses microtubules as molecular tracks, while myosins mediate transport on actin filaments. The globular motor domains associate with the cytoskeleton and perform stepwise progressive movements under ATP hydrolysis in a *hand-over-hand* manner. The coiled-coil domains of the stalk region are often responsible for homodimerization of two heavy chains, while the tail domains and associated light chains mediate the interaction with putative cargoes. Modified after Hirokawa *et al.* (2010).

In microtubule-based transport, kinesins (KIFs) are the largest protein superfamily of molecular motors, comprising 45 genes that are grouped into 14 classes (Miki *et al.*, 2001). A further classification seperates N-KIFs from M-KIFs and C-KIFs according to the position of the motor domain within the protein. Conventional kinesin (KIF5) appears as a dimeric protein of two heavy chains, each with a globular motor domain

at one end and a tail domain at the opposite end connected by a long stalk that forms a coiled-coil. N-KIFs move towards the plus end of MTs, while C-KIFs move in the opposite direction and M-KIFs depolimerize MTs in an ATP-dependent manner (Hirokawa *et al.*, 2010). The interaction with putative cargoes is mainly mediated by the tail domain of motor proteins, although in some cases the stalk was identified as the critical structure (Hirokawa & Noda, 2008). The speed at which kinesins travel along microtubules lies between 0.1 - 1.5 µm/sec (Ross *et al.*, 2008; Hirokawa & Takemura, 2005).

Like kinesins, dyneins also use microtubules as tracks for directed transport and are similarly composed of two heavy chains forming the motor domains. Dyneins are grouped into two main classes, cytoplasmic and axonemal dyneins. The latter is also termed ciliary or flagellar dynein, as it is involved in the rapid sliding movement of microtubules that drives the beating of cilia and flagella (Hirokawa *et al.*, 2010; Alberts *et al.*, 2008). Cytoplasmic dyneins are involved in intracellular protein transport where they move along microtubules towards their minus end. Besides the two motor domain-containing heavy chains, cytoplasmic dynein consists of two intermediate chains, four intermediate light chains and several light chains that make up the variable tail domain responsible for cargo interaction (Karki & Holzbaur, 1999; Pfister *et al.*, 2005). In addition to the several light chains, dynein also interacts with a number of proteins that do not belong to the dynein complex itself, but are essential for its correct function (Kardon & Vale, 2009). One example of such an accessory constituent is the dynactin complex, which was first identified as an activator of dynein-mediated transport (Gill *et al.*, 1991). The dynactin complex comprises 11 different subunits, and the inhibition of dynactin by over-expression of its subunit dynamitin is similar to a complete loss of dynein function (Kardon & Vale, 2009; Burkhardt *et al.*, 1997).

Molecular motors from the myosin superfamily are the only motor proteins utilizing actin filaments as tracks (Hirokawa *et al.*, 2010). Myosins are defined by a characteristic 80 kDa motor domain that contains the actin- and nucleotide-binding sites and mediates movement along actin filaments (Hartman *et al.*, 2011). Similar to kinesins and dyneins, the motor domain of myosin is flanked by a coiled stalk and a C-terminal tail domain conferring cargo interactions (Hartman *et al.*, 2011; Foth *et al.*, 2006). 24 different myosins have been identified, including myosin II – or conventional myosin – which mediates muscle contractions and unconventional myosins, involved in intracellular protein transport (Hartman *et al.*, 2011).

1.2.3 Motor-cargo-complexes

Because of its relevance for the maintenance of neuronal structure and functionality, microtubule-based transport has been intensively investigated (Hirokawa, 2011; Setou *et al.*, 2000; Kapitein & Hoogenraad, 2010). This led to the identification of multiple motor-cargo-complexes allowing conclusions on general principles of how intracellular protein transport is organized. The nature of cargoes that require transport into the cell periphery is very diverse, ranging from organelles such as mitochondria, to vesicles containing neurotransmitter receptors and mRNA protein complexes called *RNA granules* (Glater *et al*., 2006; Setou *et al.*, 2000; Setou *et al.*, 2002; Kanai *et al.*, 2004). The interaction between a motor and its cargo can be mediated by various factors and is likely to contribute significantly to the specificity of transport (see Chapter *1.2.4.1*; Schlager & Hoogenraad, 2009). In the case of vesicles containing neurotransmitter receptors several cases were described in which specialized adaptor proteins link motors to their respective cargoes. The motor KIF17, for instance, binds to the NR2 subunit of the NMDA receptor via the adaptor proteins LIN7, LIN2 and LIN10 (Setou *et al.*, 2000). The scaffold protein gephyrin links the glycine receptor to the motor KIF5 in the case of anterograde transport and to dynein for transport in the retrograde direction (Fuhrmann *et al.*, 2002; Maas *et al.*, 2009). KIF5 has also been shown to drive the AMPA receptor subunit GluA2 via the adaptor protein GRIP1 (GluA2-interacting protein) towards their synaptic targets into dendrites (Setou *et al.*, 2002).

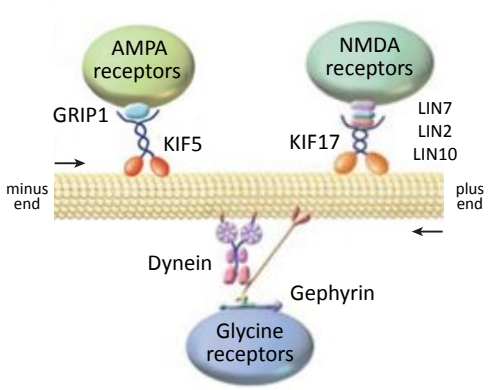

Figure 1.6. Motor-cargo-complexes
Different cargoes are transported along the microtubule network within the cell by adaptor protein-mediated binding to specific motors. In the case of AMPA receptor-containing vesicles the interaction between the motor KIF5 and the receptor is mediated by the postsynaptic protein GRIP1, while the motor KIF17 transports NMDA receptor containing-vesicles by binding to an adaptor protein complex of LIN2, LIN7 and LIN10. Transport of glycine receptor containing-vesicles performed by cytoplasmic is mediated by the postsynaptic scaffold protein gephyrin. Modified after Hirokawa *et al.* (2010).

Generally, the formation of motor-cargo-complexes serves to mediate specificity of transport into the right compartment, to the precise target and oftentimes together with proteins necessary for correct integration and function at the final location.

1.2.4 Regulation of intracellular protein transport

Intracellular transport requires exact regulation that provides for the targeted delivery of cargoes to the site where they are needed. Although many details on how transport specificity is achieved remain elusive, several regulatory mechanisms have been unravelled (Schlager & Hoogenraad, 2009).

1.2.4.1 The role of motors, adaptor proteins and cargoes in transport regulation

A first step towards an efficient regulation of intracellular transport is the assembly of specific motor-cargo-complexes as decribed above (see Chapter 1.2.3). KIF3, for instance, is a motor protein that is present almost exclusively in the axon, where it is involved in the transport of vesicles containing plasma membrane (Kondo *et al.*, 1994; Takeda *et al.*, 2000). Thus, transport of plasma membrane vesicles that are needed in axonal growth cones is automatically directed into the right compartment by association to the respective motor. Furthermore, certain motors predominantly cover certain intracellular routes, connecting specific cellular compartments. An example is the dynein motor conducting the transport of late endosomes towards lysosomal compartments (Burkhardt *et al.*, 1997; Tan *et al.*, 2011).

As mentioned above (see Chapter 1.2.3), the binding of motors to cargoes via adaptor proteins also contributes to the specificity of intracellular transport processes. An example for the impact of adaptor proteins on motor targeting is the fact that GRIP1 is sufficient to navigate KIF5 into the dendritic compartment, while the axonal scaffold protein JSAP1 attached to KIF5 predominantly steers the motor into the axon (Setou *et al.*, 2002).

Another possible mode of transport regulation is modulation of motor protein activity (Schlager & Hoogenraad, 2009). Kinesin motors, for instance, can fold their stalk creating close proximity of motor and tail domain, which renders the motor protein

inactive (Coy *et al.*, 1999; Thirumurugan *et al.*, 2006). Accessory proteins such as the dynactin complex for the dynein motor can also influence the processivity (King & Schroer, 2000).

Regulation of intracellular protein transport can also be achieved by the attachment of multiple motors to one cargo vesicle. Kinesins and dyneins at the same vesicle allow bidirectional transport along microtubules, while myosins can mediate the transfer to actin-based transport (Schlager & Hoogenraad, 2009). The different motors associated to individual transport vesicles are likely to be regulated by GTPases, scaffolding and signaling proteins also attached to the vesicles, controlling the direction of transport by differentially activating certain motors only (Karcher *et al.*, 2002; Welte, 2004).

Motors and adaptor proteins as well as cargoes can further be modified by covalent attachment of chemical residues or small proteins, influencing the function of the respective protein. The process is termed posttranslational modification (PTM) and is relevant because it can alter a protein's physical and chemical properties, i.e. its activity, localization or stability (Farley & Link, 2009). Examples for PTMs are, among others, phosphorylation, glycosylation or ubiquitinylation. As an example, phosphorylation of KIF5 or dynein has been shown to affect their motor activities and their ability to interact with putative cargoes (Thaler & Haimo, 1996).

1.2.4.2 The role of the microtubule network in transport regulation

Besides the multiple possibilities to regulate transport on the side of motor proteins, adaptors and cargoes, the underlying tracks namely microtubules can also be subject to modifications.

A major contribution towards the correct sorting of proteins into the somato-dendritic or the axonal compartment is thought to originate from the differences in microtubule orientation between these two compartments. Within proximal dendrites, microtubules have mixed orientations which means that MT plus ends can either point away or towards the cell body (Baas & Lin, 2011; Kapitein & Hoogenraad, 2010). N-KIFs that travel on these tracks are therefore not necessarily anterograde motors, but can move either direction depending on the orientation of the respective MT. Within distal dendrites and the axon, microtubules are oriented uniformly with their plus ends pointing towards the cell periphery (Heidemann & McIntosh, 1980; Baas *et al.*, 1988). The uniform orientation of microtubules in the distal dendrites or the axon designates

kinesins to perform anterograde transport, while dyneins drive retrograde transport, so that the selective activation of either motor determines the direction (Vale *et al.*, 2003, Welte, 2004; Kapitein & Hoogenraad, 2010). In proximal dendrites however, selective motor activation can not determine directionality of transport since microtubules are not uniformily oriented and both motor types can travel into either direction. It has therefore been proposed, that minus end-directed transport as performed by dynein, might play a central role in the sorting process into cellular compartments, as it allows transport of proteins into the periphery in dendrites but not in axons (Baas *et al.*, 1989). A recent study could show that the recruitment of dynein is indeed sufficient to induce transport of selective cargoes into dendrites (Kapitein *et al.*, 2010).

Not only microtubule orientation plays a role in sorting and the regulation of intracellular transport but modifications on tubulin subunits within MTs can also influence motor protein targeting and activity. An array of different posttranslational modifications on α- and β-tubulin can generate functional diversity of microtubules that can be recognized by motors, thereby establishing specifically "marked" transport routes (Westermann & Weber, 2006; Schlager & Hoogenraad, 2010). Tubulin can aquire several different types of PTMs including polyglutamylation, polyglycylation, detyrosination, acetylation, phosphorylation and palmitoylation (Verhey & Gaertig, 2007).

The reversible removal of a gene-encoded tyrosine residue at the C-terminal of tubulin called detyrosination was the first PTM to be described (Barra *et al.*, 1973). The enzyme responsible for the removal of tyrosine is unknown, the reverse reaction however, is performed by an enzyme called tubulin tyrosine ligase (TTL) (Schröder *et al.*, 1985; Ersfeld *et al.*, 1993). After detyrosination, α-tubulin can be further modified by the irreversible removal of the following glutamate residue, generating Δ2-tubulin (Paturle *et al.*, 1989; Paturle-Lafanechere *et al.*, 1991). Both detyrosination and Δ2-modifications on tubulin have been linked to increased MT stability, since MTs with these modifications are less susceptible to depolimerization (Schulze *et al.*, 1987; Peris *et al.*, 2009). The motor protein KIF5 preferentially binds to and travels on detyrosinated MTs, a property that is crucial in the early development of neuronal polarity, when the axon can be differentiated from other neurites on the basis of KIF5

accumulation on detyrosinated MTs (Dunn *et al.*, 2008; Konishi & Setou, 2007; Hammond *et al.*, 2010).

Acetylation of tubulin is performed by a protein complex called ARD1-NAT1 (ADP-ribosylation factor domain protein 1, N-terminals acetyltransferase), while deacetylation is thought to be controlled by HDAC6 (histone deacetylase 6) (Park & Szostak, 1992; Hubbert *et al.*, 2002). Tubulin acetylation has been shown to influence transport processes in a way that KIF5 prefers movement on acetylated MTs, while KIF17 and KIF1A do not exhibit this preference (Cai *et al.*, 2009). Also, acetylation seems to stimulate both anterograde and retrograde transport mediated by KIF5 and dynein, as shown on BDNF (brain-derived neurotrophic factor) vesicle transport (Dompierre *et al.*, 2007).

Polyglycylation and polyglutamylation are polymeric modifications which means that several glycine or glutamate residues are attached to the C-terminal tails of α- or β-tubulin. In mammals, polyglycylation seems to be restricted to axonemes of motile cilia and flagella (Verhey & Gaertig, 2007). Polyglutamylation on the other hand is particularly abundant on MTs in neurons, a fact that suggested a key regulatory rule for this modification in transport processes (Wolff *et al.*, 1992; Janke & Kneussel, 2010). The enzymes responsible for the modification are called polyglutamylases and belong to the large family of TTL-like enzymes (TTLLs) since parts of their catalytic domain is homologous to TTL (Janke *et al.*, 2005). TTLL glutamylases can catalize two reactions: firstly, the initial attachment of a single glutamyl residue to the acceptor glutamate in the C-terminal tail of tubulin (initiation) and secondly, the lengthening of the side chain by continuous addition of further glutamyl residues (elongation) (Van Dijk *et al.*, 2007). Of the 7 known mammalian glutamylases (TTLL1, 4, 5, 6, 7, 11, 13) TTLL4, TTLL5 and TTLL7 exhibit a preference for the initiation reaction, while TTLL6, TTLL11 and TTLL13 tend to catalize the elongation reaction and TTLL1 seems equally capable of performing both processes (Janke *et al.*, 2008). Polyglutamylation is a reversible process and the enzyme responsible for the removal of glutamyl residues appears to be a cytosolic carboxypeptidase (CCP), since over-expression of CCP5 in mammalian cells caused a dramatic decrease in MT glutamylation (Kimura *et al.*, 2010).

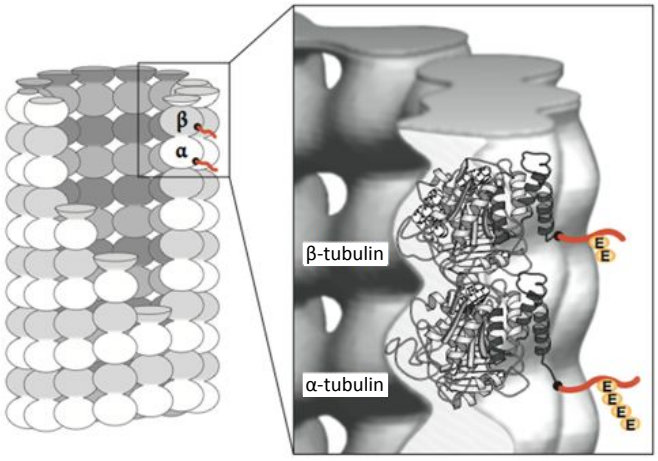

Figure 1.7: Polyglutamylation of microtubules
Polyglutamylases of the TTLL protein family catalyze the addition of glutamyl residues (E) to the C-termini of α- and β-tubulin. An acceptor glutamate residue in the terminal sequence of α- and β-tubulin is target of the initial attachment called initiation. The subsequent continuous addition of further glutamyl residues is termed elongation. Different TTLL enzymes show preferences to the type of reaction they catalyze and if the substrate is α- or β-tubulin. Modified after Janke *et al.* (2008).

Because polyglutamylation occurs within the C-terminal tail of tubulin, which is the binding site for many microtubule-associated proteins (MAPs) and molecular motors, the consequences of polyglutamylation on MTs are diverse (Janke *et al.*, 2008). Differential binding preferences for MAPs could be identified *in vitro*, depending on the length of the glutamyl side chains present on MTs (Bonnet et al., 2001; Boucher *et al.*, 1994). Changes in the interaction of MTs with motor proteins induced by differences in polyglutamylation were first investigated in neurons from mutant mice that were lacking a subunit of TTLL1 (Ikegami *et al.*, 2007). Neurons from these mice showed decreased levels of polyglutamylation and altered KIF1A localization *in vivo*, whereas KIF3A and KIF5 seemed unaffected (Campbell *et al.*, 2002; Ikegami *et al.*, 2007). More detailed insights on the complex regulatory role of polyglutamylation were gained in a study that monitored KIF5-based transport upon induction of synaptic activity in hippocampal neurons (Maas *et al.*, 2009). Increased synaptic activity induced by application of the glycine receptor inhibitor strychnine led to an increase in polyglutamylation of tubulin accompanied by MAP2 accumulation on MTs. In parallel, KIF5-based transport – visualized by fluorescently-labelled gephyrin and KIF5 – into the cell periphery was impaired (Maas *et al.*, 2009). If KIF5-based transport was monitored with GFP-tagged GRIP1, however, transport into the periphery was unchanged (Maas *et al.*, 2009). These results suggested a functional connection between MT

modifications and adaptor proteins as regulators of specific transport. The fact that these changes in protein distribution were observed after synaptic activation emphasizes the possible role of polyglutamylation as a highly modular downstream regulator of intracellar transport processes.

1.2.4.3 The role of synaptic activity in transport regulation

Besides the multiple possibilities to regulate intracellular protein transport based on motor proteins, cargoes or microtubule networks, the ultimate decision on where a given cargo has to be transported is often dictated by external stimuli. In the same way that growth cones need protein supply according to their speed of progression, synapses have changing protein requirements depending on their presynaptic input. The mechanisms that regulate activity-dependend protein transport are so far poorly understood. Several studies investigated the local trafficking of neurotransmitter receptors at synapses in response to synaptic activation (Mao et al., 2010; Lin et al., 2010; Choquet, 2010), but little is known about the effects of synaptic activity on long distance protein transport. It is known however, that the long-lasting form of LTP (late LTP or L-LTP) requires the production and distribution of newly synthesized proteins (see Chapter 1.1.4, Citri & Malenka, 2008). One theory on how this distribution might work and on how synapses growing in strength can access the contents of transport vesicles to meet their increasing protein demands is termed synaptic tagging hypothesis. The hypothesis proposes that the products of protein biosynthesis are delivered throughout the cell, but are made available only to those synpases that have been "tagged" by synaptic activity (Martin & Kosik, 2002; Redondo & Morris, 2011). However, this assumption emphasizes the role of the synapse as a recepient of gene products, rather than the regulatory processes governing the transport and distribution, i.e. motor protein activity, motor-cargo interactions and spatial cues on microtubules.

1.3 AIM OF THIS STUDY

This study aimed at elucidating some of the underlying mechanisms governing intracellular protein transport upon induction of synaptic activation. A previous study had shown that an increase in synaptic activity caused by application of the GlyR antagonist strychnine led to changes in posttranslational modifications on tubulin and subsequent changes in targeted transport of gephyrin (Maas *et al.*, 2009). In the current study, it was to be determined if AMPA receptor activation would lead to similar modifications on MTs and if these modifications are decisive in conferring regulatory effects on the intracellular transport of the scaffold protein gephyrin.
Furthermore, additional aspects of AMPA receptor activation were to be investigated to unravel general mechanisms connecting synaptic activity to intracellular protein transport processes.

2 Materials and Methods

2.1 MATERIALS

2.1.1 Chemicals and enzymes

All chemicals used in this study were of the highest degree of purity (pro analysi, p.A.) and were purchased from the following suppliers unless stated otherwise:
Sigma (Taufkirchen, Germany), Carl Roth GmbH & Co. KG (Karlsruhe, Germany), Roche (Mannheim, Germany), AppliChem (Darmstadt, Germany), Life Technologies (Darmstadt, Germany), VWR (Darmstadt, Germany) and Merck (Darmstadt, Germany).
Enzymes were purchased from the following suppliers: Restriction endonucleases from Roche (Mannheim, Germany), Fermentas (St. Leon-Rot, Germany) and New England Biolabs (Frankfurt, Germany); Phusion High Fidelity DNA Polymerase from Thermo Fisher Scientific (Asheville, USA), T4 DNA Ligase from Fermentas (St. Leon-Rot, Germany) and rAPid Alkaline Phosphatase from Roche (Mannheim, Germany). The enzyme buffers used were those provided from the supplier.
Plasticware and disposable goods were obtained from one of the below suppliers:
Sarstedt (Nümbrecht, Germany), Carl Roth GmbH & Co. KG (Karlsruhe, Germany), Greiner (Frickenhausen, Germany) and Thermo Fisher Scientific (Asheville, USA).

2.1.2 Machines

2-Photon Microscope for Ca^{2+} imaging: Olympus Fluoview F1000 MPE (Olympus, Hamburg, Germany)
Agarose gel chambers: Owl Seperation Systems B2 and B1A (Thermo Fisher Scientific, Asheville, USA)
Bacterial culture incubator: Innova 3200 Platform Shaker (New Brunswick Scientific, Nürtingen, Germany)
Cell culture incubators: HeraCell 150/150i (Thermo Fisher Scientific, Asheville, USA)

Cell culture sterile hood: SterilGARD Class II TypA/B3 (Baker Company, Sanford, USA)
Centrifuge rotors: JA-10, JA-25.5 (Beckman Coulter, Krefeld, Germany)
Centrifuges: Ultracentrifuge L7 (Beckman Coulter, Krefeld, Germany), 5417 C (Eppendorf, Hamburg, Germany), MC6 Minifuge (Sarstedt, Nümbrecht, Germany)
Confocal Microscope: Olympus Fluoview F1000 (Olympus, Hamburg, Germany), Olympus Fluoview Software Version 2.1b (Olympus, Hamburg, Germany)
DNA gel imager: Intas Gel Imager (Intas, Göttingen, Germany)
Epifluorescent Microscope: Zeiss Axiovert 200M (Zeiss, Jena, Germany), Sony CCD-Camera 12. Monochrome w/o IR-18 (Diagnostic Instruments Inc., Sterlings Heights, USA), MetaVue Imaging Software (Visitron Systems, Puchheim, Germany)
Freezer (-20°C): G 3513 Comfort (Liebherr, Ochsenhausen, Germany)
Freezer (-80°C): MDF-U74V Ultra low termperature freezer (Sanyo, Osaka, Japan)
Laboratory scales: Sartorius LC-6201 (Sartorius, Göttingen, Germany), Mettler AE240 (Mettler-Toledo, Giessen, Germany)
Microtiter plate reader: Infinite 200 PRO NanoQuant (Tecan, Männedorf, Switzerland)
PCR machine: PTC-200 Peltier Thermal Cycler (MJ Research, Waltham, USA)
pH Meter: SevenEasy (Mettler-Toledo, Giessen, Germany)
Platform shaker: Promax 2020 (Heidolph Instruments, Kelheim, Germany), WS5 (Edmund Bühler GmbH, Hechingen, Germany)
Power supplies: Power Pac 200 (Bio-Rad, Munich, Germany)
Refridgerator: G 5216 Comfort (Liebherr, Ochsenhausen, Germany)
Rolling incubator: TRM5-V (IDL GmbH & Co. KG, Nidderau, Germany)
SDS-PAGE chambers: Mini-PROTEAN Tetra Electrophoresis System (Bio-Rad, Munich)
Semi dry blotter: V20 Semi-Dry Blotter (SCIE-PLAS, Cambridge, UK)
Sequencer: ABI Prism 377 DNA Sequencer (Applied Biosystems, Darmstadt, Germany)
Spectrophotometer: NanoQuant plate for Infinite 200 PRO NanoQuant (Tecan, Männedorf, Switzerland)
Thermo mixer: Thermomixer 5436 (Eppendorf, Hamburg, Germany)
Transmission Microscope: Zeiss Axiovert 25 (Zeiss, Jena, Germany)
Vortex: REAX 2000 (Heidolph Instruments, Kelheim, Germany)
Waterbath: GFL-1012 (GFL, Burgwedel, Germany)
Western blot chemiluminescence reader: Intas ChemoCam (Intas, Göttingen, Germany)

2.1.3 Media, buffers and solutions

Water used for the production of media, buffers and solutions water had been previously purifed by a Milli-Q-System (Millipore, Schwalbach/Ts, Germany) to the degree of "Aqua bidest." purity. Whenever needed, the pH of solutions was adjusted using NaOH, KOH or HCl. For sterilisation solutions were autoclaved at 121°C and 2.1 bar over a time period of 20 min. Alternatively, solutions were sterile filtered using filter tips with a pore size of 0.22 µm (Millipore, Schwalbach/Ts, Germany). Cell sulture media were purchased from Invitrogen (Darmstadt, Germany) or Lonza (Verviers, Belgium). Standard solutions were produced according to Sambrook *et al.* (1989) or according to the manufacturer's instructions.

Blocking buffer: (Immunodetection)	5% (w/v) milk powder in 1x TBST
Blocking buffer: (Immunocytochemistry)	1% (w/v) bovine serum albumin (BSA) in 1x PBS
DNA loading buffer (6x): (Agarose gelelectrophoresis)	7.5 g Ficoll 0.125 g bromophenol blue ad 50 ml H_2O storage of aliquots at -20°C
Glycerol: (Bacterial stocks)	50% (v/v) glycerol in H_2O
HBS (2x): (Transfection)	1.6 g NaCl 0.074 g KCl 0.027 g Na_2HPO_4 0.2 dextrose 1 g HEPES ad 100 ml H_2O pH 7.05 (NaOH) sterile filter storage of aliquots at -20°C
HEK293-Medium: (Cell culture)	500 ml D-MEM (+ 4500 mg/L glucose, + GlutaMAX™ I, - pyruvate) 5 ml penicillin/streptomycin solution (10,000 U/ml) 50 ml FBS

HEPES buffer: (Transfection)	10 mM HEPES (pH 7.4) 135 mM NaCl 5 mM KCl 2 mM $CaCl_2$ 2 mM $MgCl_2$ 5 mM glucose
LB Agar: (Growth medium bacteria)	LB medium 1.5% (w/v) agar autoclave, cool down to 50°C Antibiotic supplementation: ampicillin (100 µg/ml), kanamycin (50 µg/ml)
LB Medium: (Growth medium bacteria)	10 g tryptone 5 g yeast extract 5 g NaCl ad 1000 ml H_2O pH 7.5 (NaOH) autoclave
Mini Prep Solution I: (DNA isolation)	50 mM D-glucose 20 mM Tris HCl (pH 8.0) 2.5 mM EDTA (pH 8.0)
Mini Prep Solution II: (DNA isolation)	1% (w/v) SDS 0.2 M NaOH
Mini Prep Solution III: (DNA isolation)	67.4 ml 5 M potassium acetate 12.95 ml 100% acetic acid ad 100 ml H_2O
Neurobasal medium: (Cell culture)	500 ml Neurobasal (A) 2 mM L-Glutamin 25 µg/ml Pyruvat 5 ml penicillin/streptomycin solution (10,000 U/ml) 2% (v/v) B27
Paraformaldehyde solution: (Immunocytochemistry)	40 g paraformaldehyde 40 g saccharose ad 1,000 ml 1x PBS pH 7.2 (NaOH) storage of aliquots at -20°C

PBS (10x): (Immunocytochemistry)	2 g KCl 2.4 g KH_2PO_4 14.4 g Na_2HPO_4 80 g NaCl pH 7.4 (NaOH or HCl) ad 1,000 ml H_2O autoclave
Phosphate buffer: (competent cells)	170 mM KH_2PO_4 720 mM K_2HPO_4 sterilization by autoclaving
Recording medium: (Ca^{2+} imaging)	129 mM NaCl 5 mM KCl 25 mM HEPES 1 mM $MgCl_2$ 2 mM $CaCl_2$ 30 mM glucose adjust to pH 7.3
SDS running buffer (10x): (Western blot)	250 mM Tris 2.5 M glycine 1% (w/v) SDS pH 8.3 (HCl)
SDS sample buffer (5x): (Western blot)	400 mM Tris (pH 6.8) 500 mM DTT 50% (v/v) glycerol 10% (w/v) SDS 0.8% (w/v) bromophenol blue
SOB buffer: (Competent cells)	2% (w/v) bacto tryptone 0.5% (w/v) yeast extract 10 mM NaCl 2.5 mM KCl 10 mM $MgCl_2$ 10 mM $MgSO_4$ pH 6.7 (KOH)
TAE (50x): (Agarose gelelectrophoresis)	242 g Tris 57.1 ml acetic acid 100 ml 0.5 M EDTA (pH 8.0) ad 1,000 ml H_2O

TBjap medium: (Competent cells)	10 mM PIPES 250 mM KCl pH 6.7 (KOH) 55 mM $MnCl_2$ 15 mM $CaCl_2$
TBST (10x): (Immunodetection)	100 mM Tris (pH 8.0) 1,5 M NaCl 0.5% (v/v) Triton-X-100
Transfer buffer (10x): (Western blot)	390 mM glycine 480 mM Tris-HCl 0.37% (w/v) SDS 20% methanol (added freshly) ad 1,000 ml H_2O

2.1.4 Animals, cell lines and bacterial strains

Mice: Mus muculus, C57Bl6/J (Central animal facility, University Hamburg Medical School (UKE), Hamburg)

HEK293: human embryonic kidney cells, ATCC CRL-1537 (ATTC, Manassas, USA)

E. coli: XL1-*blue*, *supE44 hsdR17 recA1 endA1 gyrA96 thi-1 relA1* lac [F' *proAB lacI*q*ZΔM15* Tn*10*(Tet_r)]
(Stratagene/Agilent Technologies, Santa Clara, USA)

2.1.5 Kits

- HiSpeed Plasmid Maxi/Midi Kit (Qiagen, Hilden)
- EndoFree Plasmid Maxi/Midi Kit (Qiagen, Hilden)
- Agarose Gel DNA Extraction Kit (Roche, Mannheim)
- Pierce BCA™ Protein Assay Kit (Thermo Fisher Scientific, Asheville, USA)
- Immobilon™ Western Chemiluminescent HRP Substrate (Millipore, Schwalbach/Ts)

2.1.6 Antibodies

Primary Antibodies

Antibody	*Host species*	*Mode of application*	*Origin*
β-Actin (Phalloidin Atto-488)	-	1:500 (ICC)	Sigma Aldrich (Buchs, Switzerland)
F-Actin	Rabbit	1:5,000 (WB)	Sigma Aldrich (Buchs, Switzerland)
Ankyrin G	Rabbit	1:300 (ICC)	Santa Cruz Biotechnology (Dallas, USA)
CaMKII	Rabbit	1:1,000 (WB)	Life Technologies (Darmstadt)
CaMKII (phosphorylated, Thr 286)	Rabbit	1:1,000 (WB)	Cell Signaling Technology (Danvers, USA)
Early Endosome Antigen 1	Mouse (Clone 14)	1:100 (ICC)	BD Biosciences (San José, USA)
$GABA_A$ Receptor γ_2	Goat	1:100 (ICC)	Abcam (Cambridge, UK)
Glycine Receptor	Mouse (mAb2b)	1:100 (ICC)	Synaptic Systems (Göttingen, Germany)
Golgi Apparatus	Mouse (Clone 35/GM130)	1:100 (ICC)	BD Biosciences (San José, USA)
Neuroligin-2	Mouse	1:200 (ICC)	Synaptic Systems (Göttingen, Germany)
Neuron Specific Enolase	Chicken	1:5,000 (WB)	Novus Biologicals (Littleton, USA)
Polyglutamylated Tubulin	Mouse (Clone GT335)	1:20,000 (ICC) 1:4,000 (WB)	Adipogen (Liestal, Switzerland)
Tyrosinated Tubulin	Mouse (Clone TUB-1A2)	1:4,000 (WB)	Sigma Aldrich (Buchs, Switzerland)

Table 2.1: Primary antibodies used in the current study
ICC = Immunocytochemistry, WB = Western blot

Secondary Antibodies

Antibody	*Host species*	*Mode of application*	*Origin*
α-mouse Alexa 488-conjugated	Donkey	1:500 (ICC)	Dianova (Hamburg, Germany)
α-rabbit Cy5-conjugated	Donkey	1:500 (ICC)	Dianova (Hamburg, Germany)
α-goat Alexa 488-conjugated	Donkey	1:500 (ICC)	Dianova (Hamburg, Germany)
α-chicken HRP-conjugated	Donkey	1:2,500 (WB)	Thermo Fisher Scientific (Asheville, USA)
α-mouse HRP-conjugated	Goat	1:10,000 (WB)	Dianova (Hamburg, Germany)
α-rabbit HRP-conjugated	Goat	1:10,000 (WB)	Dianova (Hamburg, Germany)

Table 2.2: Secondary antibodies used in the current study
ICC = Immunocytochemistry, WB = Western blot

2.1.7 Vectors and constructs

Name	*Preparation/Origin*	*Application*
ptdtomato-C1	Clonetech (Saint-Germain-en-Laye, France)	Expression of C-terminally-tagged double-tandem tomato fusion proteins in eukaryotic cells
pEGFP-C1	Clonetech (Saint-Germain-en-Laye, France)	Expression of EGFP in eukaryotic cells
ptdtomato-gephyrin	PCR using *LR Geph Hin s* and *LR Geph Sal as* from mRFP-gephyrin (C. Maas, ZMNH, Hamburg), restriction and ligation into ptdtomato-C1 (*Hin*dIII/*Bam*H1)	Expression of tomato-labelled gephyrin in eukaryotic cells
pEGFP-TTLL6	C. Janke, Orsay-Cedex, France	Expression of EGFP-labelled TTLL6 in eukaryotic cells
pEGFP-TTLL6 mut	C. Janke, Orsay-Cedex, France	Expression of EGFP-labelled TTLL6 mut in eukaryotic cells
pYFP-TTLL4	C. Janke, Orsay-Cedex, France	Expression of YFP-labelled TTLL4 in eukaryotic cells
pYFP-TTLL4 mut	C. Janke, Orsay-Cedex, France	Expression of YFP-labelled TTLL4 mut in eukaryotic cells
pEGFP-Dynamitin	R. Vallee, Columbia University, USA (Palazzo *et al.*, 2001)	Expression of EGFP-labelled dynamitin in eukaryotic cells
pEGFP-PSD95	M. Kneussel, ZMNH, Hamburg	Expression of EGFP-labelled PSD95 in eukaryotic cells

Table 2.3: Vectors and constructs used in the current study

2.1.8 Oligonucleotides

Name	*Purpose*	*Sequence (5' – 3')*
LR Geph Hin s	Amplification of gephyrin ORF from pmRFP-gephyrin (C. Maas, ZMNH, Hamburg) with PCR	CACGAAAGCTTAC**ATG**GCGACCG
LR Geph Sal as	Amplification of gephyrin ORF from pmRFP-gephyrin (C. Maas, ZMNH, Hamburg) with PCR	TGTTGTCGACCATCATAGCCGTC
LR Geph Seq 0as	Sequencing of ptdtomato-gephyrin	CTATCACTCACTGTGAGGAC
LR Geph Seq 1as	Sequencing of ptdtomato-gephyrin	CTCTGGAGTGACATCTCGT
LR Geph Seq 2as	Sequencing of ptdtomato-gephyrin	CTTCAAGTTCATCATGCACC
LR Geph Seq 3as	Sequencing of ptdtomato-gephyrin	CCCATTCCATCTCGGTAA
LR Geph Seq 5as	Sequencing of ptdtomato-gephyrin	CCAAGTCAGTATACACCG
CM Geph Seq 2s	Sequencing of ptdtomato-gephyrin	CTAAGAGCCAGTCACAG
CM Geph Seq 3s	Sequencing of ptdtomato-gephyrin	GGGGAGTGTGTTTTGGC
CM Geph Seq 4s	Sequencing of ptdtomato-gephyrin	CCTGCAACCTCTTTGTTG
CM Geph Seq 6as	Sequencing of ptdtomato-gephyrin	CCTGTTGACATAACGGCAAC

Table 2.3: Oligonucleotides used in the current study
Oligonucleotides were used for amplification or sequencing of DNA. Start-codons within the displayed sequences are indicated in bold letters. s = sense, as = antisense, ORF = open reading frame.

2.2 METHODS

2.2.1 Molecular biology

2.2.1.1 Polymerase chain-reaction (PCR)

The PCR is an *in vitro* method to synthesize and amplify DNA sequences, which was originally established by Saiki *et al*. (1988). The method involves the cyclic repetition of 3 major steps: (1) the separation of DNA double-strands (template DNA) by thermal denaturation at 95°C, (2) cooling of the single stranded DNA fragments to 52 - 69°C for annealing of oligonucleotide primers and (3) enzymatic DNA synthesis of the sequences adjacent to the oligonucleotide primers according to the template DNA at 72°C. For DNA synthesis, specifically heat-resistant DNA polymerases are used to allow DNA elongation at elevated temperatures in an automated fashion. In this study, *Phusion High Fidelity DNA Polymerase* (Finnzymes, Thermo Scientific, Asheville, USA) was used for DNA amplification. After 30 - 35 cycles, the amount of DNA increases exponentially so that after n cycles 2^n copies of the template DNA are present. A representative PCR reaction mix contained ~50 ng plasmid-DNA or 100 ng cDNA library, 20% 5x PCR-buffer (*Phusion GC buffer*, Finnzymes, Thermo Scientific, Asheville, USA), 400 nM forward and reverse primer, 200 µM dNTPs and 2 U *Phusion* polymerase in a total volume of 50 µl. Usually, 30 cycles of the 3 steps described above were performed in a *PTC-200 Thermal Cycler* (MJ Research, Waltham, USA). After completion of all cycles the samples were cooled to 4°C and were ready for further use.

2.2.1.2 Agarose gel electrophoresis

DNA molecules can be electrophoretically separated in agarose gels. Due to their steady ribose-phosphate-backbone DNA fragments exhibit an evenly distributed negative charge relative to their size (Takahashi *et al.*, 1969). Since agarose gels form equally sized pores, DNA fragments can be separated according to their size once an electric potential is applied. Smaller fragments migrate faster than large fragments since they can penetrate the gel more easily. For the production of gels, 1 - 2% (w/v) agarose (Eurogentech, Cologne, Germany) was solubilized in TAE-buffer by heating.

After the solution had cooled down, 0.5 µg/ml *Roti safe* (Carl Roth, Karlsruhe, Germany) was added. The solution was poured into a cast containing combs to form loading pockets. After polymerization, the gel was put into an electrophoresis chamber and covered with TAE-buffer. DNA samples were loaded onto the gel in individual pockets after being mixed with 6x *DNA* loading buffer. A current of 90 - 120 V was applied for approximately 45 min. The *Roti safe* contained in the gel interferes with the DNA molecules and excitation with UV light causes a strong fluorescence. The fluorescence was made visible by an *Intas Gel Imager* (Intas, Göttingen, Germany), which provided a camera for photographic documentation. A marker (*Hyperladder I*, Bioline, Luckenwalde, Germany) containing DNA fragments of known size and concentration was run along with the samples on the gel, so the size of DNA fragments of interest could be determined.

2.2.1.3 Restriction of DNA with restriction enzymes

Restriction endonucleases are enzymes capable of recognizing and cleaving specific duplex DNA sequences. In this study, DNA restriction was performed with class II restriction endonucleases according to the manufacturer's manual. For cloning purposes 1 µg of DNA was mixed with 4 µl 10x *Fermentas FastDigest buffer* (Fermentas, St. Leon-Rot, Germany) and diluted in H_2O to a total volume of 40 µl. 1 U of the respective enzymes was added to the reaction. Restriction with *FastDigest* enzymes (Fermentas, St. Leao-Rot, Germany) was performed in 15 - 30 min at 37°C. After incubation, samples were directly used for dephosphorylation reactions (Chapter 2.2.1.4).

2.2.1.4 Dephosphorylation of DNA fragments

To prevent restricted DNA fragments from re-ligating, the 5'-phosphate groups were removed by enzymatic reaction. In a total volume of 50 µl, 5 µl *rAPid Alkaline 10x buffer* (Roche, Mannheim, Germany) was mixed with 4 µl H_2O and 1 µl *rAPid Alkaline Phosphatase* (Roche, Mannheim, Germany) while 40 µl sample were used directly from the previous restriction reaction (Chapter 2.2.1.3). The sample was incubated for 10 min at 37°C and then loaded onto an agarose gel for band seperation (Chapter 2.2.1.2) and subsequent purification (Chapter 2.2.1.5).

2.2.1.5 Purification of DNA fragments

DNA fragments obtained from restriction or dephosphorylation reactions were applied to agarose gels for seperation of cleaved fragments by size (Chapter 2.2.1.2). Fragments of interest were removed from the gel by excision with a scalpel and purified with the *Agarose Gel DNA Extraction Kit* (Roche, Mannheim, Germany) according to the manufacturer's manual. Isolated DNA was eluted in 30 µl H_2O.
PCR fragments were purified by precipitation with alcohol. To a 50 µl PCR reaction sample, 500 µl isopropanol were added and mixed thoroughly. The sample was centrifuged at approximately 14,000 x g for 20 min at 4°C. The supernatant was discarded and replaced by 300 µl 70% ethanol, followed by an additional centrifugation step at 14,000 x g for 5 min. Again, the supernatant was removed and the DNA-containing pellet dried for approximately 15 min at RT. The DNA was dissolved in 50 µl H_2O for further uses.

2.2.1.6 Determination of DNA concentration

Concentration and purity of isolated DNA was determined photometrically. 2 µl sample were used for analysis with the NanoQuant plate of the *Infinite 200 PRO NanoQuant microplate reader* from Tecan (Männedorf, Switzerland).

2.2.1.7 Ligation of DNA fragments

T4 DNA ligase catalyses the synthesis of phosphodiester bonds between adjacent 5'-phosphoryl and 3'-hydroxyl groups in duplex DNA in an ATP-dependent manner (Lehman, 1974). In this study, T4 DNA ligase from the *Rapid DNA Ligation Kit* (Fermentas, St. Leon-Rot, Germany) was used to ligate DNA fragments into expression vectors. In 20 µl total volume 50 ng of vector DNA were mixed with a 3- to 5-fold molar excess of insert and 2 µl 10x *T4 quick ligase buffer* (Fermentas, St. Leon-Rot, Germany) was added as well as 1 U *T4 ligase*. This mix was incubated at room temperature for 1 hour and subsequently used for transformation of chemically competent *E. coli* XL1-*blue* (Chapter 2.2.1.11).

2.2.1.8 Production of chemically competent bacteria

Chemically competent bacterial cells were produced according to Inoue *et al*. (1990). A 3 ml pre-culture of the *E. coli* strain XL-1 *blue* was inoculated in TB medium and grown at 37°C over night. The pre-culture was used to inoculate 1,000 ml TB medium and the culture was grown at 18°C until an OD_{600} of 0.6 was reached (approximately 24 - 40 hours). At that point, the culture was incubated on ice for 10 min, followed by centrifugation at 4°C for 10 min at 3,000 rpm in the JA-10 rotor from Beckmann Coulter (Krefeld, Germany). The pellet was resuspended in 380 ml cold TBjap medium containing 2% (v/v) DMSO and again incubated on ice for 10 min. The suspension was centrifuged as before and the resulting bacterial pellet was resuspended in 74.4 ml cold TBjap without DMSO. 5.6 ml DMSO were added subsequently and the readily competent cells were aliquoted and shock-frozen in liquid nitrogen. Competent cells were stored at -80°C.

2.2.1.9 Cloning of DNA expression constructs

For cloning of fluorescently-labelled expression constructs, a PCR was performed to amplify the gene of interest from a cDNA library or from an existing template construct (see Chapter 2.2.1.1). The primers used for amplification contained endonuclease restriction sites at their ends for subsequent digestion and targeted insertion into an expression vector. The PCR sample was purified by precipitation with alcohol (Chapter 2.2.1.5) and digested with the same restriction enzymes as the target vector (Chapter 2.2.1.3). The vector was dephosphorylated to prevent re-ligation (Chapter 2.2.1.4), the two fragments (PCR product and vector backbone) were purified by gel extraction and the DNA concentration was quantified (Chapters 2.2.1.5 and 2.2.1.6). As a next step, both fragments were ligated and immediately used for transformation of chemically competent *E. coli* XL-1 *blue* (Chapters 2.2.1.7 and 2.2.1.11). Antibiotic-resistant clones were picked and plasmid DNA was extracted (Chapter 2.2.1.12). An analytical restriction reaction was performed to identify plasmids containing an insert of correct size, and positive candidates were sequenced at the sequencing core facility of the ZMNH (Chapter 2.2.1.13).

2.2.1.10 Transformation of chemically competent bacteria

Transformation of chemically competent *E. coli* XL1-*blue* cells (Chapter 2.2.1.8) with plasmid DNA was performed according to a protocol modified after Inoue *et al.* (1990). 100 µl of chemically competent cells per transformation reaction were thawed on ice. 50 - 100 ng plasmid DNA or 20 µl ligation sample were added and incubation on ice continued for another 20 min. A heat shock was performed in a 42°C warm water bath for 45 sec followed by a 2 min incubation on ice after which 800 µl of pre-warmed SOC medium were added. The sample was incubated shaking at 37°C for 45 min and afterwards plated on LB agar plates containing antibiotics for selection. For bacterial cells to grow, agar plates were incubated at 37°C over night.

2.2.1.11 Isolation of plasmid DNA from bacteria

Isolation of plasmid DNA from small volumes of bacterial cultures for analytical purposes was performed following a procedure introduced by Birnboim and Doly (1979). 2 ml bacterial culture were centrifuged in a 5417C centrifuge (Eppendorf, Hamburg, Germany) at maximal speed for 1 min to obtain a bacterial pellet. After decantation of the supernatant, the bacterial pellet was resuspended in 200 µl *Mini Prep Solution I* and 1 µl of *RNase A* was added. Next, 200 µl *Mini Prep Solution II* was added and the sample was mixed by gently inverting the reaction tube several times before incubation on ice for 5 min. The lysis reaction was stopped by addition of 200 µl *Mini Prep Solution III*, subsequent mixing and incubation on ice for 10 min. Afterwards, a 10 min centrifugation step at maximal speed was applied and the resulting supernant was used for DNA precipitation with alcohol (Chapter 2.2.1.5) using 100% isopropanol and 70% ethanol. The DNA pellet was air-dried at RT and resuspended in 50 µl H_20.
Isolation of larger quantities of plasmid DNA was performed with the help of DNA preparation kits from Qiagen (Hilden, Germany) (Chapter 2.1.5).

2.2.1.12 Sequencing of DNA

Sequencing of DNA was performed using the chain-terminating method (Sanger *et al.*, 1977), which involves the incorporation of fluorescently-labelled didesoxynucleotides. All sequencing reactions were performed by a core facility unit of the ZMNH that is

supervised by PD Dr. Sabine Hoffmeister-Ullerich. Each individual sample contained between 0.5 µg and 1 µg DNA and 10 pmol primer. Samples were analyzed with an *ABI Prism 377 DNA Sequencer* (Applied Biosystems, Darmstadt, Germany) and sequences were analyzed using the software *DNA Strider 1.4f1* (CEA, Gif-sur-Yvette Cedex, France).

2.2.2 Protein biochemistry

2.2.2.1 SDS-polyacrylamide gel electrophoresis (SDS-PAGE)

SDS-polyacrylamide gel electrophoresis is a method used to separate proteins according to their size. Proteins that are to be separated are treated with sodium dodecyl sulfate (SDS), which introduces a surplus of negative charge. Disulfide bonds in proteins are denatured with dithiothreitol or β-mercaptoethanol so that migration within the gel is solely dependent on protein size. Polyacrylamide gels were produced according to Sambrook *et al.* (1989). For this study stacking gels containing 5 % acrylamide (Carl Roth, Karlsruhe, Germany) and resolving gels containing 15% acrylamide were used since they were most suitable for the separation of the proteins of interest. Before protein samples were loaded onto gels they were diluted with 4x SDS loading buffer and heated to 95°C for 10 minutes. Gels were fixed in an electrophoresis chamber (Bio Rad, Munich, Germany) and covered with running buffer. 120 V per gel were applied for approximately 90 minutes until sufficient separation of the marker bands of known size (*Presicion Plus Protein Dual Color Standard*, Bio-Rad, Munich, Germany) was achieved. Polyacrylamide gels were subsequently used for the transfer of seperated proteins onto PVDF membrane for western blot analysis (Chapter 2.2.2.2).

2.2.2.2 Western blotting

The western blot method allows the transfer of proteins from polyacrylamide gels (Chapter 2.2.2.1) onto carrier-membranes by electrophoresis. For semi-dry western blot, a methanol-activated PVDF (polyvinyldifluoride)-membrane (Amersham, GE

Healthcare, Freiburg, Germany) and the acrylamide gel were stacked between two Whatman papers (Whatman, GE Healthcare, Freiburg, Germany) which were soaked in blotting buffer. Together, these components were put directly between two electrodes with the PVDF-membrane facing the anode. Protein transfer was performed at RT for 2 hours at 2 mA/cm^2 in a V20 Semi-Dry Blotter (SCIE-PLAS, Cambridge, UK).

2.2.2.3 Immunodetection of immobilized proteins

Proteins immobilized on PVDF-membranes (Chapter 2.2.2.2) can be specifically detected with the use of primary antibodies and horse raddish peroxidase (HRP)-coupled secondary antibodies. Previous to antibody application, the PVDF-membrane was reduced in its protein binding capacity by incubation in blocking buffer, thereby enhancing the specificity of antibody binding. Incubation with primary antibody diluted in 5% milk powder/TBS/0.05% Tween (w/v/v) was either performed over night shaking at 4°C or for 2 hours at RT. Afterwards, excess primary antibody was removed by four washing steps for 15 min with TBS/0.05% Tween (TBST). The secondary HRP-coupled antibody was then applied for 45 min at RT in 5% milk powder/TBST (w/v). Again, the PVDF-membrane was washed four times for 15 min in TBST and afterwards sparsely covered with *ImmobilonWestern HRP substrate* (Millipore, Schwalbach/Ts, Germany). The peroxidase coupled to the secondary antibody catalyses the oxidation of luminol in the substrate, which leads to the emission of light. For documentation of emitted signals, the camera system *Intas ChemoCam* (Intas, Göttingen, Germany) was used.

2.2.3 Cell biology

2.2.3.1 Cultivation of HEK293 cells

Human embryonic kidney (HEK293) cells were cultivated in HEK medium and passaged every 2 to 3 days by splitting the culture 1:4 to 1:8. For that purpose, cells were rinsed with PBS once and incubated with 1 ml 0.05% trypsine-EDTA solution (Life Technologies, Darmstadt, Germany) for 2 minutes at 37°C. Trypsination caused the

cells to dissociate from each other and the cell culture dish, and was then stopped by the addition of serum-containing D-MEM. Cells were further dissociated by pipetting up and down and aliquots of the cell suspension were distributed into fresh culture dishes and complemented with pre-warmed HEK medium. Cells were kept at 37°C and 5% CO_2.

2.2.3.2 Preparation and cultivation of primary hippocampal neurons

One day prior to the preparation of hippocampal neurons, 12 mm sterile glass coverslips (Roth) were placed into 24-well plates (Sarstedt, Nümbrecht, Germany). Coverslips were coated with 50 µg/ml poly-D-lysine (Sigma, Taufkirchen, Germany) and incubated at 37°C over night. The following day, the coverslips were washed twice with sterile H_2O and 1 ml Neurobasal medium was added to each well. The 24-well plates were then placed at 37°C to pre-heat the medium before cells were plated. Primary hippocampal neurons were obtained from neonatal mice (P0) or from mouse embryos (E16). In both cases, the animals were decapitated and the hippocampus was seperated from other brain structures in ice-cold PBS/10 mM glucose. For dissociation of the tissue, PBS/10 mM glucose was removed and replaced by 5 ml HBSS (Invitrogen, Darmstadt, Germany) containing 0.5 ml trypsine (Invitrogen, Darmstadt, Germany; 2.5% for P0 animals, 0.05% for E16) and incubated at 37°C for 10 min. Afterwards, cells were washed once with DMEM-F12 resuspended in 2 ml HBSS and dissociated by gently pipetting cells up and down through three fire-polished pasteur pipettes with decreasing opening diameter. Dissociated cells were counted in a Neubauer counting chamber and plated at a density of 110,000 (P0) to 60,000 (E16) cells per well and cultivated at 37°C and 5% CO_2. After 5 to 7 days, 1 ml of Neurobasal medium (-glucose) containing 3 µM 1-β-D-arabinofuranosyl cytosine (AraC) was added to each well to stop astrocyte proliferation.

2.2.3.3 Cell lysis for protein biochemistry

To harvest cultured HEK293, N2A (Chapter *2.2.3.1*) or neuronal cells (Chapter *2.2.3.2*) from culture dishes, a PBS-based lysis buffer containing 1% Triton-X100, protease inhibitor (cOmplete, Roche, Mannheim, Germany) and 1 mM PMSF was freshly prepared and pre-cooled to 4°C. Culture medium was removed and the cells were

rinsed once with ice-cold PBS, before the dishes were transferred onto ice. PBS was replaced by lysis buffer (300 µl for 3.5 cm dishes, 150 µl for 12 mm coverslips) and the cells were harvested mechanically with a cell scraper and transferred to 1.5 ml reaction tubes (Sarstedt, Nümbrecht, Germany). To complete lysis of cell membranes, samples were incubated on ice for 45 min before centrifugation at 1,000 x g and 4°C for 10 min. After centrifugation the supernatant was transferred into fresh reaction tubes and shock frozen in liquid nitrogen. Small aliquots were retained to determine the total protein concentration using the *BCA Protein Assay Kit* (Pierce Biotechnology, Thermo Scientific, Asheville, USA), while samples were stored at -80°C.

2.2.3.4 Transfection of HEK293 cells and primary hippocampal neurons

Transfection of mammalian cells was performed according to the calcium phosphate transfection method (Chen & Okayama, 1987; Kingston *et al.*, 1996). In HEK293 cells transfection as performed when cultures had reached approximately 50% confluency. For transfection of 3.5 cm dishes, 4 µg plasmid DNA were mixed with 12.5 µl 1 M $CaCl_2$ and diluted with H_2O to a total volume of 50 µl. Also, a seperate reaction tube containing 50 µl 2x HBS buffer was prepared. The contents of both tubes were mixed slowly under constant agitation on a vortex mixer. The resulting transfection solution was incubated for 15 min at RT before being added to the cell culture medium dropwise. Cells were placed at 37°C and 5% CO_2 for 24 - 48 hours. Expression of fluorescently-labelled proteins was confirmed visually with a Zeiss Axiovert 200M epifluorescence microscope (Zeiss, Jena, Germany).

For primary neurons a few variations had to be added to the above protocol for transfection with DNA. Transfection was performed between DIV 10 and DIV 12. A transfection mix was set up containing 2 µg DNA, 6.25 µl 1 M $CaCl_2$ and H_2O to a volume of 25 µl. This solution was slowly mixed with 25 µl 2x HBS under constant agitation on a vortex mixer and subsequently incubated at RT for 15 min. Meanwhile, culture medium was removed from the cell culture well that was to be transfected until approximately 400 µl remained on the cells. The calcium phosphate solution was slowly added to the remaining medium and cells were incubated at 37°C and 5% CO_2 for 45 min. Afterwards, the medium containing the transfection solution was removed and the cells were rinsed twice with pre-warmed HEPES buffer before 1 ml of the

previously removed conditioned medium was added to the cells. Expression of plasmid DNA lasted between 8 and 48 hours. In case of double transfections, 1 µg of each plasmid DNA was used.

2.2.3.5 Immunocytochemistry

For immunostainings neurons cultured on 12 mm coverslips were carefully rinsed with PBS once, before application of paraformaldehyde (PFA) solution. PFA fixation lasted for 12 min before being washed off thoroughly 3x with PBS. Next, a solution of 5% (v/v) donkey serum (Sigma, Taufkirchen) in PBS containing 0,25% (v/v) Triton-X100 was applied to the cells for 20 min in order to permeabilize the cell membrane and block unspecific binding sites. Cells were briefly rinsed with PBS afterwards before primary antibodies were applied in PBS containing 1% (w/v) bovine serum albumine (BSA). Incubation with primary antibodies lasted either 2 hours at RT or over night at 4°C. As a next step, primary antibodies were washed off in 5 washing steps with PBS before secondary antibodies were applied in PBS/1% (w/v) BSA. Secondary antibody treatment lasted 45 min at RT, followed by 5 washing steps with PBS. Coverslips were mounted on glass slides with AquaPoly/Mount (Polysciences, Eppelheim, Germany) and left to dry in the dark at RT for approximately 18 hours. Excess AquaPoly/Mount was removed with 70% ethanol when preparing the slides for microscopy. Epifluorescent or confocal laser scanning microscopy was performed as stated in Chapters 2.2.4.1 and 2.2.4.2.

2.2.3.6 Live cell surface stainings

For live cell surface stainings cultured hippocampal neurons were rinsed with ice-cold PBS once, to halt cellular endocytic processes. Afterwards, antibody was applied in ice-cold HEPES buffer and cells were incubated at 4°C for 20 min. The neurons were then rinsed once more with ice-cold PBS followed by fixation with PFA solution, permeabilization and further immunostanings as stated in Chapter 2.2.3.5.

2.2.3.7 Pharmacological treatment of cultured hippocampal neurons

For stimulation experiments of primary hippocampal neurons cultured on 12 mm coverslips, the culture medium except 600 µl was removed. 400 µl conditioned culture medium were mixed with the stimulation agent. For AMPA receptor activation, 2 µl of a 10 mM stock of AMPA solved in H_2O were added to the 400 µl conditioned medium, mixed thoroughly and returned to the remaining culture medium (f.c. = 20 µM). Stimulation continued for 6 hours at 37°C and 5% CO_2 before the cells were either fixed in PFA solution or the entire medium was replaced with fresh *Neurobasal medium* for recovery experiments. Control samples were stimulated with 10 µM (f.c.) DNQX (1 µl from 10 mM stock in DMSO) or 2 µl H_2O/1 µl DMSO respectively and treated equally.

For kinase inhibitor experiments, the procedure was similar in that all compounds were mixed with 400 µl conditioned medium before administration to the cells in a total volume of 1 ml. All kinase inhibitors except for lithium chloride were solved in DMSO. For each experiment, four 12 mm coverslips with cultured neurons were transfected with ptdtomato-gephyrin (Chapter 2.2.3.4) and each sample was treated as follows:

(1) control samples were treated with 2 µl H_2O (as a control for AMPA application) and DMSO in a volume respective to the volume of kinase inhibitor applied.

(2) kinase inhibitors were applied as follows: 20 µM f.c. GF109203X (Tocris, Bristol, UK) for inhibition of PKC; 2 µM (f.c.) KN62 (Tocris, Bristol, UK) for inhibition of CaMKII; 10 µM (f.c.) UO126 (Sigma, Taufkirchen, Germany) for MAPK blockade; 2 mM (f.c.) lithium chloride (Sigma, Taufkirchen, Germany) for blockade of GSK3β and 5 µM (f.c.) GSK-IX (Merck, Darmstadt, Germany) for GSK3β blockade.

(3) AMPA was applied at 20 µM (f.c.).

(4) 20 µM (f.c.) AMPA were applied together with a respective volume of kinase inhibitor as listed under (2).

Treatment of cells lasted for 6 hours before cells were fixed in PFA solution (Chapter 2.2.3.5).

2.2.4 Imaging

2.2.4.1 Epifluorescent microscopy

To determine the distribution of fluorescently-labelled protein clusters throughout the cell, fixed neurons (Chapter 2.2.3.5) were imaged with epifluorescent microscopy at a Zeiss Axiovert 200M (Zeiss, Jena, Germany) using MetaVue 6.2r6 software (Molecular Devices, Munich, Germany). A 40 x objective (N/A 0.8) was used to aquire two images of each cell, one with an exposure time of 500 ms to visualize protein clusters in the cell soma and one with an exposure time of 2,000 ms to capture small clusters in the cell periphery.

2.2.4.2 Confocal laser scanning microscopy

Confocal laser scanning microscopy was performed with an Olympus Fluoview FV1000 (Olympus, Hamburg, Germany) using the Olympus Fluoview software (Version 2.1b). A 60 x objective (N/A 1.35) was used. The pinhole was set at 120 µm and sequential line scans were performed. Laser power and computational gain were adjusted depending on the intensity of the fluorescent signals, but kept constant within one group of experiments.

2.2.4.3 Ca^{2+} imaging with epifluorescent microscopy

Imaging changes in intracellular calcium concentrations was performed on cultured hippocampal neurons at DIV12 - DIV14. Culture medium was removed from cells and replaced by fresh neurobasal medium (-glucose, Invitrogen) containing 0.5 mM FURA-2 calcium indicator previously dissolved in DMSO. After 20 minutes incubation of the cells with calcium indicator at 37°C, all medium was removed and the coverslip was transferred into a dish containing 1.5 ml pre-warmed ACSF for Ca^{2+} imaging.
Imaging was performed using an Olympus Fluoview FV1000 MPE (Olympus, Hamburg) and the imaging software Olympus *xcellence* (Version 1.1, Olympus soft imaging solutions GmbH, Munich). The objective was placed in an upright position and a 60 x (N/A 1) water objective was used for images aquisition. During recording the

microscope stage was heated to 37°C, but no perfusion with medium was applied. Three to five cells from the same field of view were chosen to be monitored at the same time, and regions of interest (ROIs) were drawn into the cell somata. Image aquisition was started with alternating excitation at 340 and 380 nm. FURA-2 that is not bound to Ca^{2+} ions emits light after excitation at 340 nm, while FURA-2 in complex with Ca^{2+} is excited by light with a wavelength of 380 nm. By aquisition of emitted signals after alternated excitation, free FURA-2 is visualized as well as Ca^{2+}-bound FURA-2. The ratio of emission after 340/380 nm excitation is determined instantaneously, reflecting changes in calcium levels within each cell.

After approximately 4 minutes of recording baseline Ca^{2+} levels, 500 ml ACSF containing 80 µM AMPA were added to the recording chamber, so that a final concentration of AMPA at 20 µM was obtained. Recording of changes in intracellular Ca^{2+} levels was continued for approximately 30 minutes. For control experiments, Ca^{2+} levels were recorded for similar times, but H_2O was added to the recording chamber instead of AMPA.

Aquired data was grouped into AMPA-treated and untreated data sets and initial baseline measurement values set to 100%. Traces as shown in Figure 3.4 show the average change in intracellular Ca^{2+} from at least 20 cells from 3 independent experiments.

2.2.5 Quantitative analysis and statistics

2.2.5.1 Analysis of cluster distribution with Perkin Elmer Volocity

Images aquired with MetaVue software (see Chapter *2.2.4.1*) or Olympus Fluoview software (see Chapter 2.2.4.2) were analyzed using Volocity Demo 5.4 (Perkin Elmer, Waltham, USA). Images were loaded into the software and *Auto Contrast* was applied to each image seperately. Furthermore, pixel size was readjusted to 0.185 µm/pixel for images aquired with MetaVue, while images imported from Olympus Fluoview automatically displayed the correct pixel size according to the objective and zoom used during aquisition. To determine the number of protein clusters in the neurites, a measurement protocol was written, including the following steps: (1) identification of

fluorescent objects above a certain intensity threshold, (2) exclusion of objects larger than 10 µm^2, (3) separation of touching objects and (4) exclusion of objects smaller than 0.07 µm^2 (2 pixels) in order to exclude background noise from the calculation. As a next step, all neurites were traced with a measuring tool and the sum of all neurite lengths was calculated. The number of protein clusters was later divided by the sum of neurite length and multiplied by 100 to obtain the number of protein clusters per 100 µm neurite length.

When quantifying of axonal clusters, a ROI was drawn along the axon, which was marked by immunochemical labelling of ankyrin G (Chapter 2.2.3.5). Next, the image was clipped to the selected ROI, before applying the 4 steps above for cluster quantification.

2.2.5.2 Quantification of band intensities in Western blot experiments

For a quantitative analysis of immunodetection signal intensities from Western blots the software *ImageJ* (Version 1.42q, National Institutes of Health, Bethesda, USA) was used. All quantitative data were raised as signal intensity values after subtraction of background signals. Afterwards, experimental data were normalized to loading controls. Signal intensities are finally expressed as percentages relative to control experiments which equal 100%.

2.2.5.3 Statistical analysis with Microsoft Excel

Quantified data is always stated as mean values ± standard error of the mean (SEM). Data were obtained from at least three individual experiments. To check for statistical significance a Student's t-test was applied and significance levels were defined as follows: $p \leq 0.05$ (*), $p \leq 0.01$ (**) and $p \leq 0.001$ (***). All calculations were performed with the use of Microsoft Excel for Mac (2008 or 2011, Microsoft).

3 Results

3.1 REGULATION OF INTRACELLULAR TRANSPORT PROCESSES FOLLOWING AMPA RECEPTOR ACTIVATION

In this study, the postsynaptic scaffold protein gephyrin was used as a model protein to elucidate regulatory processes that govern activity-dependent protein transport within neurons. Gephyrin is located at inhibitory postsynaptic sites and is actively transported within cells along the microtubule network by the motor proteins KIF5 and cytoplasmic dynein (Maas *et al.*, 2006; Maas *et al.,* 2009). It was investigated in what manner synaptic activity influences the subcellular distribution of gephyrin and which regulatory mechanisms are involved.

3.1.1 Distribution of tomato-gephyrin upon AMPA receptor activation

To evaluate the impact of synaptic activity on the distribution of newly-synthesized gephyrin, cultured hippocampal neurons were transfected with a plasmid encoding a fluorescently-labelled gephyrin fusion protein (tomato-gephyrin) and treated with 20 µM AMPA to activate the AMPA-type of ionotropic glutamate receptors two hours after transfection (Chapter *2.2.3.4* and *2.2.3.6*). After 6 hours of continuous stimulation with AMPA, neurons were fixed and the subcellular distribution of tomato-gephyrin clusters was analyzed.

The number of tomato-gephyrin clusters within the neurites of individual cells was assessed and displayed as the number of gephyrin clusters per 100 µm neurite. Figure 3.1 shows representative images of hippocampal neurons that were treated with solvent (Control), AMPA or the AMPA receptor antagonist DNQX.

Quantification revealed significant differences between the individual forms of treatment. The number of gephyrin clusters per 100 µm neurite was reduced by nearly 50% in AMPA-treated cells when compared to control values (Figure 1d). Upon activation of AMPA receptors in neurons, fewer clusters of newly-synthesized tomato-

gephyrin were transported into neurites than in cells from cultures that were treated with solvent or the AMPA receptor antagonist DNQX.

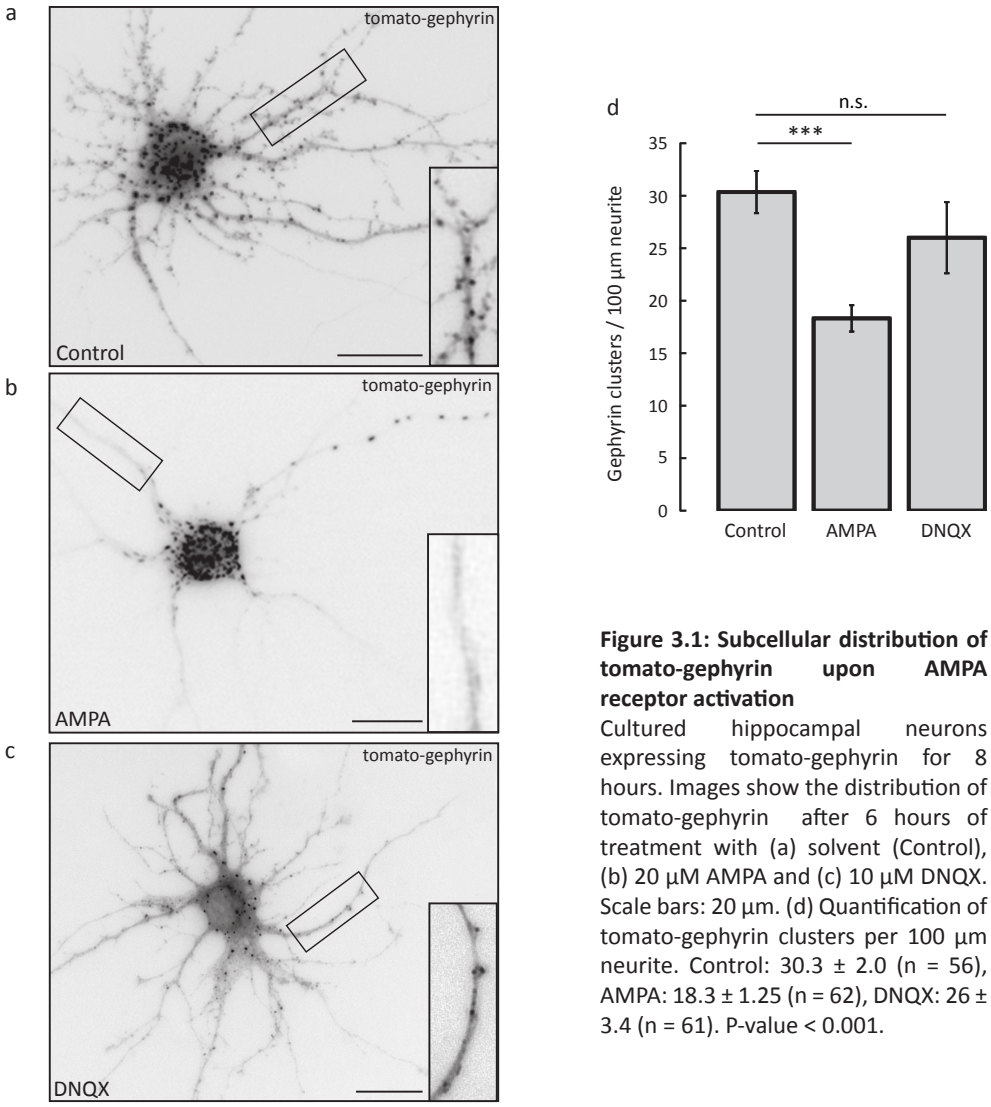

Figure 3.1: Subcellular distribution of tomato-gephyrin upon AMPA receptor activation
Cultured hippocampal neurons expressing tomato-gephyrin for 8 hours. Images show the distribution of tomato-gephyrin after 6 hours of treatment with (a) solvent (Control), (b) 20 µM AMPA and (c) 10 µM DNQX. Scale bars: 20 µm. (d) Quantification of tomato-gephyrin clusters per 100 µm neurite. Control: 30.3 ± 2.0 (n = 56), AMPA: 18.3 ± 1.25 (n = 62), DNQX: 26 ± 3.4 (n = 61). P-value < 0.001.

3.1.2 Posttranslational modifications of tubulin upon AMPA receptor activation

Next, it was attempted to investigate the underlying mechanisms responsible for the reduction of gephyrin cluster numbers in the cell periphery of AMPA-treated cells. A previous study had identified posttranslational modifications on microtubules as regulators of intracellular transport (Maas *et al.*, 2009). Microtubules serve as molecular tracks for active transport within cells and modifications on individual

tubulin subunits are thought to have a considerable impact on transport processes (Verhey & Gaertig, 2007). Different kinds of posttranslational modifications of tubulin have been described (Janke & Kneussel, 2010) and one that has been shown to influence the transport of gephyrin is polyglutamylation (Maas *et al.*, 2009). Therefore, the level of polyglutamylation and other modifications of tubulin was determined in cell lysates from hippocampal neuron cultures that had been stimulated with AMPA. For that purpose hippocampal neuron cultures were treated with either solvent (Control), AMPA or DNQX for six hours prior to analysis of tubulin modifications by immunodetection on PVDF membranes (see Chapter *2.2.2.3*). Significant changes in tubulin polyglutamylation as well as tubulin tyrosination could be detected in lysates from cultures that had been treated with AMPA, compared to cultures that had been treated with solvent (Figure 3.2). Treatment with DNQX did not result in significant changes in tubulin modifications when compared to controls.

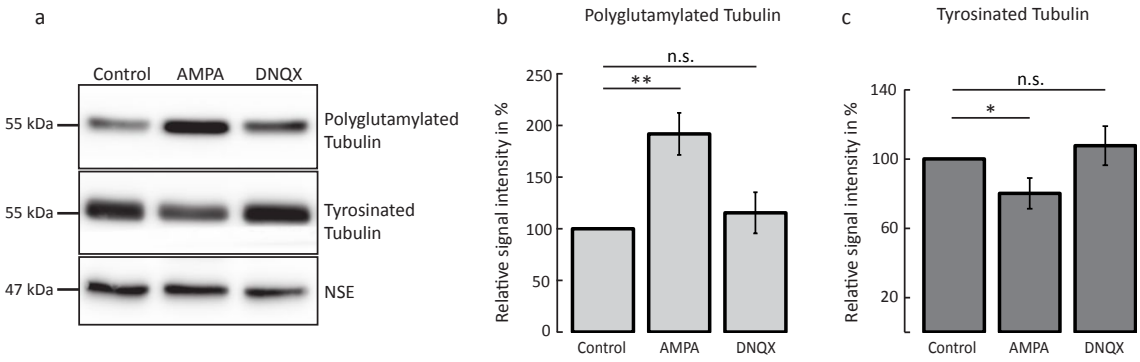

Figure 3.2: Changes in posttranslational modifications of tubulin upon AMPA receptor activation
(a) Immunodetection of posttranslational modifications of tubulin and the cytosolic protein neuron specific enolase (NSE) in lysates from hippocampal neuron cultures after treatment with solvent (Control), 20 µM AMPA or 10 µM DNQX for 6 hours. (b) Quantification of polyglutamylated tubulin signals normalized to NSE signals. Signal intensities from control samples were set to 100%. Control: 100% (n = 4), AMPA: 191.8% ± 20.4 (n = 4), DNQX: 115.4% ± 19.9 (n = 4). P-value = 0.004. (c) Quantification of tyrosinated tubulin signals normalized to NSE signals. Signal intensities from control samples were set to 100%. Control: 100% (n = 10), AMPA: 80.1 ± 8.8 (n = 10), DNQX: 107.6 ± 11.3 (n = 10). P-value = 0.04.

Signal intensities for polyglutamylated tubulin increased in cultures that were treated with AMPA to almost 200% of the control level which was set to 100% (Figure 3.2.b). Also, tubulin tyrosination was affected by AMPA receptor activation, as shown in a reduction of the normalized signal for tyrosinated tubulin by 20% compared to control values (Figure 3.2.c).

3.1.3 Intracellular calcium responses to AMPA receptor activation

AMPA receptors display fast kinetics, with activation, deactivation and desensitization occuring within milliseconds (Hansen *et al.*, 2007). Desensitization typically occurs when receptors are continuously exposed to their agonists, which is the case in this study (Traynelis *et al.*, 2010; Chapter *2.2.3.6*). Intracellular Ca^{2+} concentration changes rapidly upon synaptic activity due to an influx through Ca^{2+} channels and Ca^{2+}-permeable receptors (Redmond, 2008). Because it is a reliable indicator for synaptic activation (Chapter *1.1.2.2*; Okubo *et al.*, 2011), the amplitude and duration of intracellular Ca^{2+} increase upon continuous AMPA receptor activation was determined.
To monitor changes in intracellular Ca^{2+} levels elicited by AMPA receptor activation over a time period of 30 minutes, the Ca^{2+} indicator FURA-2 was used (see Chapter *2.2.4.3*). FURA-2 is a ratiometric calcium indicator, requiring two different wavelengths for excitation. Light with a wavelength of 340 nm excites Ca^{2+}-bound FURA-2, while 380 nm light excites free FURA-2 (Tsien *et al.*, 1985). The ratio of emmission signals after alternating excitation allows determination of Ca^{2+} levels within the cell while effects such as differences in cell thickness, local differences in dye concentration or bleaching are minimized. For Ca^{2+} recording, cultured hippocampal neurons were loaded with the Ca^{2+} indicator FURA-2 and measurements were started immediately afterwards (Chapter *2.2.4.3*). The relative changes in Ca^{2+} levels upon AMPA receptor activation are shown in Figure 3.
The red trace indicates Ca^{2+} levels in neurons that were exposed to AMPA, while the black trace stands for Ca^{2+} levels in solvent-treated cells (Control). The arrow indicates the timepoint at which AMPA or solvent were added to the recording medium. Application of AMPA instantaneously caused a strong increase in intracellular calcium levels. Notably, despite the fast kinetics and desensitization of AMPA receptors this elevation of intracellular Ca^{2+} levels continued over the entire time period measured, indicating that AMPA application causes long-lasting intracellular changes.

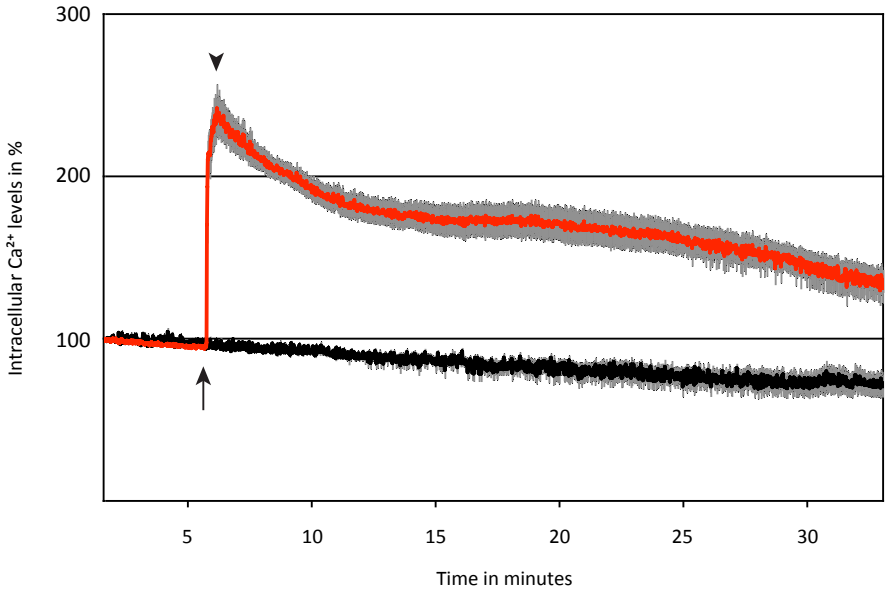

Figure 3.3: Changes in intracellular Ca^{2+} levels upon AMPA receptor activation
Intracellular Ca^{2+} levels as determined with the ratiometric Ca^{2+} indicator FURA-2. The red trace indicates Ca^{2+} levels in cultured hippocampal neurons treated with 20 µM AMPA, while the black trace shows Ca^{2+} levels in neurons treated with H_2O (Control). The arrow indicates the beginning of treatment. Maximal difference between both traces as indicated by arrowhead: 146 % ± 14.5 (n = 20). P-value < 0.001.

3.1.4 Phosphorylation of CaMKII upon AMPA receptor activation

Ca^{2+}/Calmodulin-dependent protein kinase II (CaMKII) is activated by an increase in postsynaptic Ca^{2+} concentration upon synaptic activation (Lisman *et al.*, 2002). Once activated, CaMKII is able to autophosphorylate its subunits, keeping itself in an active state (Hudmon & Schulman, 2002). The active kinase phosphorylates a number of substrates – a process that is essential for the induction and maintenance of long-term potentiation (Lisman *et al.*, 2012).

To evaluate the effects of AMPA receptor activation on the activational state of CamKII, a quantification of CaMKII and phosphorylated CaMKII in lysates from neuronal cell cultures was performed. Samples were prepared from hippocampal neuron cultures that were treated with either solvent (Control), AMPA or DNQX for six hours and subsequently lysed (see Chapter *2.2.3.3*). Cell lysates were then analyzed by western blot and immunodetection. To determine the total amount of CaMKII an antibody recognizing both, the dephosphorylated and phosphorylated form was used. Another

antibody, specifically recognizing phosphorylated CaMKII was employed to assess the amount of active CaMKII in each sample. NSE served as a loading control (Figure 3.4 a).

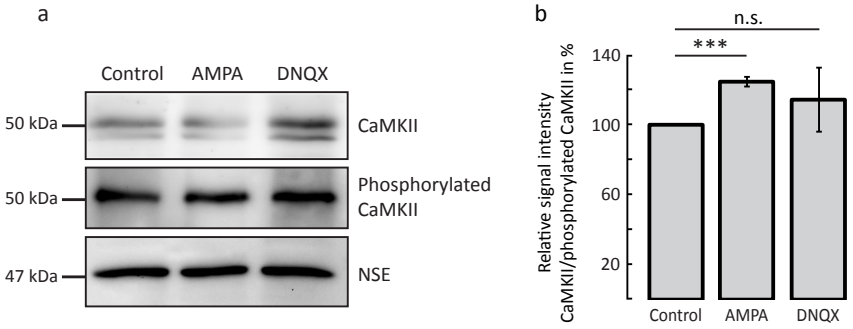

Figure 3.4: Relative increase in phosphorylated CaMKII upon AMPA receptor activation
(a) Immunodetection of total CaMKII, phosphorylated CaMKII and the loading control NSE in lysates from cultured hippocampal neurons. (b) Signal intensities were normalized to NSE signals and displayed as total CaMKII/phosphorylated CaMKII. Signal intensities from control samples were set to 100%. Control: 100% (n = 4), AMPA: 124.6% ± 2.7 (n = 4), DNQX: 114.3% ± 18.3 (n = 4). P-value < 0.001.

Figure 3.4 b shows the quantitative analysis of the detected signals normalized to NSE, expressed as the ratio of total/phosphorylated CaMKII. Cell lysates from neurons that had been treated with AMPA showed a significant increase in this ratio, whereas DNQX treatment did not result in a change when compared to control values.

3.1.5 Effects of polyglutamylation on tomato-gephyrin targeting

Analysis of posttranslational modifications of tubulin upon AMPA receptor activation had revealed a significant increase in polyglutamylated tubulin in neurons that had been treated with AMPA (Chapter 3.1.2, Figure 2). To assess, if this modification of tubulin has a direct impact on the transport of tomato-gephyrin in hippocampal neurons, polyglutamylation of tubulin was enhanced by over-expression of TTLL enzymes in neurons (Chapter *1.2.4.2*) and the effects on the distribution of tomato-gephyrin were determined. Two enzymes, TTLL6 and TTLL4 were chosen to evaluate the effects of polyglutamylation on microtubule-based transport. TTLL6 displays a preference for α-tubulin and generates long glutamyl chains, while TTLL4 preferably attaches short side chains to β-tubulin (Janke et al., 2008). Inactive mutants for both

enzymes (TTLL6 mut and TTLL4 mut) with non-functional ATPase domains were used as controls (provided by C. Janke, Orsay-Cedex, France).

Functionality of all enzymes was confirmed by detection of polyglutamylated tubulin in lysates from HEK293 cells expressing fluorescently-labelled forms of the glutamylases. (Figure 3.5 a). GFP-TTLL6, GFP-TTLL6 mut, YFP-TTLL4 and YFP-TTLL4 mut were expressed in HEK293 cells for 24 hours before lysis and subsequent immunodetection. Cells expressing GFP only served as a control.

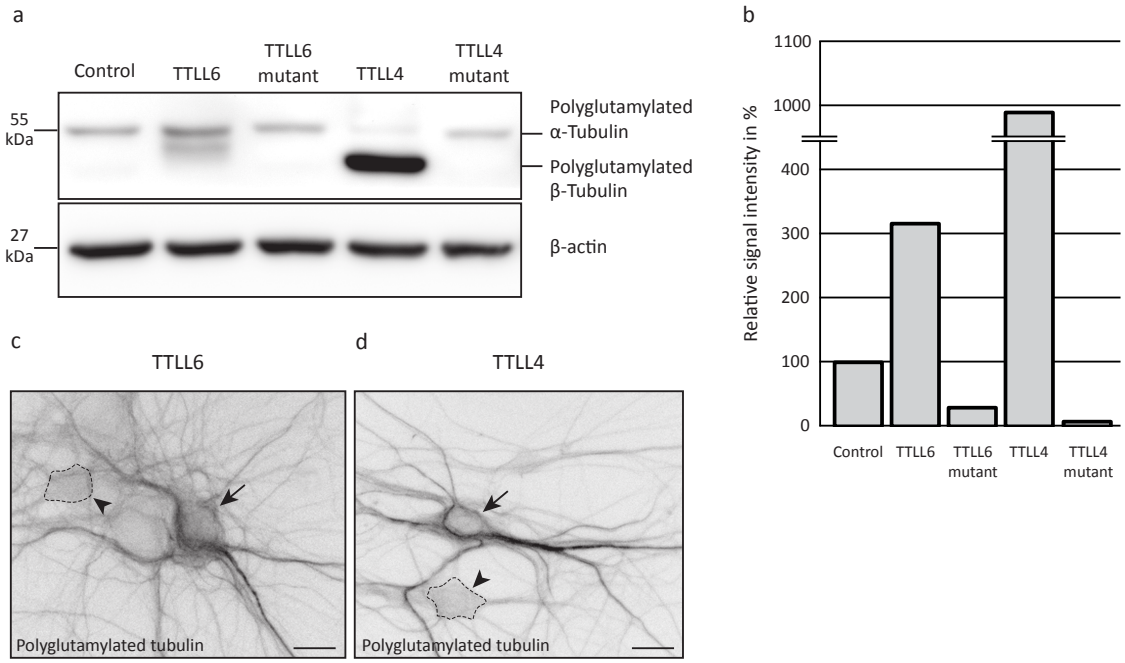

Figure 3.5: Functional characterization of the glutamylating enzymes TTLL6 and TTLL4
(a) Immunodetection of polyglutamylated tubulin with the monoclonal antibody GT335. Cell lysates were prepared from HEK293 cells expressing GFP (control), GFP-TTLL6, GFP-TTLL6 mut, YFP-TTLL4 or YFP-TTLL4 mut. (b) Quantification of the signal intensities shown in (a) normalized to β-actin signals. Only one experiment was quantified, but results could be reproduced several times. Signal intensities from control experiments were set to 100%. Control: 100%, GFP-TTLL6: 316%, GFP-TTLL6 mut: 29%, YFP-TTLL4: 990%, YFP-TTLL4 mut: 7%. (c) Immunostaining of polyglutamylated tubulin in cultured hippocampal neurons expressing GFP-TTLL6. (d) Immunostaining of polyglutamylated tubulin in cultured hippocampal neurons expressing YFP-TTLL4. Arrows indicate transfected cells, the cell bodies of untransfected, neighbouring cells are outlined and marked by arrowheads. Scale bars: 20 µm.

Figure 3.5 a shows, that GFP-TTLL6 over-expression caused an increase of polyglutamylated α-tubulin, while over-expression of the mutant enzyme GFP-TTLL6-mut did not induce such an increase. Over-expression of YFP-TTLL4 in HEK293 cells led to a strong increase of polyglutamylated β-tubulin, while YFP-TTLL4 mut over-expression did not have this effect. These results confirmed the functionality of the

glutamylases in HEK293 cells and attested the differences in substrate preference between the two enzymes. Next, hippocampal neurons over-expressing GFP-TTLL6 and YFP-TTLL4 for 8 hours were immunostained with an antibody recognizing polyglutamylated tubulin. The differences in immunoreactive signal between TTLL-transfected cells and neighbouring non-transfected cells are shown in Figure 3.5 c and 3.5 d. The immunoreactive signals for polyglutamylated tubulin was increased in the cell soma as well as in the neurites of TTLL-expressing cells, while neighbouring cells show only weak signals (cell somata are indicated by dashed lines). These results show, that over-expression of GFP-TTLL6 or YFP-TTLL4 leads to an increase of polyglutamylated tubulin in HEK293 cells as well as in cultured hippocampal neurons, confirming functionality of their enzymatic activity.

To evaluate the effect of increased polyglutamylation on gephyrin transport, GFP-TTLL6 and tomato-gephyrin were co-expressed in cultured hippocampal neurons. In control cells, tomato-gephyrin was co-expressed with GFP-TTLL6 mut. Neurons were fixed 8 hours after transfection and the number of tomato-gephyrin clusters per 100 µm neurite was determined. The obtained results are displayed in Figure 3.6.

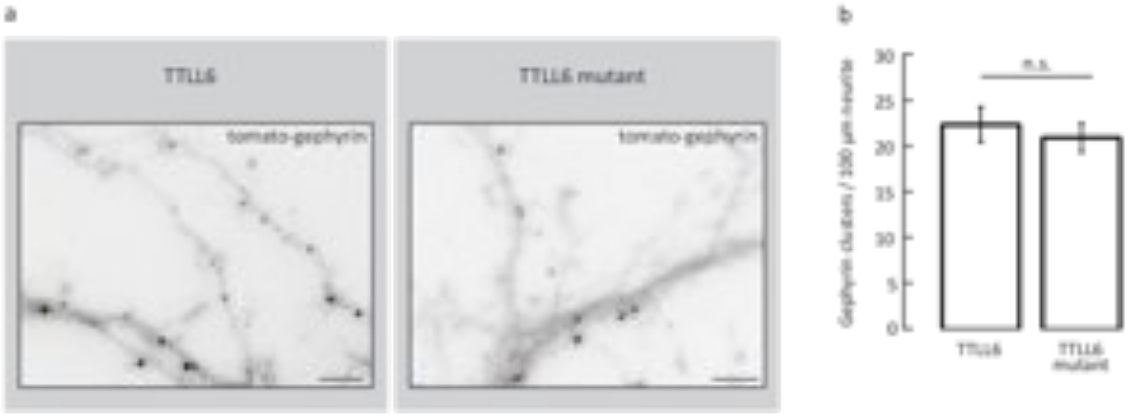

Figure 3.6: Distribution of tomato-gephyrin clusters in neurons expressing TTLL6
(a) Representative images of neurites from cultured hippocampal neurons co-expressing GFP-TTLL6 or GFP-TTLL6 mut together with tomato-gephyrin. Scale bars: 5 µm. (b) Quantification of tomato-gephyrin clusters per 100 µm neurite. TTLL6: 22.5 ± 1.9 (n = 33), TTLL6 mut: 21.04 ± 1.6 (n = 33).

A comparison of tomato-gephyrin cluster numbers within neurites of cells expressing GFP-TTLL6 or GFP-TTLL6 mut revealed no significant difference. The result suggests that the over-expression of GFP-TTLL6, which leads to increased levels of

polyglutamylated tubulin (Figure 3.5), does not cause reduced targeting of tomato-gephyrin clusters into neurites as observed after AMPA receptor activation (Figure 3.6). The number of tomato-gephyrin clusters in the cell periphery of GFP-TTLL6-expressing neurons is comparable to control values in reference experiments (Chapter 3.1.1, Figure 3.1) and is unchanged in cells expressing the non-functional TTLL6 mutant.

When testing the impact of YFP-TTLL4 over-expression on tomato-gephyrin targeting in cultured hippocampal neurons, results similar to those of GFP-TTLL6 over-expression were obtained (Figure 3.7). The increase in polyglutamylated tubulin as induced by YFP-TTLL4 expression (Figure 3.5) did not lead to changes in tomato-gephyrin distribution reminiscent of those observed upon AMPA receptor activation. In an additional experiment, hippocampal neurons co-expressing YFP-TTLL4 and tomato-gephyrin or YFP-TTLL4 mut and tomato-gephyrin, were treated with H_20 or AMPA two hours after transfection.

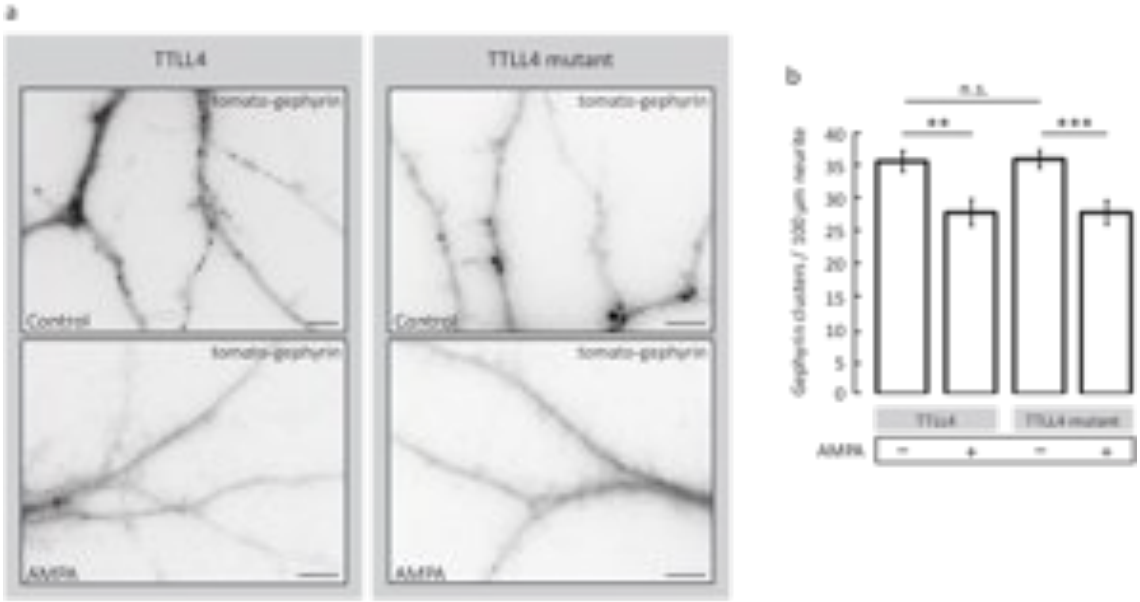

Figure 3.7: Distribution of tomato-gephyrin clusters in neurons expressing TTLL4
(a) Representative images of neurites from cultured hippocampal neurons co-expressing YFP-TTLL4 or YFP-TTLL4 mut together with tomato-gephyrin. Additionally, samples were treated with H_2O (Control) or 20 µM AMPA. Scale bars: 5 µm. (b) Quantification of tomato-gephyrin clusters per 100 µm neurite. TTLL4 (- AMPA): 35.5 ± 1.6 (n = 30), TTLL4 (+ AMPA): 27.7 ± 2.03 (n = 31), TTLL4 mut (- AMPA): 35.8 ± 1.4 (n = 25), TTLL4 mut (+ AMPA): 27.71 ± 1.8 (n = 29). P-values: TTLL4 (-/+ AMPA) = 0.004, TTLL4 mut (-/+ AMPA) < 0.001.

AMPA receptor activation led to the expected decrease of tomato-gephyrin cluster numbers in the cell periphery as observed previously (Chapter 3.1.1, Figure 3.1), but

this effect was independent of the over-expression of YFP-TTLL4 or its mutant (Figure 3.7). These results suggest, that an increase of polyglutamylated tubulin caused by the over-expression of GFP-TTLL6 or YFP-TTLL4 as performed here is not sufficient to elicit a significant impact on tomato-gephyrin distribution.

3.1.6 Identification of protein kinases involved in the regulation of tomato-gephyrin targeting upon AMPA receptor activation

Since increased polyglutamylation of tubulin as induced by over-expresio of TTLL6 or TTLL4 did not influence tomato-gephyrin targeting (3.1.5), it was attempted to clarify whether protein kinases involved in intracellular signaling cascades play a role in the regulation of the intracellular transport. The initiation of intracellular signaling cascades following AMPA receptor activation in the form of an increase in intracellular Ca^{2+} concentration (Chapter 3.1.3, Figure 3.3) and an increase in phosphorylated CaMKII (Chapter 3.1.4, Figure 3.4) could already be shown. Both events lead to downstream effects such as the activation of protein kinases, which in turn evoke cellular responses. Several signaling pathways following synaptic activation are well investigated with the respective protein kinases, the order of their activation and the cellular responses well understood (Amadio *et al.*, 2006; Cohen & Greenberg, 2008; Wiegert & Bading, 2010). This allowed the targeted inhibition of individual pathways by blockade of specific protein kinases.

In this study, identification of signaling pathways that contribute to the regulation of tomato-gephyrin transport was attempted by selective blockade of individual kinases, thereby bringing specific signaling cascades to a halt. For this purpose, three kinases that were shown to be involved in the majority of signaling processes within neurons were analyzed: protein kinase C (PKC) (Amadio *et al.*, 2006), Ca^{2+}/Calmodulin kinase II (CaMKII) (Rongo, 2002) and MAP kinase (MAPK/ERK) (Wiegert & Bading, 2010). For each one, a specific blocker could be obtained: GF109203X (PKC inhibitor, Toullec *et al.*, 1991), KN62 (CaMKII inhibitor, Tokumitsu *et al.*, 1990) and UO126 (MAPK kinase inhibitor, Favata *et al.*, 1998).

To investigate the effects of kinase inhibitors on AMPA receptor-dependent signaling, cultured hippocampal neurons expressing tomato-gephyrin for 8 hours were treated

with (1) solvent, (2) kinase inhibitor, (3) AMPA and (4) both, AMPA and kinase inhibitor two hours after transfection. Neurons were fixed 6 hours after application of the compounds and the distribution of tomato-gephyrin clusters within the neurites was evaluated. The results, expressed as the number of tomato-gephyrin clusters per 100 µm neurite are shown in Figure 3.8.

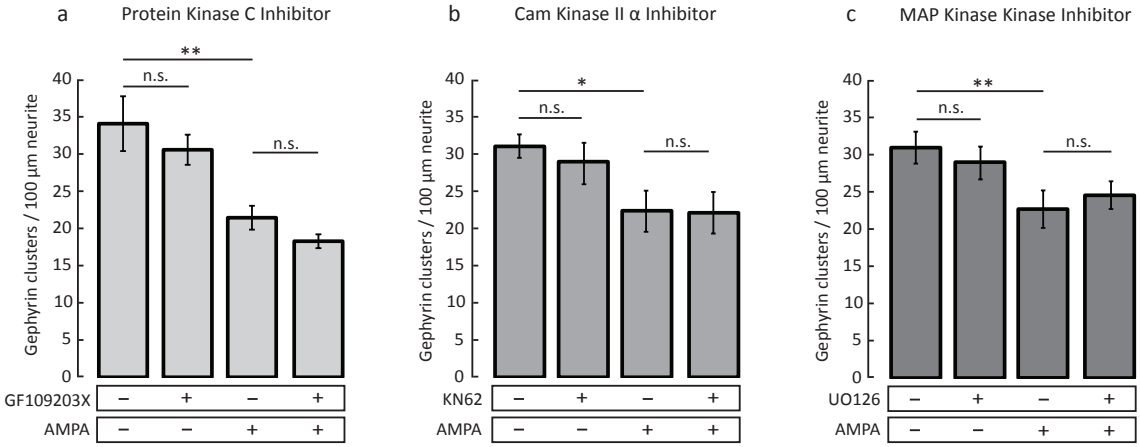

Figure 3.8: Effects of kinase inhibitors on the distribution of tomato-gephyrin upon AMPA receptor activation
(a) Cultured hippocampal neurons expressing tomato-gephyrin were treated with solvent (-/-), 20 µM GF109293X (+/-), 20 µM AMPA (-/+) or 20 µM GF109203X and 20 µM AMPA (+/+). The number of tomato-gephyrin clusters per 100 µm neurite was quantified. (-/-): 34 ± 3.7 (n = 16), (+/-): 30.5 ± 2 (n = 11), (-/+): 21.4 ± 1.6 (n = 16), (+/+): 18.3 ± 0.9 (n = 17). P-value = 0.004. (b) Cultured hippocampal neurons expressing tomato-gephyrin were treated with solvent (-/-), 2 µM KN62 (+/-), 20 µM AMPA (-/+) or 2 µM KN62 and 20 µM AMPA (+/+). The number of tomato-gephyrin clusters per 100 µm neurite was quantified. (-/-): 30.9 ± 2.1 (n = 10), (+/-): 28.9 ± 2.8 (n = 9), (-/+): 22.3 ± 2.7 (n = 11), (+/+): 22 ± 2.8 (n = 11). P-value = 0.02. (c) Cultured hippocampal neurons expressing tomato-gephyrin were treated with solvent (-/-), 10 µM UO126 (+/-), 20 µM AMPA (-/+) or 10 µM UO126 and 20 µM AMPA (+/+). The number of tomato-gephyrin clusters per 100 µm neurite was quantified. (-/-): 32.2 ± 2.7 (n = 12), (+/-): 29.3 ± 2.1 (n = 11), (-/+): 22.6 ± 1.9 (n = 10), (+/+): 24.5 ± 2.5 (n = 13). P-value = 0.01.

A significant decrease in the cluster number could be detected for neurons treated with AMPA compared to control cells, however, this effect was unaltered by the addition of any of the three kinase inhibitors. Blockade of PKC (GF109203X), CaMKII (KN62) or MAPK (UO126) alone did not alter tomato-gephyrin distribtion. These results suggest that none of the blocked signaling pathways contributes significantly to the regulation of tomato-gephyrin transport upon AMPA receptor stimulation.

As a next approach the blockade of another protein kinase, namely glycogen synthase kinase 3β (GSK3β) was chosen. Although having a multitude of substrates within the

cell (Grimes & Jope, 2001) it had recently been discovered that GSK3β phosphorylates gephyrin at serine residue 270 (Chapter 1.1.3; Tyagarajan *et al.*, 2010). Furthermore, the lack of gephyrin phosphorylation upon GSK3β blockade led to stronger clustering of gephyrin at inhibitory synapses and an increase in miniature GABAergic post-synaptic currents (Tyagarajan *et al.*, 2010).

Due to these findings the effects of GSK3β blockade on gephyrin distribution upon AMPA receptor activation were investigated. To block GSK3β activity in neurons, two different inhibitors were selected: lithium chloride and GSK-IX. The ability of lithium chloride to inhibit GSK3β has been described previously (Klein & Melton, 1996). Furthermore, its effects as a form of treatment for bipolar disorders are well-described (Du *et al.*, 2010) and the impact of lithium chloride treatment on gephyrin clustering and GABAergic transmission is thought to contribute to its therapeutic function (Tyagarajan *et al.*, 2010). GSK-IX is a highly specific inhibitor of GSK3β derived from the natural product 6-bromoindirubin that inhibits GSK3β by occupying the ATP binding pocket of the kinase (Meijer *et al.*, 2003).

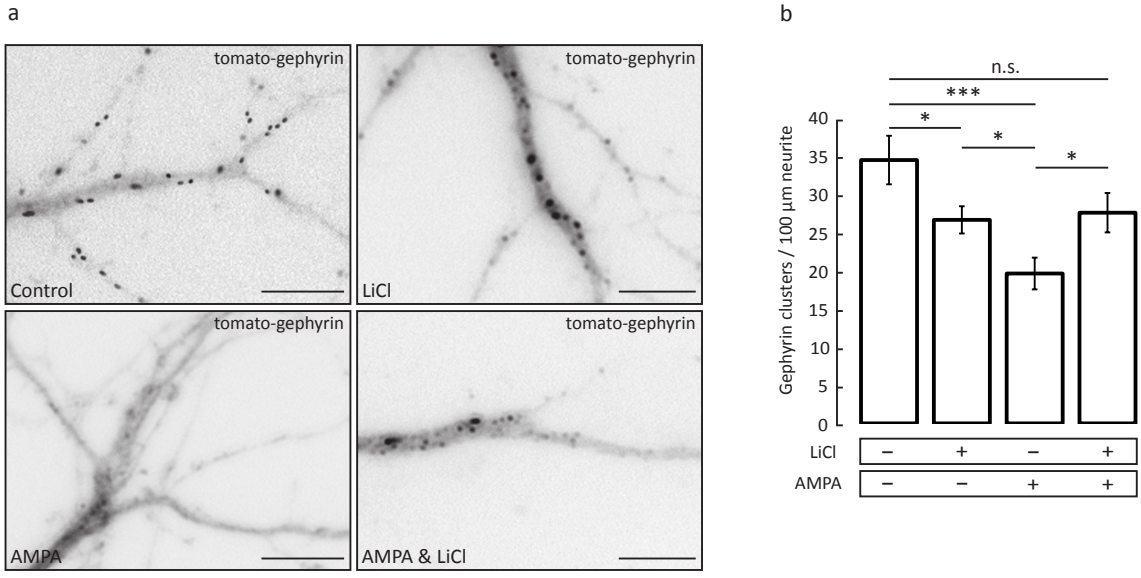

Figure 3.9: Blockade of glycogen synthase 3β with lithium chloride
(a) Representative images of neurites from cultured hippocampal neurons expressing tomato-gepyhrin. Neurons were treated with either solvent (Control) (-/-), 2 mM lithium chloride (LiCl) (+/-), 20 µM AMPA (-/+) or 20 µM AMPA and 2 mM LiCl (+/+). Scale bars: 5 µm. (b) Quantification of tomato-gephyrin clusters per 100 µm neurite. (-/-): 34.5 ± 3.2 (n = 8), (+/-): 26.7 ± 1.8 (n = 12), (-/+): 19.6 ± 2.1 (n = 10), (+/+): 27.6 ± 2.6 (n = 12).
P-values: *** < 0.001, * [(-/-)/(+/-)] = 0.033, * [(+/-)/(-/+)] = 0.02, * [(-/+)/(+/+)] = 0.03.

To test both compounds, cultured hippocampal neurons expressing tomato-gephyrin for 8 hours were treated with (1) solvent, (2) kinase inhibitor, (3) 20 µM AMPA and (4) kinase inhibitor in addition to 20 µM AMPA. 6 hours after drug application, neurons were fixed and the number of tomato-gephyrin clusters per 100 µm neurite was determined. The results for the blockade of GSK3β with lithium chloride are shown in Figure 3.9.

Quantification revealed that lithium chloride itself elicited an effect on the distribution of tomato-gephyrin within the cell. Compared to solvent control cells, the number of tomato-gephyrin clusters per 100 µm neurite was significantly reduced. AMPA receptor activation led to a strong reduction in tomato-gephyrin cluster numbers, as was expected from previous results (Chapter 3.1.1, Figure 3.1). Combined treatment with AMPA and lithium chloride showed a reduction in the number of tomato-gephyrin clusters in the cell periphery when compared to control samples but this reduction was not significant ($P = 0.1$). Compared to AMPA-treated cells, the combined treatment led to a significant increase in the number of tomato-gephyrin clusters in 100 µm neurite.

The results from experiments in which GSK-IX was used to block GSK3β are displayed in Figure 3.10. Quantification of this data revealed, that inhibtion of GSK3β with GSK-IX caused an effect on the distribution of tomato-gephyrin similar to that of GSK3β blockade with lithium chloride. Again, the inhibitor alone caused a significant decrease in tomato-gephyrin cluster numbers in the cell periphery when compared to control values. The combined effects of AMPA receptor activation and GSK-IX treatment also caused a reduction in the number of tomato-gephyrin clusters within neurites in comparison to control samples and in this case the reduction was significant ($P = 0.02$). Compared to AMPA-treated cells, the combined treatment with AMPA and GSK-IX led to a significant increase in peripheral tomato-gephyrin cluster numbers.

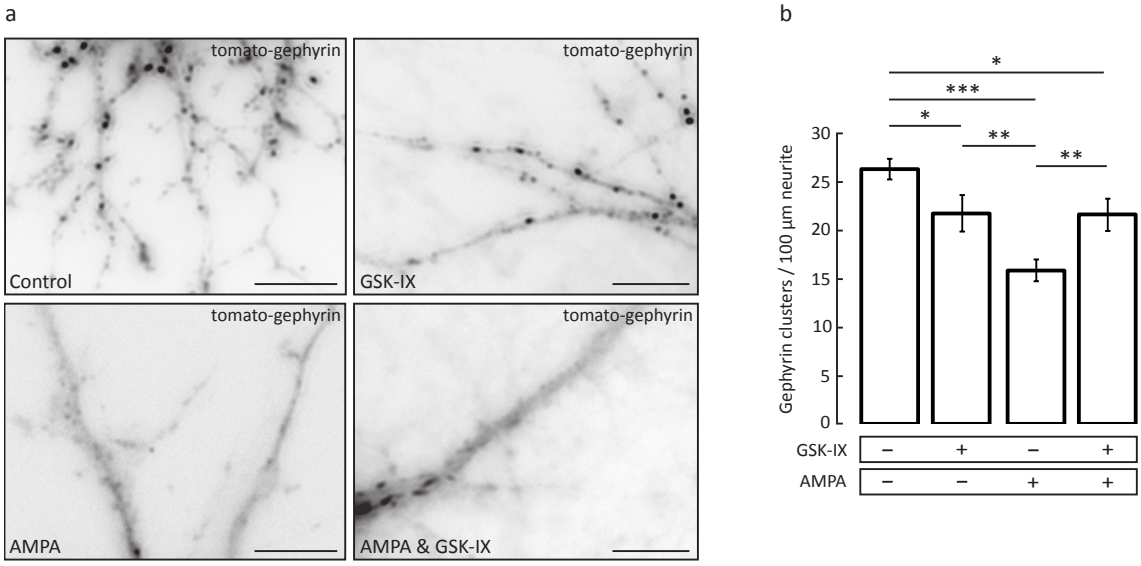

Figure 3.10: Blockade of glycogen synthase 3β with GSK-IX
(a) Representative images of neurites from cultured hippocampal neurons expressing tomato-gepyhrin. Neurons were treated with either solvent (Control) (-/-), 5 µM GSK-IX (+/-), 20 µM AMPA (-/+) or 20 µM AMPA and 5 µM GSK-IX (+/+). Scale bars: 5 µm. (b) Quantification of tomato-gephyrin clusters per 100 µm neurite. (-/-): 26 ± 1.04 (n = 10), (+/-): 21.6 ± 1.8 (n = 11), (-/+): 15.5 ± 1.1 (n = 10), (+/+): 21.3 ± 1.6 (n = 11).
P-values: *** < 0.001, ** [(+/-)/(-/+)] = 0.01, ** [(-/+)/(+/+)] = 0.008, * [(-/-)/(+/+)] = 0.02, * [(-/-)/(+/-)] = 0.048.

Summarizing, this series of experiments in which several different protein kinases were inhibited did not lead to the identification of a single signaling pathway essential for the regulation of gephyrin transport in neurons after AMPA receptor activation. However, the lack of gephyrin phosphorylation as a result of GSK3β blockade may be a relevant regulatory factor contributing to the reduction of tomato-gephyrin cluster numbers in the cell periphery.

3.1.7 Distribution ot tomato-gephyrin after recovery from AMPA receptor activation

Neither an increase in polyglutamylation, nor the inhibition of specific protein kinase signaling cascades led to the identification of a key regulator for transport of tomato-gephyrin in cultured hippocampal neurons, even though phosphorylation of gephyrin might be a critical determinant. Nevertheless, it remained to be investigated whether or not the reduction of tomato-gephyrin cluster numbers within neurites was a result

of excessive AMPA receptor activation, leading to the inhibition of house-keeping functions and distributional artefacts due to excitotoxicity.

To adress this problem, cultured hippocampal neurons expressing tomato-gephyrin were with solvent or AMPA two hours after transfection for a time period of 6 hours. Afterwards, the culture medium was removed entirely, replaced with fresh medium and the neurons were left to recover over night. The following day, neurons were fixed and the subcellular distribution of tomato-gephyrin clusters was analyzed. The results as presented in Figure 3.11 show that there is no significant difference in the number of tomato-gephyrin clusters in the periphery between solvent- and AMPA-treated neurons, after recovery for a sufficient amount of time. This suggests, that the effect on tomato-gephyrin distribution elicited by AMPA receptor activation is reversible and does not harm neurons, as intracellular transport processes are continuously carried out.

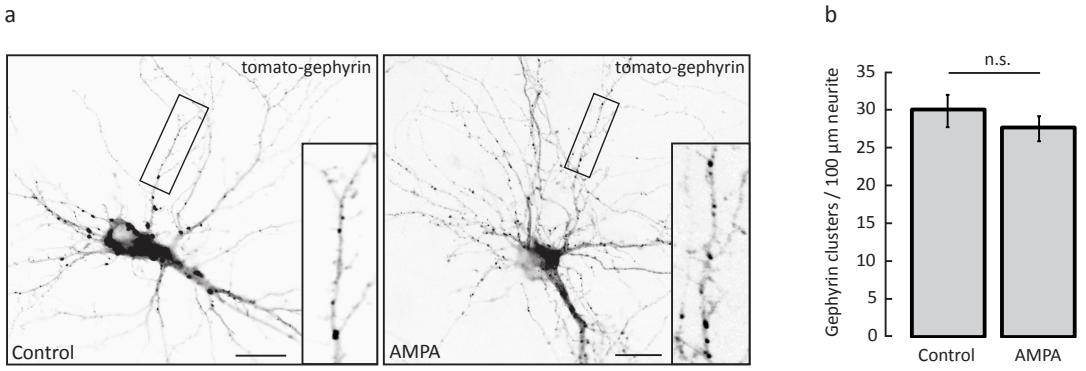

Figure 3.11: Distribution of tomato-gephyrin in neurons after recovery from AMPA receptor activation
(a) Cultured hippocampal neurons expressing tomato-gephyrin were treated with solvent (Control) or 20 µM AMPA. After 6 hours, stimulation was stopped by addition of fresh medium to the cells before recovery over night. Scale bars: 20 µm. (b) Quantification of tomato-gephyrin clusters per 100 µm neurite after recovery. Control: 30.1 ± 2.1 (n = 22), AMPA: 27.7 ± 1.6 (n = 27).

3.2 PROTEIN REDISTRIBUTION FOLLOWING AMPA RECEPTOR ACTIVATION

It could be shown that continuous stimulation of hippocampal neuron cultures with the glutamate receptor agonist AMPA has a considerable effect on the subcellular distribution of the postsynaptic scaffolding protein gephyrin (Chapter 3.1.1, Figure 3.1). In the first part of this study, several approaches were taken to elucidate the underlying mechanisms leading to a reduction of tomato-gephyrin cluster numbers within the neurites upon AMPA receptor activation.

Irrespective of mechanisms that regulate the intracellular transport of tomato-gephyrin, a possible reason for this reduction might be the accumulation of gephyrin in the cell soma caused by retention of the protein at somatic compartments. It was shown previously, for instance, that in HEK293 cells gephyrin colocalizes with γ-tubulin, a constituent of the microtubule organizing centre (MTOC) (Maas *et al.*, 2006; Oakley & Akkari, 1999). Another possible reason for the reduction of tomato-gephyrin cluster numbers located in neurites may be disruptions in protein sorting mechanisms mediated by AMPA receptor activation.

3.2.1 Alterations in tomato-gephyrin cluster shape

The stimulation of AMPA receptors in cultured hippocampal neurons caused a notable change in the shape of tomato-gephyrin clusters present in the cell soma.

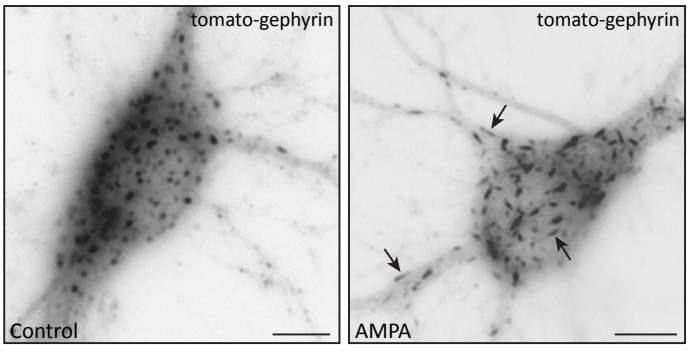

Figure 3.12: Alterations in tomato-gephyrin cluster shape upon AMPA receptor activation
Cultured hippocampal neurons expressing tomato-gephyrin were treated with solvent (Control) or 20 µM AMPA for 6 hours before fixation. Under control conditions tomato-gephyrin clusters assume a circular shape, while AMPA receptor activation causes cluster formation in elongated structures (arrows). Scale bars: 10 µm.

While untreated neurons displayed tomato-gephyrin clusters of circular shape, tomato-gephyrin clusters took on an elongated, rod-like form upon AMPA receptor activation (Figure 3.12).

3.2.2 Redistribution of tomato-gephyrin clusters into the axon

In addition to the change in cluster shape (Chapter 3.2.1) AMPA receptor activation led to a redistribution of tomato-gephyrin clusters into the axon. When cultured hippocampal neurons were treated with AMPA for 6 hours, their axons contained an unsually high number of clusters (Figure 3.13). Identification of the axon was achieved after fixation with an immunostaining against ankyrin G (AnkG), a protein enriched in the axon initial segment (AIS) (Kordeli *et al.*, 1995). The number of tomato-gephyrin clusters within the axon was determined in neurons that had been treated with H_2O and in neurons after AMPA receptor activation.

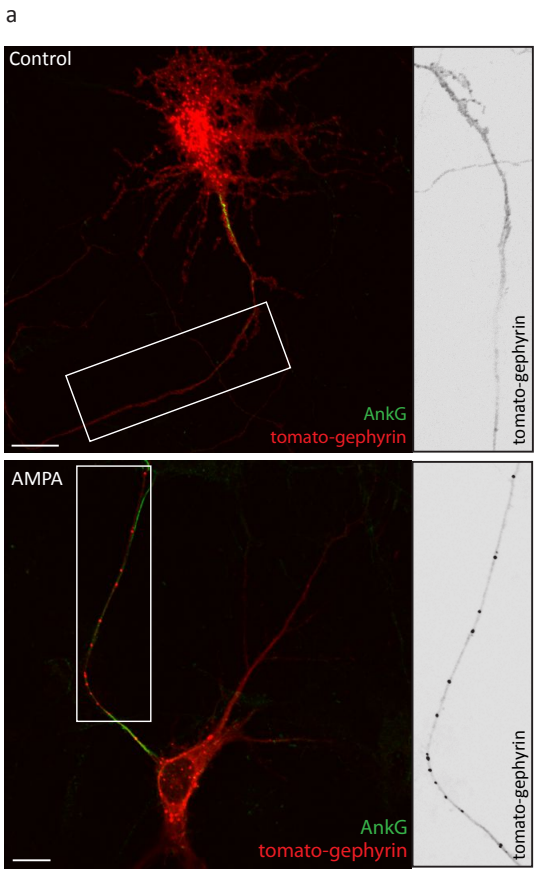

Figure 3.13: Redistribution of tomato-gephyrin into the axon upon AMPA receptor activation
(a) Cultured hippocampal neurons expressing tomato-gephyrin were treated with solvent (Control) or 20 µM AMPA for 6 hours. After fixation an immunostaining against ankyrin G (AnkG) was performed. Scale bars: 20 µm. (b) Quantification of tomato-gephyrin clusters per 100 µm axon. Control: 11.2 ± 0.7 (n = 52), AMPA: 18.7 ± 0.8 (n = 57). P-value < 0.001.

The quantified data was expressed as the number of tomato-gephyrin clusters per 100 µm axon and the results revealed a significant difference between the two forms of treatment (Figure 3.13 b). Not only did the number of tomato-gephyrin clusters differ, but also the localization within the axon or, more specifically, the distance of clusters from the cell soma. If only those clusters were taken into account that were localized beyond the initial 50 µm of the axon – here defined as „distal“ axon – the difference between the two forms of treatment became even more pronounced (Figure 3.14). Quantification revealed that in distal parts of the axon the number of tomato-gephyrin clusters is increased approximately 5-fold upon AMPA receptor activation, compared to control values (Figure 3.14 b).

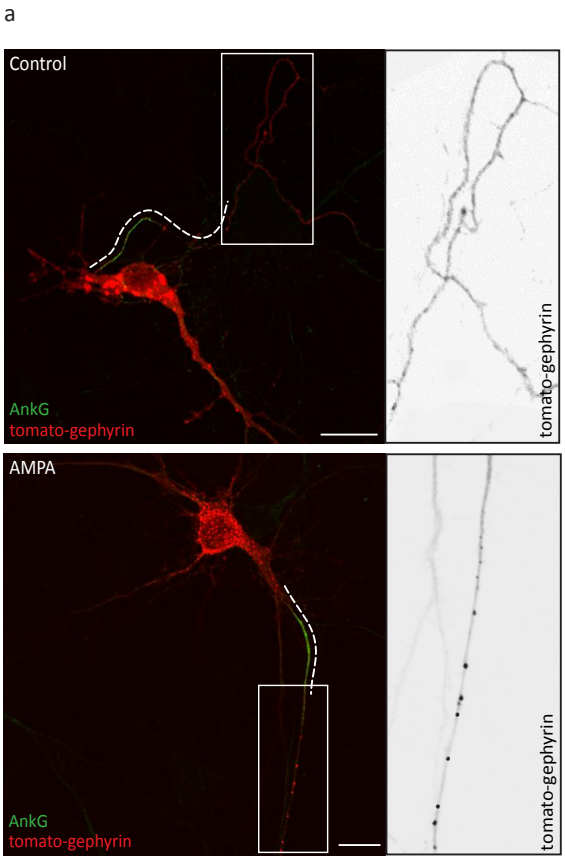

Figure 3.14: Redistribution of tomato-gephyrin into the distal axon upon AMPA receptor activation
(a) Cultured hippocampal neurons expressing tomato-gephyrin were treated with solvent (Control) or 20 µM AMPA for 6 hours. After fixation an immunostaining against ankyrin G (AnkG) was performed. Dashed lines indicate the initial 50 µm axon. Scale bars: 20 µm. (b) Quantification of tomato-gephyrin clusters per 50 µm distal axon. Control: 1.97 ± 0.3 (n = 39), AMPA: 9.8 ± 0.8 (n = 49). P-value < 0.001.

Since gephyrin anchors inhibitory neurotransmitter receptors at postsynaptic membrane specializations, it is considered to be a somato-dendritic protein and should not be present within the axon. Taken together the obtained results suggest, that the activation of AMPA receptors not only causes a reduction of tomato-gephyrin cluster

numbers in dendrites, but also leads to a relocation of tomato-gephyrin clusters into the axon and promotes the distribution of such clusters into the distal periphery.

3.2.3 Dynein-function is not required for AMPA receptor-mediated redistribution of tomato-gephyrin

Several attempts have been made to unravel the underlying mechanism of protein sorting, i.e. the assignment of proteins to either the axonal or the somato-dendritic compartment, prior to the actual transportation process into the distal periphery. Although some insight could be gained, many aspects remain elusive (Arnold, 2009; Burack *et al.*, 2000; Sampo *et al.*, 2003; Song *et al.*, 2009). One hypothesis on how protein sorting is achieved, assignes a central role to the molecular motor dynein and is based on the differences in cytoskeletal organisation in axons and dendrites (Chapter *1.2.4.2*; Kapitein *et al.*, 2010). Dynein is a molecular motor that moves along microtubules towards their minus end. Within proximal dendrites, this allows movement into both, anterograde and retrograde direction, since microtubules in this compartment have mixed orientations (Baas & Lin, 2010). Within the axon, however, microtubules are uniformly directed with their plus ends pointing towards the cell periphery, allowing dynein to perform retrograde transport only (Kapitein & Hoogenraad, 2010). Given the differences in microtubule orientation between the axon and the dendrites and the limitations this has on dynein function, it was proposed that dynein is critically involved in protein sorting processes (Kapitein *et al.*, 2010). Dynein could transport dendritic proteins in an anterograde fashion into the proximal dendrites, where a kinesin motor could take over and perform the transport into distal parts of dendrites (Kapitein *et al.*, 2010). Since gephyrin has been shown to bind to dynein as well as to KIF5 (Maas *et al.*, 2006; Maas *et al.*, 2009), it would be possible that this mechanism applies to the sorting process of gephyrin and its anterograde transport into dendrites. If dynein fulfilled such a role in the sorting of gephyrin into the dendrites, then AMPA receptor activation might hamper its correct function, resulting in a faulty sorting process. Disrupted sorting of gephyrin might account for its accumulation within the axon upon AMPA receptor activation.

To determine whether the dynein motor has an impact on the correct targeting of tomato-gephyrin, dynein function was inhibited by over-expression of the protein

dynamitin. Dynamitin is part of the dynactin protein complex and its over-expression leads to a loss of dynein function (Kardon & Vale, 2009; Burkhardt *et al.*, 1997). Cultured hippocampal neurons were co-transfected with a cDNA encoding a GFP-dynamitin fusion protein (R. Vallee, Columbia University, USA) and the plasmid encoding tomato-gephyrin. As a control, hippocampal neuron cultures were expressing GFP and tomato-gephyrin.

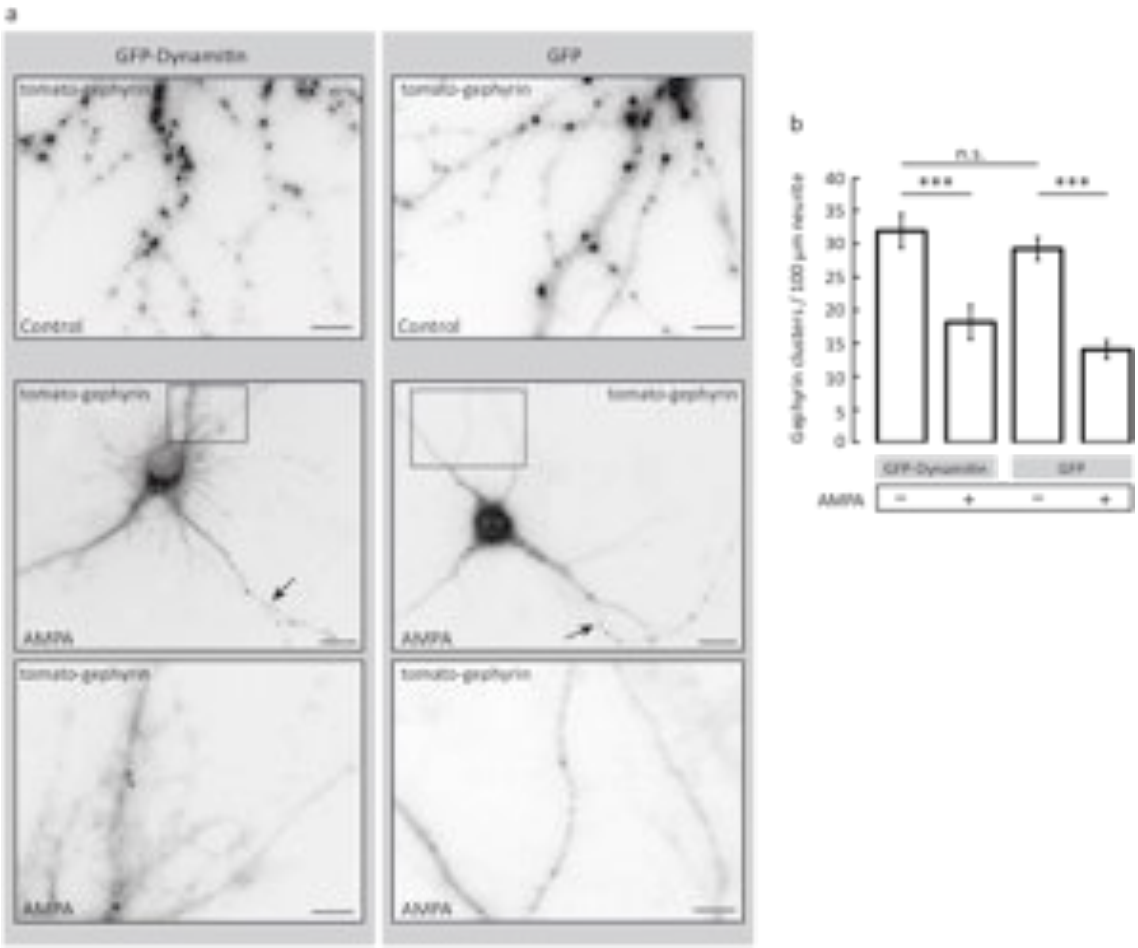

Figure 3.15: Dynein function is not required for AMPA receptor activation-mediated redistribution of tomato-gephyrin
(a) Cultured hippocampal neurons co-expressing GFP-dynamitin and tomato-gephyrin (left column) or GFP and tomato-gephyrin (right column). Neurons were treated with H_2O (Control) or AMPA for 6 hours. Upper panel: Distribution of tomato-gephyrin in dendrites under control conditions. Scale bars: 5 µm. Middle panel: Distribution of tomato-gephyrin upon AMPA receptor activation. Arrows mark the axons. Scale bars: 20 µm. Lower panel: Dendritic detail from cells shown in the panel above. Scale bars: 5 µm.
(b) Quantification of tomato-gephyrin clusters per 100 µm neurite. GFP-dynamitin: Control = 31.8 ± 2.6 (n = 15), AMPA = 18.1 ± 1.7 (n = 16). GFP: Control = 29.2 ± 1.4 (n = 11), AMPA = 14 ± 2.3 (n = 13). P-values < 0.001.

Two hours after transfection samples were treated with either H_20 or AMPA for six hours. Cells were fixed and the distribution of tomato-gephyrin clusters was

determined. As shown in Figure 3.15, over-expression of dynamitin did not affect distribution of tomato-gephyrin clusters into the cell periphery. The number of tomato-gephyrin clusters per 100 µm neurite did not differ between neurons over-expressing GFP-dynamitin or GFP. In case of additional treatment with AMPA, the number of tomato-gephyrin clusters in the cell periphery was reduced, as observed before (Chapter 3.1.1, Figure 3.1) but this was also independent of GFP-dynamitin or GFP expression. Axons of neurons could be identified by the accumulation of tomato-gephyrin clusters upon AMPA receptor activation (Figure 3.15 a, middle panel, arrows), but this effect was also not influenced by dynamitin over-expression.

These results permit two conclusions: (1) The anterograde distribution of tomato-gephyrin clusters from the cell soma into dendrites under control conditions does not appear to rely on dynein function, as it is unaffected by dynamitin over-expression. (2) The redistribution of tomato-gephyrin into the axon, as observed upon AMPA receptor activation is independent of dynein-mediated protein sorting, since it takes place even if dynein function is inhibited.

3.2.4 Retention of tomato-gephyrin at intracellular compartments

Next, it was attempted to elucidate the reasons for the formation of rod-shaped gephyrin clusters (Chapter 3.2.1, Figure 3.12). AMPA receptor activation caused tomato-gephyrin to accumulate in unregular, elongated clusters. Gephyrin has been shown to interact with the actin cytoskeleton via profilin and Mena at synpatic sites and a colocalization of gephyrin and γ-tubulin at the MTOC has also been described (Giesemann *et al.*, 2003; Maas *et al.*, 2006). To investigate if tomato-gephyrin is retained in the cell soma due to interactions with cellular components upon AMPA receptor activation, several immunostainings in hippocampal neurons expressing tomato-gephyrin were performed. Antibodies against the Golgi apparatus (GM130), and the actin cytoskeleton (Phalloidin) were used to label intracellular structures. Figure 3.16 displays examples of hippocampal neurons in which the Golgi apparatus (Figure 3.16 a) and the actin cytoskeleton (Figure 3.16 b) were labelled after AMPA receptor activation.

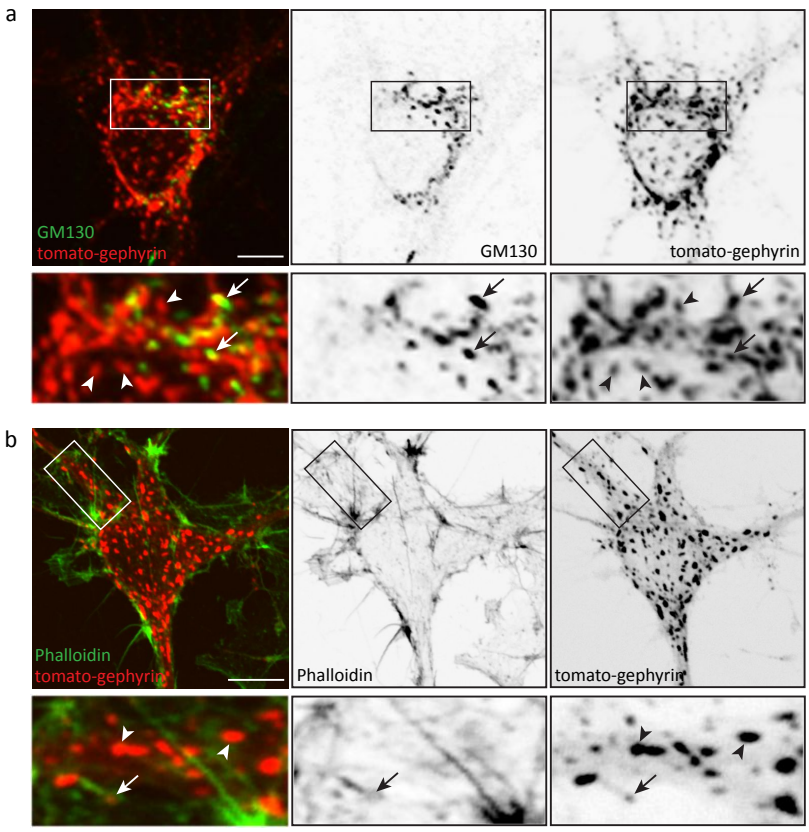

Figure 3.16: Tomato-gephyrin shows no colocalization with the Golgi apparatus or the actin cytoskeleton upon AMPA receptor activation
(a) Cultured hippocampal neurons expressing tomato-gephyrin were treated with AMPA for 6 hours. After fixation, a staining of the Golgi apparatus (GM130) was performed. Although tomato-gephyrin and GM130 signals colocalize in some places (arrows), most tomato-gephyrin clusters are distributed throughout the cell soma without colocalizing with GM130 (arrow heads). (b) Cultured hippocampal neurons expressing tomato-gephyrin were treated with AMPA for 6 hours, before an immunostaining against the actin cytoskeleton (Phalloidin) was performed. Most tomato-gephyrin clusters do not colocalize with Phalloidin signals. Arrows: colocalization, arrowheads: no colocalization. Scale bars: 10 µm.

The golgi apparatus occupies a space in the perinuclear region of the cell soma but is limited to one side of the nucleus. Figure 3.16 a shows that tomato-gephyrin clusters accumulate around the entire nucleus upon AMPA receptor activation, thereby showing colocalization with Golgi structures only on one side of the nucleus. The characteristic unilateral distribution of the Golgi apparatus is not reflected in the arrangement of tomato-gephyrin clusters. The immunostaining against the actin cytoskeleton shown in Figure 3.16 b reveals that the elongated tomato-gephyrin clusters colocalize with F-actin only in individual cases.

Taken together, these results suggest that tomato-gephyrin is neither retained at the Golgi apparatus nor at actin-containing structures within the cell soma upon AMPA receptor activation.

3.2.5 Redistribution of glycine, but not γ_2-containing $GABA_A$ receptors

The scaffold protein gephyrin colocalizes with inhibitory neurotransmitter receptors at postsynaptic specialization of inhibitory synapses (Fritschy *et al.*, 2008). It binds to a sequence motif in the β subunit of the glycine receptor, and colocalizes with $GABA_A$ receptors containing the α_2 or γ_2 subunits (Kirsch *et al.*, 1995; Kneussel *et al.*, 1999; Sassoe-Pognetto *et al.*, 1995). It could be shown that in the case of AMPA receptor activation, tomato-gephyrin is redistributed into the axon of hippocampal neurons (Chapter 3.2.2, Figure 3.13). To assess, if AMPA receptor activation also causes the redistribution of inhibitory neurotransmitter receptors, immunostainings against both, the glycine receptor and the $GABA_A$ receptor γ_2 subunit ($GABA_AR\gamma_2$) were performed.

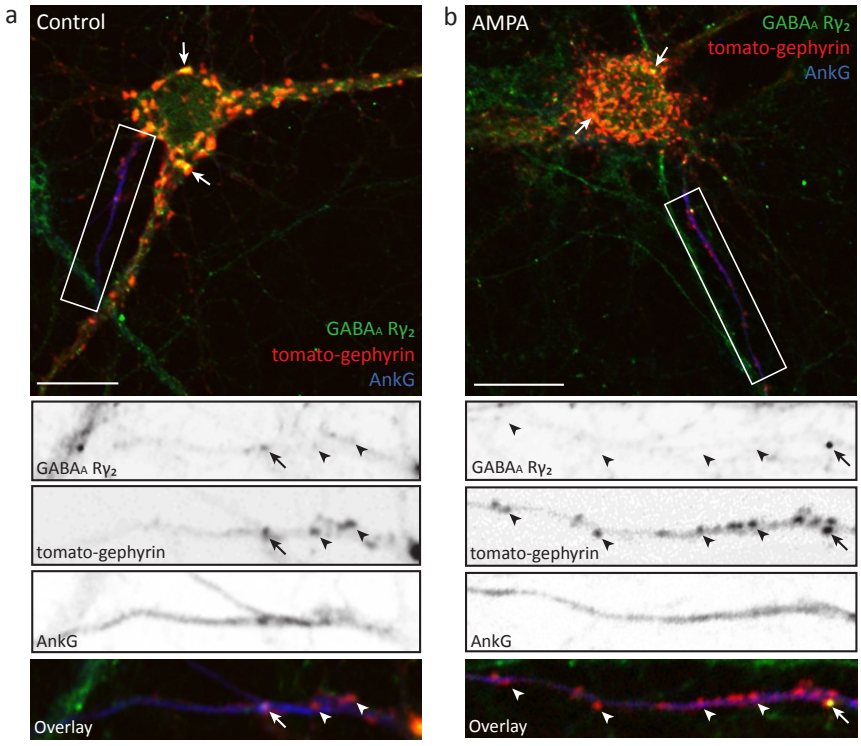

Figure 3.17: Colocalization of tomato-gephyrin and γ_2-containing $GABA_A$ receptors
Cultured hippocampal neurons expressing tomato-gephyrin were treated with solvent (a, Control) or 20 µM AMPA (b) for 6 hours. After fixation immunostainings against $GABA_A$ Rγ_2 and ankyrin G (AnkG) were performed. Colocalizations of tomato-gephyrin and $GABA_A$ Rγ_2 signals are marked by arrows, while tomato-gephyrin clusters that do not colocalize with $GABA_A$ Rγ_2 are indicated by arrow heads. Scale bars: 20 µm.

Cultured hippocampal neurons expressing tomato-gephyrin were treated with H_2O or AMPA for 6 hours. After fixation, immunostainings against $GABA_A$ Rγ_2 or the glycine receptor were performed in addition to an immunostaining against Ankyrin G to identify the axon. Representative images for $GABA_A$ Rγ_2 stainings in cultured hippocampal neurons are shown in Figure 3.17. Colocalization of tomato-gephyrin and immunoreactive signals for $GABA_AR\gamma_2$ occured within the somato-dendritic compartment in both, AMPA-treated and control neurons (Figure 3.17, arrows). However, tomato-gephyrin clusters that were redistributed into the axon upon AMPA receptor activation showed very little colocalization with $GABA_AR\gamma_2$ signals.

When performing immunostainings against the α_1 subunit of the glycine receptor in cultured hippocampal neurons after AMPA receptor stimulation, colocalization with tomato-gephyrin not only occured in the somato-dendritic compartment but also with tomato-gephyrin clusters within the axon (Figure 3.18 a). The relocation of the glycine receptor into the axon was quantified and it was revealed that approximately 15 glycine receptor immunosignals were detectable per 100 µm axon in neurons under control conditions. Upon AMPA receptor activation, this number increased by nearly 70% to approximately 25 glycine receptor signals per 100 µm axon (Figure 3.18 b). The amount of colocalization between tomato-gephyrin clusters and glycine receptor signals within the axon upon AMPA receptor activation was quantified as 88%.

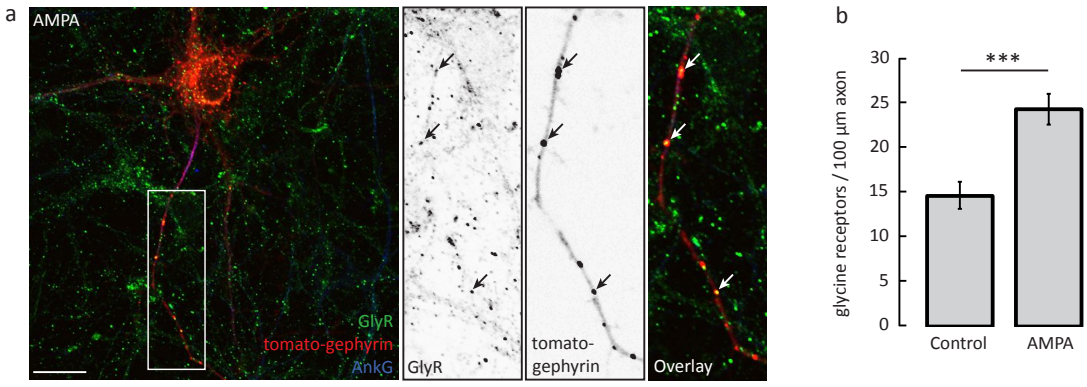

Figure 3.18: Colocalization of tomato-gephyrin and α_1-containing glycine receptors
(a) Cultured hippocampal neurons expressing tomato-gephyrin were treated with 20 µM AMPA for 6 hours. After fixation immunostainings against the glycine receptor (GlyR) and ankyrin G (AnkG) were performed. Colocalizations of tomato-gephyrin and GlyR signals within the axon are marked by arrows. Scale bar: 20 µm. (b) Quantification of GlyR signals per 100 µm axon. Control: 14.5 ± 1.6 (n = 18), AMPA: 24.3 ± 1.7 (n = 20). P-value < 0.001.

It was concluded from these findings that the glycine receptor, like tomato-gephyrin, is redistributed into the axon upon AMPA receptor activation. This is not the case for γ_2-subunit-containing $GABA_A$ receptors.

To confirm the previously obtained results, a live cell surface staining (Chapter *2.2.3.6*) against the glycine receptor was performed. Cultured hippocampal neurons expressing tomato-gephyrin were washed with ice-cold PBS in order to halt cellular endocytic events and then incubated with a monoclonal antibody against the extracellular N-terminus of the glycine receptor at 4°C without prior permeabilisation. This allowed antibody-binding to the α_1 subunit of the glycine receptors at the cell surface, but prevented labelling of intracellular receptors. Afterwards, neurons were fixed and an immunostaining against ankyrin G was performed to identify the axon.

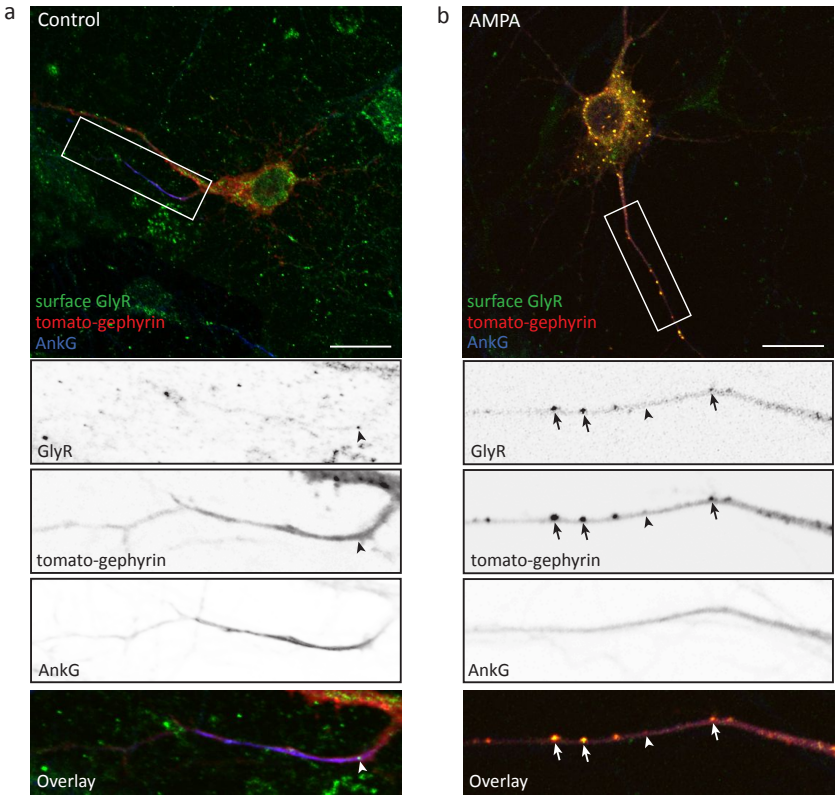

Figure 3.19: Colocalization of tomato-gephyrin and glycine receptors at the cell surface
Cultured hippocampal neurons expressing tomato-gephyrin were treated with solvent (a, Control) or 20 µM AMPA (b) for 6 hours. Before permeabilization a cell surface staining against the glycine receptor (GlyR) was performed. After fixation an immunostaining against ankyrin G (AnkG) was performed. Colocalizations of tomato-gephyrin clusters with glycine receptors at the cell surface are marked by arrows. Arrow heads indicate sites where no colocalization occured. Scale bars: 20 µm.

Examples of glycine receptor surface stainings in neurons that were treated with solvent or AMPA are shown in Figure 3.19. The stainings confirmed that upon AMPA receptor activation, glycine receptors are redistributed into the axon and revealed that tomato-gephyrin clusters within the axon colocalize with glycine receptor surface signals. The number of glycine receptors within the axon increased upon AMPA treatment, as was shown with the conventional staining method (Figure 3.18). Taken together, these results suggest that glycine receptors that are redistributed into the axon upon AMPA receptor activation can be incorporated into the plasma membrane.

3.2.6 Colocalization of tomato-gepyhrin with early endosome antigen 1 and neuroligin-2 within the axon

In further experiments, immunostainings revealed that tomato-gephyrin clusters redistributed into the axon as a result of AMPA receptor activation colocalized with early endosomal vesicles marked by early endosome antigen 1 (EEA1). A representative image for cultured hippocampal neurons that were treated with AMPA and subsequently immunolabelled for EEA1 and ankyrin G is shown in Figure 3.20 a. The number of EEA1-positive vesicles per 100 µm axon was quantified and a significant increase upon AMPA receptor activation compared to control conditions was found (Figure 3.20 b).

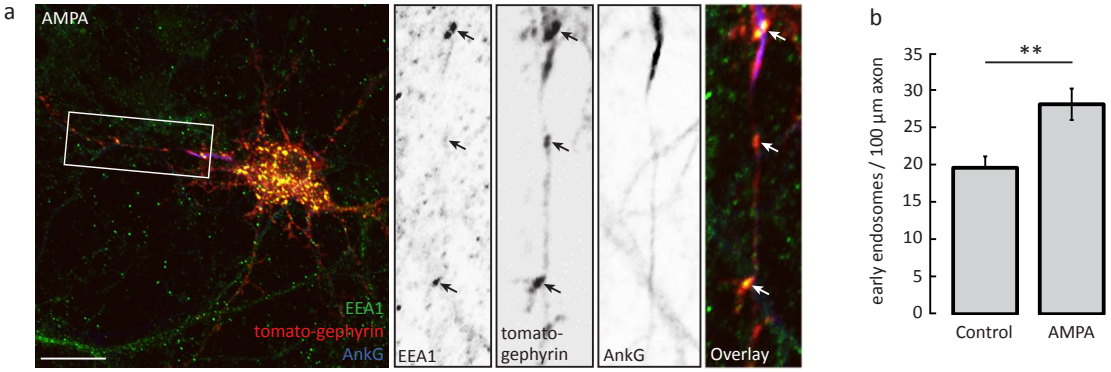

Figure 3.20: Colocalization of tomato-gephyrin and early endosomes
(a) Cultured hippocampal neurons expressing tomato-gephyrin were treated with 20 µM AMPA for 6 hours. After fixation immunostainings against early endosomes (EEA1) and ankyrin G (AnkG) were performed. Colocalizations of tomato-gephyrin and EEA1 signals within the axon are marked by arrows. Scale bar: 20 µm. (b) Quantification of EEA1 signals per 100 µm axon. Control: 19.6 ± 1.5 (n = 17), AMPA: 28.1 ± 2.1 (n = 17). P-value = 0.003.

While approximately 20 EEA1-positive vesicles per 100 µm axon were detected in neurons under control conditions, this number increased to more than 28 EEA1-positive vesicles per 100 µm axon in neurons upon AMPA receptor stimulation. Furthermore, the percentage of colocalization of tomato-gephyrin clusters and EEA1-positive vesicles upon AMPA receptor activation amounted to 71%.
These findings allow for two possibilities: either, tomato-gephyrin clusters and EEA1-positive vesicles were distributed into the axon together upon AMPA receptor activation, or tomato-gephyrin clusters colocalize with early endosomes that were endocytosed at the axonal membrane.

A redistribution of two components of inhibitory postsynapses – gephyrin clusters and glycine receptors – into the axon upon AMPA receptor activation had been discovered using immunocytochemistry (Figure 3.18). Next, immunostainings against another postsynaptic component, neuroligin-2 (NLG2) were performed (Figure 3.21).
Neuroligin-2 is a postsynpatic cell adhesion molecule that is targeted to inhibitory synapses and is involved in their formation (Patrizi *et al.*, 2008). Cultured hippocampal neurons were treated with H_2O or AMPA for 6 hours, before immunostainings against NLG2 and ankyrin G were performed. Analysis of NLG2 stainings revealed that the number of NLG2 signals in the axon is the same for control AMPA-treated cells (Figure 3.21 c). However, the level of colocalization between tomato-gephyrin clusters and NLG2 signals within the axon increased to 89% upon AMPA receptor activation compared to 71% under control conditions (Figure 3.21 d).

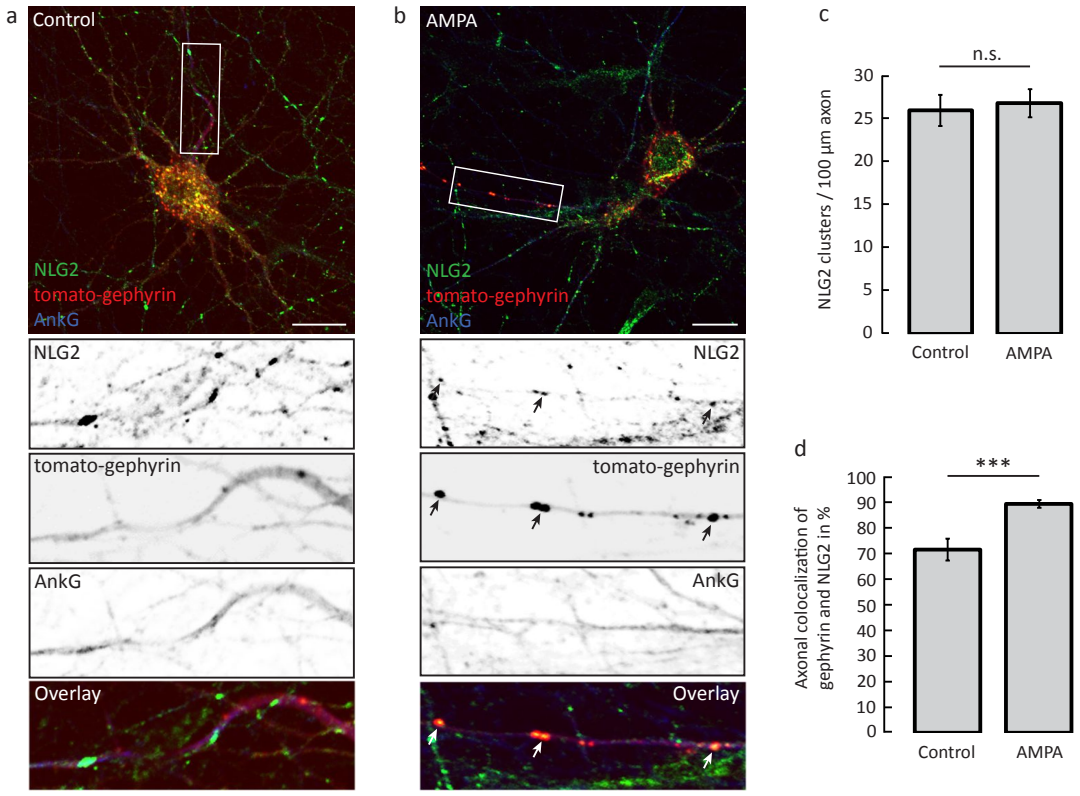

Figure 3.21: Colocalization of tomato-gephyrin and neuroligin-2
Cultured hippocampal neurons expressing tomato-gephyrin were treated with solvent (a, Control) or 20 µM AMPA (b) for 6 hours. After fixation immunostainings against neuroligin-2 (NLG2) and ankyrin G (AnkG) were performed. Colocalizations of tomato-gephyrin and NLG2 signals within the axon are marked by arrows. Scale bars: 20 µm. (c) Quantification of neuroligin-2 clusters per 100 µm axon. Control: 25.8 ± 1.8 (n = 17), AMPA: 26.6 ± 1.6 (n = 17). (d) Quantification of tomato-gephyrin clusters that colocalize with NLG2 signals in percent. Control: 71% ± 4.3 (n = 17), AMPA: 89% ± 1.5 (n = 20). P-value < 0.001.

Summarizing, immunocytochemical experiments revealed that tomato-gephyrin is redistributed into the axon (identified by positive staining against ankyrin G) upon AMPA receptor activation (Figures 3.13 and 3.14). Also, glycine receptors are redistributed into the axon where they colocalize to a large extend (88%) with tomato-gephyrin clusters (Figure 3.18) and are potentially incorporated into the axonal plasma membrane (Figure 3.19), while γ_2 subunit-containing $GABA_A$ receptors are not relocated into the axon upon AMPA receptor activation. The incidence of EEA1-positive vesicles within the axon is significantly increased upon AMPA receptor stimulation (Figure 3.20) and 71% of EEA1-positive vesicles colocalize with tomato-gephyrin clusters. Furthermore, the colocalization of tomato-gephyrin clusters and the postsynaptic cell adhesion molecule neuroligin-2 within the axon increases significantly after AMPA receptor activation (Figure 3.21).

3.2.7 Redistribution of tomato-gephyrin from the somato-dendritic compartment to the axon

The protocol used for the stimulation of cultured hippocampal neurons with AMPA had been designed to affect the distribution of newly-synthesized tomato-gephyrin (Chapter 3.1.1). Only two hours after transfection with the tomato-gephyrin-encoding plasmid, AMPA was added to the culture medium in order to influence the sorting and transport of newly synthesized protein (Chapter *2.2.3.7*). Even though it could be shown that this effect was reversible if AMPA was removed from the culture medium (Chapter 3.1.7), the possibility remained that the increased number of gephyrin clusters within the axon was an artefact caused by the combination of over-expression and AMPA receptor activation, rather than a redistributional process. For that reason it was to be investigated if the relocation of tomato-gephyrin into the axon would still take place if the protein had already been distributed throughout the cell. The experimental protocol was changed in that transfection of neurons with the plasmid encoding tomato-gephyrin was performed 24 hours before the application of AMPA. In that case tomato-gephyrin could be expressed and distributed throughout the cell before AMPA receptor activation would occur. Representative images of cultured hippocampal neurons that were treated with H_2O or AMPA for 6 hours 24 hours after transfection are shown in Figure 3.22.

Quantification revealed that the number of tomato-gephyrin clusters within axons of neurons that received AMPA treatment was significantly increased, similar to the results obtained previously (Chapter 3.2.2, Figure 3.13). This finding supports the assumption that the increase in tomato-gephyrin cluster within the axon upon AMPA receptor stimulation is due to specific redistribution rather than an artefact of over-expression.

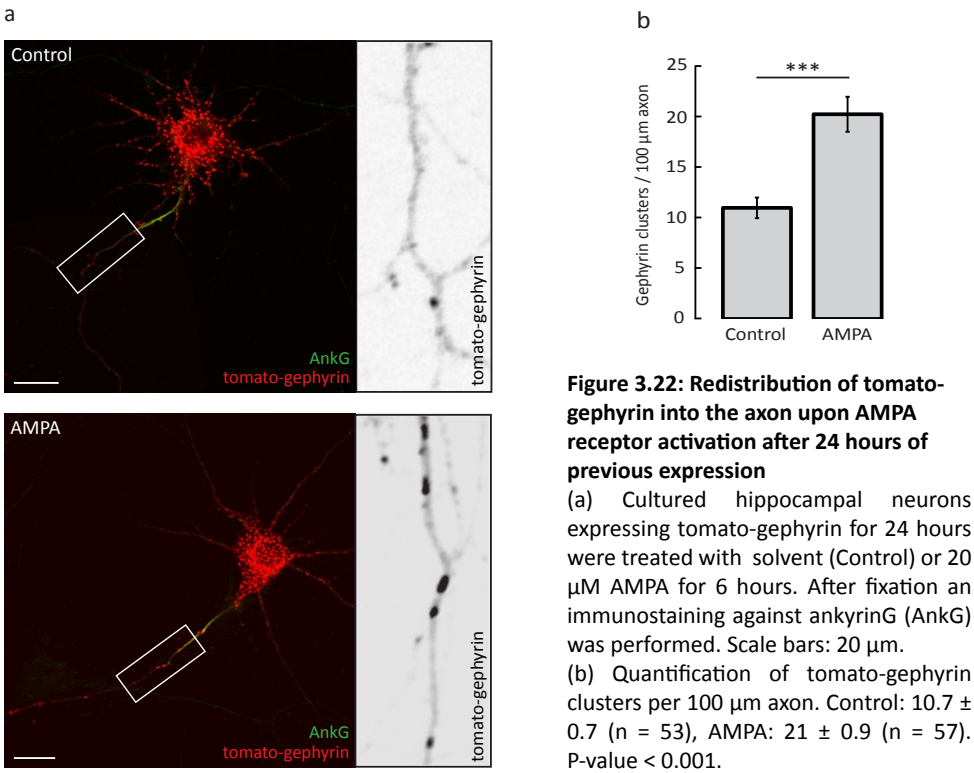

Figure 3.22: Redistribution of tomato-gephyrin into the axon upon AMPA receptor activation after 24 hours of previous expression
(a) Cultured hippocampal neurons expressing tomato-gephyrin for 24 hours were treated with solvent (Control) or 20 µM AMPA for 6 hours. After fixation an immunostaining against ankyrinG (AnkG) was performed. Scale bars: 20 µm.
(b) Quantification of tomato-gephyrin clusters per 100 µm axon. Control: 10.7 ± 0.7 (n = 53), AMPA: 21 ± 0.9 (n = 57). P-value < 0.001.

To support these results, recovery experiments were performed. Cultured hippocampal neurons expressing tomato-gephyrin for 24 hours were stimulated with H_2O or AMPA. After 6 hours of AMPA receptor activation, the culture medium was replaced with fresh medium and the neuronal cultures were incubated at 37°C and 5% CO_2 for recovery over night. Upon fixation the following day, an immunostaining against ankyrin G was performed to identify the axon. The distribution of tomato-gephyrin clusters within neurons was analyzed and the number of clusters per 100 µm axon was determined (Figure 3.23).

Quantification revealed that the number of tomato-gephyrin clusters per 100 µm axon was not increased significantly after recovery from AMPA receptor activation (Figure 3.23 b). This result implies, that the observed redistribution of tomato-gephyrin clusters into the axon is a reversible effect that is no longer detectable after sufficient recovery from AMPA receptor activation. These findings are in line with previously obtained results, that suggested the reversibility of the effect AMPA receptor activation had on the dendritic distribution of tomato-gephyrin clusters (Chapter 3.1.7, Figure 3.11).

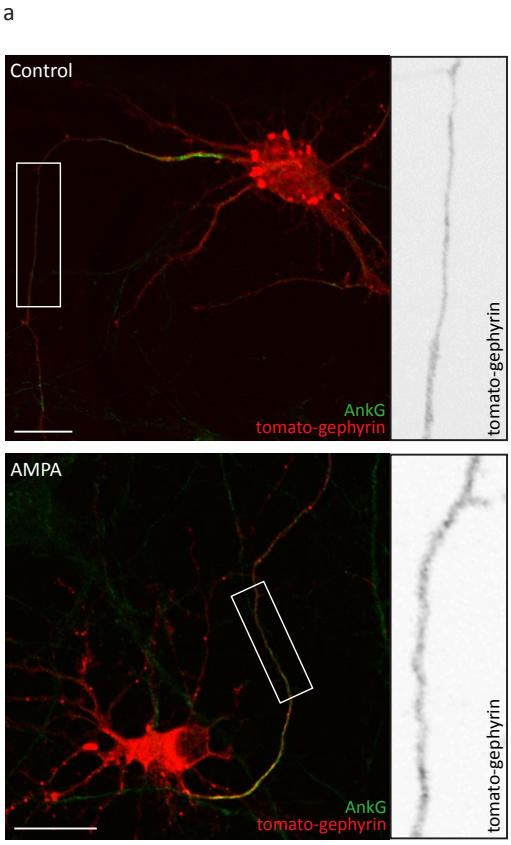

Figure 3.23: The redistribution of tomato-gephyrin into the axon upon AMPA receptor activation is reversible
(a) Cultured hippocampal neurons expressing tomato-gephyrin for 24 hours were treated with solvent (Control) or 20 µM AMPA for 6 hours. After treatment, neurons recovered in fresh medium for 14 hours. After fixation an immunostaining against ankyrin G (AnkG) was performed. Scale bars: 20 µm. (b) Quantification of tomato-gephyrin clusters per 100 µm axon. Control: 11.3 ± 1.6 (n = 13), AMPA: 13.7 ± 1.4 (n = 14).

3.2.8 Distribution of PSD95 upon AMPA receptor activation

The observed effects on the distribution of tomato-gephyrin and other components of inhibitory postsynaptic sites such as the glycine receptor and neuroligin-2 upon AMPA receptor activation raised the question if the underlying mechanisms also applied to the distributional regulation of other postsynaptic proteins.

PSD95 is a postsynaptic scaffold protein, anchoring excitatory neurotransmitter receptors at excitatory synapses (Chapter *1.1.2.1*, Kornau *et al.*, 1995; Kornau *et al.*, 1997). To investigate if AMPA receptor activation leads to changes in the distribution of this protein, fluorescently-labelled PSD95 (GFP-PSD95) was expressed in cultured hippocampal neurons. 24 hours after transfection, neurons were treated with H_2O or 20 µM AMPA, to activate AMPA receptors. Treatment lasted for 6 hours before fixation of the cells and subsequent immunostaining against ankyrin G to identify the axon. Representative images are shown in Figure 3.25.

Quantification was performed for two parameters: (1) the overall number of GFP-PSD95 clusters within the neurites was determined and expressed as GFP-PSD95 clusters per 100 µm neurite (Figure 3.25 c) and (2) the number of GFP-PSD95 clusters per 100 µm axon was determined (Figure 3.25 d). Both quantifications revealed no significant difference in GFP-PSD95 cluster numbers between neurons treated with H_2O and neurons in which AMPA receptors were activated. The number of GFP-PSD95 clusters per 100 µm neurite was approximately 48 under control conditions and after AMPA receptor stimulation. Within the axon, only 1.7 GFP-PSD95 clusters were detected under control conditions, while this value was 1.4 upon AMPA receptor activation.

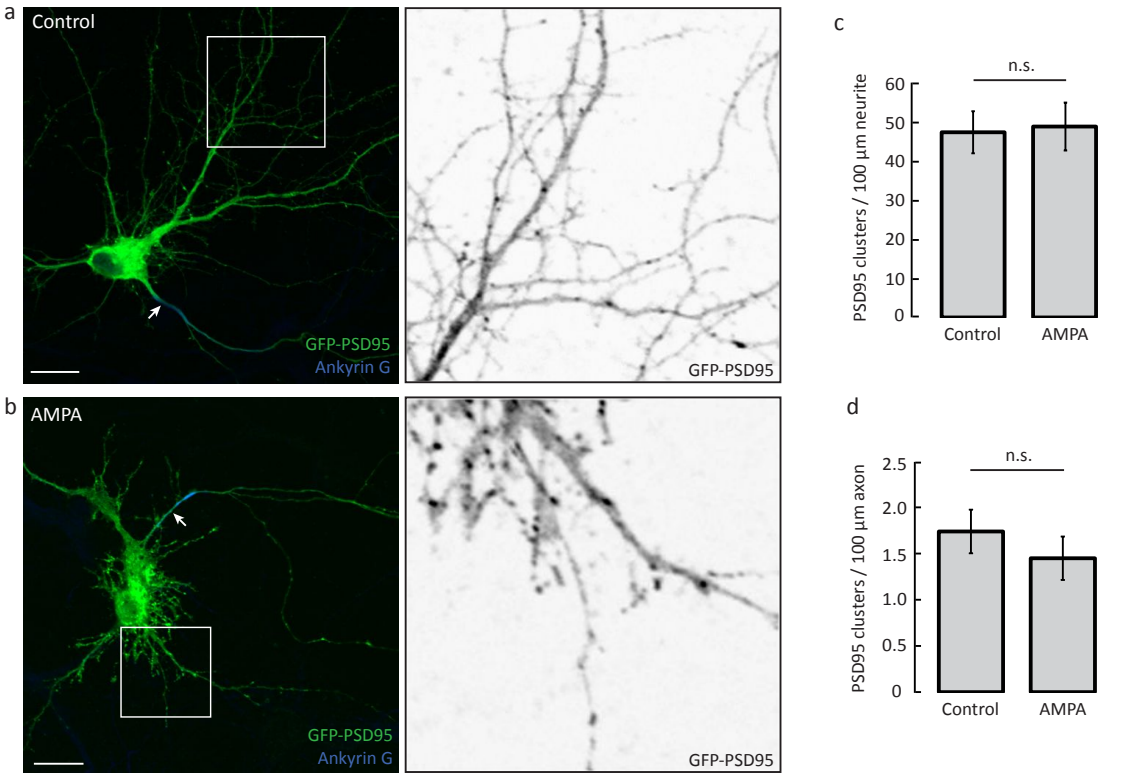

Figure 3.24: Subcellular distribution of GFP-PSD95 upon AMPA receptor activation
Hippocampal neurons expressing GFP-PSD95 for 24 hours were treated with solvent (a, Control) or 20 µM AMPA (b) for 6 hours. After fixation an immunostaining against ankyrin G (AnkG) was performed (arrows). Scale bars: 20 µm. (c) Quantification of PSD95 clusters per 100 µm neurite. Control: 47.3 ± 5.4 (n = 9), AMPA: 48.8 ± 6.1 (n = 10). (d) Quantification of PSD95 clusters per 100 µm axon. Control: 1.7 ± 0.23 (n = 9), AMPA: 1.4 ± 0.3 (n = 9).

These findings suggest, that the redistribution of proteins such as tomato-gephyrin into the axon upon AMPA receptor activation is not a general mechanism, since it does not apply to GFP-PSD95.

4 Discussion

4.1 MECHANISMS UNDERLYING THE REGULATION OF INTRACELLULAR PROTEIN TRANSPORT

The complex morphology of neurons requires targeted transport to deliver proteins synthesized in the cell soma to the periphery (Chapter 1.2). Protein composition at synaptic sites can change upon neuronal activity and the ability to strengthen individual synapses while weakening others in accordance with their presynaptic input is called synaptic plasticity (Chapter 1.1.4; Esteban, 2003; Kennedy & Ehlers, 2006). On the level of transport, synaptic plasticity requires precise targeting of newly synthesized proteins to individual synapses and it is not yet understood how this selectivity is achieved (Maas *et al.*, 2009).

4.1.1 Distibution of tomato-gephyrin upon AMPA receptor activation

In this study, the subcellular distribution of the postsynaptic scaffold protein gephyrin upon AMPA receptor activation was investigated. It was attempted to shed light on the mechanisms that regulate directed transport of proteins from the cell soma into the periphery upon an increase in synaptic activity. A previous study had shown that transport of fluorescently-labelled gephyrin is attenuated upon glycine receptor blockade induced by strychnine application (Maas *et al.*, 2009). Since blockade of the inhibitory glycine receptor resembles an overall increase in neuronal activity, it was also investigated if the activation of excitatory ionotropic glutamate receptors with the agonist AMPA leads to comparable effects (Maas *et al.*, 2009). Indeed, the consequences of decreased synaptic inhibition or increased synaptic activation were similar in their outcome, although the mechanisms underlying AMPA receptor activation-mediated transport regulation were not investigated in more detail (Maas *et al.*, 2009). The current study aimed to elucidate the underlying mechanisms regulating targeted protein transport upon AMPA receptor activation.

In line with the results presented by Maas *et al.* (2009) it could be shown in the current study that the number of tomato-labelled gephyrin clusters targeted into neurites is significantly reduced upon AMPA receptor stimulation (Chapter 3.1.1, Figure 3.1). Since gephyrin mediates the transport of glycine receptors to and from inhibitory synapses via the motor proteins KIF5 and cytoplasmic dynein respectively (Chapter 1.1.3; Maas *et al.*, 2006; Maas *et al.*, 2009), the obtained results suggest that an increase in synpatic activity as induced by AMPA receptor activation reduces the delivery of glycine receptor-containing transport complexes into the cell periphery. One could hypothesize that the increase in synaptic activity after AMPA receptor activation would lead to the strengthening of inhibitory synapses to counterbalance excitation (Turrigiano, 2012), but this hypothesis is not supported by the obtained results showing a decrease in gephyrin targeting into neurites.

4.1.2 Posttranslational modifications of tubulin upon AMPA receptor activation

In a next step it was attempted to elucidate the mechanisms underlying the reduced targeting of newly-synthesized tomato-gephyrin into the cell periphery. Intracellular transport can be regulated via several mechanisms, for instance on the level of motor proteins and motor-cargo-adaptor proteins (Chapter *1.2.4.1*) or on the level of the cytoskeletal tracks, i.e. microtubules (Chapter *1.2.4.2*). The study conducted by Maas *et al.* (2009) had revealed changes in posttranslational modifications (PTMs) on tubulin, the fundamental unit of microtubules upon glycine receptor blockade. Polyglutamylation, a modification that involves the addition of up to 20 glutamyl units to an acceptor glutamate residue in the C-terminus of tubulin (Janke *et al.*, 2008), was significantly increased in neurons that had been treated with strychnine when compared to untreated controls (Maas *et al.*, 2009). It could be shown in the current study, that polyglutamylation of tubulin was also significantly increased in neurons upon AMPA receptor activation (Chapter 3.1.2, Figure 3.2). Furthermore, the level of tubulin tyrosination, a modification in which a single tyrosine residue is attached to the C-terminus of tubulin by an enzyme called tubulin tyrosine ligase (TTL), was significantly reduced upon AMPA receptor activation (Chapter 3.1.2, Figure 3.2), while this was not the case upon strychnine-induced glycine receptor blockade (Maas *et al.*, 2009). No differences in tubulin acetylation could be detected between neurons

treated with AMPA and untreated controls (data not shown), which is in line with the results obtained by Maas *et al.* (2009) after glycine receptor blockade.

The changes in two types of PTMs on tubulin as found upon AMPA receptor activation but not glycine receptor blockade suggest the activation of differential signaling pathways following the different types of stimulation. Furthermore, the results obtained upon AMPA receptor activation might point towards a combinatorial effect of the two types of PTMs on intracellular protein transport. This means that not just one modification such as polyglutamylation or tyrosination alone mediates regulatory effects on transport processes, but a combination of several modifications together. For instance, a study investigating the effects of acetylation on axonal development revealed that not acetylation alone, but a combination of enhanced acetylation, detyrosination and polyglutamylation on tubulin determines axonal fate (Hammond *et al.*, 2010). However, individual types of PTMs of tubulin have also been shown to mediate effects on motor protein trafficking. For example, it was revealed that KIF5C moves significantly slower on detyrosinated microtubules, yet prefers those tracks over tyrosinated ones (Dunn *et al.*, 2007). Furthermore, tubulin tyrosination was shown to guide the KIF5 motor domain into the axon, rather than dendrites and it was found that this regulation is required for the maintenance of neuronal polarity (Konishi & Setou, 2009). Whether the changes in tubulin PTMs observed in this study occurred predominantly on microtubules within the somato-dendritic compartment or within the axon could not be determined with the detection method used, but it might be possible to detect these differences in future experiments with the use of advanced cell culture techniques. It can be realized, for instance, to grow primary neurons in cell culture dishes that promote the extension of the axons along indented lines in the bottom of the dish. Seperating the somato-dendritic from the axonal compartment in a spatial manner would allow the preparation of lysates from either part of the cell, and the differential analysis of protein modifications on western blots.

4.1.3 Targeted manipulation of polyglutamylation of tubulin by over-expression of polyglutamylating enzymes

It was attempted in the current study to investigate the significance of increased polyglutamylation of tubulin on intracellular transport processes in more detail. An

increase in polyglutamylation of tubulin was induced by over-expression of two different polyglutamylating enzymes: TTLL6 and TTLL4 (Chapter 3.1.5, Figure 3.5). Theses two polyglutamylases differ in their modes of action, as TTLL6 preferentially modifies α-tubulin by elongating existing glutamyl chains, while TTLL4 preferably attaches primary glutamyl residues to the C-termini of β-tubulin (Chapter *1.2.4.2*; Janke *et al.*, 2008).

Over-expression of TTLL6 or TTLL4 in cultured hippocampal neurons did not affect tomato-gephyrin targeting into neurites, as shown in Figure 3.5 (Chapter 3.1.5). These findings suggest, that the changes on tubulin induced by the over-expression of the individual polyglutamylating enzymes TTLL6 or TTLL4 were not sufficient to mediate regulatory effects on intracellular transport processes that are similar to those induced by AMPA receptor activation. Although the over-expression of TTLL6 enhances the elongation of glutamyl chains on α-tubulin and the over-expression of TTLL4 promotes the attachment of primary glutamyl residues to β-tubulin, the effects caused by AMPA receptor activation might lead to a far more complex orchestration of microtubule modifications. Several approaches would be resonable to further investigate the impact of tubulin modifications on intracellular transport processes. First of all, with respect to polyglutamylation, the combined over-expression of several polyglutamylating enzymes might lead to changes in protein targeting. Polyglutamylating enzymes display different preferences towards their substrate (α- or β-tubulin) and the reaction they catalyze (elongation or initiation), as well as different subcellular localizations (Hammond *et al.*, 2010). In total, 7 different polyglutamylase enzymes have been characterized (Chapter 1.2.4.2; Janke *et al.*, 2008) and only the co-expression of several enzymes to complement each others limitations may lead to the formation of polyglutamylation modifications that exhibit a significant effect on tomato-gephyrin targeting. Another option to investigate the significance of polyglutamylation on MT-based transport would be the use of enzymes that remove this modification from tubulin, such as cytosolic carboxypeptidases (CCPs) (Kimura *et al.*, 2010). Possibly, tomato-gephyrin distribution would be unaltered upon AMPA receptor activation, if a co-expressed CCP enzyme could prevent an increase in polyglutamylation of tubulin. A similar approach was used by Maas *et al.* (2009), when polyglutamylation was downregulated by microinjection of antibodies specific for polyglutamylase subunit 1 (PGs1). The reduction in targeting of mRFP-gephyrin that

had been observed after GlyR blockade with strychnine, could be reversed with the use of this method (Maas *et al.*, 2009).

Another approach to study the impact of tubulin modifications on transport in more detail would be to selectively manipulate more than one type of tubulin modification, such as polyglutamylation and tyrosination together. As mentioned above (Chapter 4.1.2), only the combined effects of enhanced acetylation, detyrosination and polyglutamylation are sufficient to determine axonal fate during development (Hammond *et al.*, 2010). It is possible, that a similar combinatorial effect is necessary to mediate the regulation of specific transport processes.

A detail that might also be of importance for the evaluation of the obtained data involves a technical limitation inherent to the method of transfection applied in this study. The Ca^{2+} phosphate transfection method used for transfection of cultured hippocampal neurons in this study (Chapter *2.2.3.4*) leads to the delivery and expression of plasmid DNA in roughly 0.05% of the neurons in culture. Co-transfection of individual cells with two different expression plasmids is achieved with high probability, since individual Ca^{2+} phosphate precipitates that form tend to contain both plasmids, meaning that they are delivered to neurons at the same time. However, the expression of exogenous protein within neurons can vary depending on the size of the protein, the fluorescent tag it is labelled with or the maturation time it requires to become functional. In the case of co-expression of tomato-gephyrin with GFP-TTLL6 or YFP-TTLL4 the difference in maturation time after transfection might be of importance. Possibly, tomato-gephyrin is made available to the intracellular transport machinery, long before the expression of glutamylating enzymes leads to significant increases in polyglutamylation of tubulin. In that case, it can hardly be achieved to influence tomato-gephyrin targeting. Consecutive transfections of neurons with the plasmid coding for the polyglutamylating enzyme first and the plasmid encoding tomato-gephyrin a certain time period later is not possible with the Ca^{2+} phosphate method. Due to the low efficiency of the method with only approximately 0.05% of neurons being transfected, the probability that an individual neuron becomes transfected with both plasmids in two separate transfection reactions is extremely low. A possible solution to this problem is offered by the use of methods that deliver plasmid DNA into eukaryotic cells with higher efficiency. If polyglutamylating enzymes could be delivered to cultured neurons by viral transduction for instance, leading to the infection of approximately 80% of the neurons, a subsequent delivery of the plasmid encoding

tomato-gephyrin with the Ca^{2+} phosphate method would likely result in several cells expressing both, the enzyme and tomato-gephyrin. However, a viral expression system for polyglutamylating enzymes was not available during data aquisition for this study.

4.1.4 Analysis of intracellular signaling cascades following AMPA receptor activation

The results discussed above addressed the role of tubulin modifications in the regulation of intracellular transport processes. Additionally, this study focused on the intracellular signaling cascades following AMPA receptor activation and the function these cascades might fulfil in the transmission of signals linking synaptic activity to transport regulation.

Immediately after the binding of AMPA to its receptor at the cell surface the intrinsic cation channel opens, leading to an influx of Na^{+} ions and a depolarization of the postsynaptic membrane (Chapter *1.1.2.2*). This leads to an increase in intracellular Ca^{2+} concentration due to an influx through voltage-gated Ca^{2+} channels (VGCCs), NMDA receptors, Ca^{2+}-permeable AMPA receptors and by release of Ca^{2+} from intracellular stores, such as the endoplasmatic reticulum (Bloodgood & Sabatini, 2007; Jonas *et al.*, 1994; Rizzuto & Pozzan, 2006; Yuste *et al.*, 1999). In this study, somatic Ca^{2+} levels were monitored using the ratiometric indicator FURA-2. Somatic increases in Ca^{2+} are mainly caused by ion influx through VGCCs that are activated by backpropagating action potentials and synaptically-mediated depolarization of dendritic spines (Spruston *et al.*, 1995; Waters *et al.*, 2005; Reid *et al.*, 2001). The relative Ca^{2+} levels depicted in Figure 3.3 (Chapter 3.1.3), show a significant increase in somatic Ca^{2+} upon application of AMPA to the recording medium. This increase lasted for a considerable time period and did not reach baseline levels within the time of recording (30 min). This result was crucial for the evaluation of the protein distribution analyses that were performed. It had to be confirmed that a significant increase in synaptic activity was achieved by continuous AMPA application, despite the fast desensitization kinetics of AMPA receptors. Depending on subunit composition, individual AMPA receptors desensitize within 0.9 - 9.9 ms after activation (Partin *et al.*, 1996; Mosbacher *et al.*, 1994; Quirk *et al.*, 2004; Traynelis *et al.*, 2010) and in the case of continuous application of AMPA this could result in an overall decrease in synaptic activity due to

collective desensitization of receptors. However, the lasting increase in somatic Ca^{2+} confirmed the successful induction of AMPA receptor-mediated neuronal activity over time periods long enough to induce systemic intracellular effects. These results are in line with published data on Ca^{2+} transients following pharmacological AMPA receptor activation. Brünig and colleagues recorded synaptic Ca^{2+} concentrations after application of 10 µM AMPA and found that intracellular Ca^{2+} increased by more than 400% following AMPA receptor activation (Brünig et al., 2004). Bellinger et al. (2006) recorded changes in somatic Ca^{2+} levels over 25 min using FURA-2 as an indicator. After application of 100 µM AMPA, Ca^{2+} concentrations rapidly increased followed by a gradual decrease, but not reaching baseline levels within the time period recorded (Bellinger et al., 2006).

The intracellular responses to Ca^{2+} transients are versatile, ranging from the local activation of Ca^{2+}-dependent kinases to changes in gene transcription (Chapter *1.1.2.2*). At the synaptic level, free Ca^{2+} in the cytoplasm binds calmodulin. Calmodulin activates a number of proteins, including Ca^{2+}/Calmodulin-dependent kinase II (CaMKII), adenylyl cyclases and Ras-guanine-nucleotide-releasing factors (Lisman *et al.*, 2012; Cohen & Greenberg, 2008; Redmond, 2008). Of these activated proteins some will act locally on structures such as the cytoskeleton, while others will propagate signals towards the nucleus and activate gene regulation by binding to transcription factors (Wiegert & Bading, 2010; Redmond, 2008).

CaMKII is a critical component of the postsynaptic signaling cascade during the induction of LTP and it is highly concentrated in dendritic spines (Kennedy *et al.*, 1983). Upon initial activation by local increases in Ca^{2+} concentration, CaMKII can autophosphorylate, thereby becoming persistently active and Ca^{2+}-independent (Miller & Kennedy, 1986). This independence allows the conversion of brief Ca^{2+} transients into long-lasting biochemical changes (Lisman, 1994; Mayford, 2007). In the current study, elevated levels of phosphorylated CaMKII could be detected 6 hours after the initial activation of AMPA receptors (Chapter 3.1.4, Figure 3.4). This suggests, that continuous AMPA receptor activation and the increase in intracellular Ca^{2+} concentration following AMPA application (Chapter 3.1.3, Figure 3.3.), is converted into long-lasting changes that trigger intracellular responses. This confirms the suitability of this form of receptor activation for the current study, in which the downstream, systemic effects of AMPA receptor activation on intracellular protein transport were evaluated.

4.1.5 Analysis of intracellular signaling cascades following AMPA receptor activation by specific blockade of individual protein kinases

It could be shown in this study that the intracellular Ca^{2+} concentration significantly increases and that Ca^{2+}-dependent signaling cascades are induced upon AMPA receptor activation (Chapter 4.1.4). To determine the impact of individual signaling pathways on the regulation of intracellular protein transport, specific protein kinases were inhibited and the effect on the subcellular distribution of tomato-gephyrin was evaluated (Chapter 3.1.6). Possibly, this approach would allow the identification of signaling pathways that are essential in propagating signals regarding the regulation of transport processes.

Protein kinase C (PKC) is involved in several intracellular processes following synaptic activity. Upon activation by diacylglycerol (DAG) and Ca^{2+} active PKC influences cellular components like neurotransmitter receptors, local translation machinery, the cytoskeleton or nuclear transcription factors (Amadio *et al.*, 2006). However, blockade of PKC with the selective inhibitor GF109203X did not influence the distribution of tomato-gephyrin clusters into the cell periphery. Furthermore, it did not affect the reduction of tomato-gephyrin targeting as a result of AMPA receptor activation (Chapter 3.1.6, Figure 3.8). This suggests, that the processes leading to the reduction of tomato-gephyrin targeting upon AMPA receptor activation, do not depend on the activity of PKC, although a general contribution of PCK activity to transport-related regulatory mechanisms can not be ruled out.

The implications of CaMKII activation on several cellular processes have already been discussed (Chapter 4.1.4). It was therefore attempted to evaluate the impact of CaMKII activation on the regulation of intracellular transport by blocking its kinase activity with the selective inhibitor KN62. Treatment of cultured hippocampal neurons with KN62 did not lead to changes in tomato-gephyrin distribution. Also, AMPA receptor activation-mediated effects on tomato-gephyrin distribution were not influenced by CaMKII inhibition (Chapter 3.1.6, Figure 3.8). It was therefore concluded, that albeit having a multitude of cellular functions CaMKII does not directly influence the targeting of tomato-gephyrin and is not involved in AMPA receptor activation-mediated transport regulation. Again, however, a general contribution to transport-related regulatory mechanisms can not be excluded.

The MAP kinase cascade presents a central module for the transduction of signals from the site of local Ca^{2+} increases to the nucleus (Wiegert & Bading, 2010). UO126 was used as a selective inhibitor for this family of kinases to determine if MAPK blockade has an influence on activity-mediated transport processes. Application of UO126 alone did not result in a change of tomato-gephyrin cluster quantities in the cell periphery and combined treatment with AMPA and UO126 led to reduced tomato-gephyrin targeting as observed previously after AMPA receptor activation alone (Chapter 3.1.6, Figure 3.8). These results imply that the MAPK signaling cascade does not directly interfere with the mechanisms leading to the reduction in tomato-gephyrin targeting upon AMPA receptor activation.

Taken together, these results did not lead to the identification of a specific key regulator of intracellular transport processes following synaptic activation. However, several aspects need to be taken into account for the evaluation of the obtained results. First of all, the experimental protocol used had several limitations. During experiments, kinase inhibitors were applied to hippocampal neuron cultures at the same time as AMPA. This might have induced intracellular responses to AMPA receptor activation, before the individual kinase inhibitor could effectively elicit its function. A second limitation was that inhibitor concentrations were chosen relatively low in order to allow cell survival for at least 6 hours. Since all previous results were obtained after AMPA receptor activation for 6 hours this time period was to be kept constant. This time frame was chosen to permit the expression of a sufficient amount of tomato-gephyrin fusion protein over 8 hours in total. Although the inhibitor concentrations used for the blockade of protein kinases were all within the recommended effective range (Toullec *et al.*, 1991, Tokumitsu *et al.*, 1990, Favata *et al.*, 1998), they might have been too low to induce efficient inhibition or the compounds might have been degraded over the 6 hour time period, so that their functionality could not be secured.

Similar to the regulatory effects of several types of PTMs on tubulin (Chapters 4.1.2 and 4.1.3), the effect of AMPA receptor activation on the targeting of tomato-gephyrin might be mediated by several signaling pathways simultaneously. In that case, blockade of an individual kinase might not elicit an effect strong enough to be detected in the subcellular distribution of tomato-gephyrin. In future experiments, a combinational blockade of several signaling pathways at the same time might be of

interest, although this might lead to severe damage of cells and an appropriate protocol would have to be designed.

Glycogen synthase kinase 3β (GSK3β) is a protein kinase that was of particular interest for this study, because of two notable properties. Firstly, inhibition of GSK3β prevents long-term depression in acute rat hippocampal slices when triggered by low frequency stimulation (Peineau *et al.*, 2007). This indicates towards a decisive role in activity-regulated processes. Secondly, GSK3β has been shown to phosphorylate gephyrin at serine residue 270 and inhibition of this modification reaction led to an increase in the size of dendritic gephyrin clusters (Tyagarajan *et al*., 2010). To determine if GSK3β is involved in the regulation of tomato-gephyrin targeting upon AMPA receptor activation, the distribution of tomato-gephyrin was evaluated after GSK3β blockade. One compound used for the blockade of GSK3β was lithium chloride, as this was shown to directly inhibit the kinase (Klein & Melton, 1996; O'Brien & Klein, 2009). The second compound used to block GSK3β activity was GSK-IX, which occupies the ATP binding site of the kinase and thereby inhibits its function (Meijer *et al.*, 2003).

Upon blockade of GSK3β in cultured hippocampal neurons with lithium chloride or GSK-IX, the distribution of tomato-gephyrin was changed in comparison to control cells. A significant decrease of tomato-gephyrin cluster numbers within neurites could be detected, similar to the effects of AMPA receptor activation, although to a lesser extend (Chapter 3.1.6, Figures 3.9 and 3.10).

Under resting conditions GSK3β exists in a dephosphorylated, active state in which it can phosphorylate gephyrin at S270. This reaction is prevented in the presence of a GSK3β inhibitor, leaving gephyrin in an unphosphorylated state. In the study performed by Tyagarajan *et al.* (2010), it was found that a lack of gephyrin phosphorylation as induced by GSK3β inhibition, leads to the formation of larger gephyrin clusters than under control conditions. Interestingly, this change in cluster size was only observed if GSK3β was blocked with lithium chloride, but not in the case of GSK3β inhibition with GSK-IX (Tyagarajan *et al.*, 2010).

With regards to the distribution of tomato-gephyrin upon GSK3β blockade with lithium chloride, this change in cluster size might have different implications. For quantification of the experiments performed in this study, tomato-gephyrin distribution was expressed as the number of clusters per 100 µm neurite. Cluster size however, was not taken into consideration, mainly because no striking difference was

noticed between cells that were treated with GSK3β inhibitor and control cells. The possibility exists however, that the distribution of tomato-gephyrin was not directly affected by GSK3β blockade with lithium chloride, but that several clusters within neurites formed fewer, larger ones upon GSK3β inhibition. This effect would not be detectable with the method used for quantification. As mentioned above, the increase in gephyrin cluster size was only described for GSK3β blockade with lithium chloride, not with GSK-IX pointing towards a difference in their mode of action (Tyagarajan *et al.*, 2010). In this study however, quantification of tomato-gephyrin clusters in the cell periphery resulted in similar reductions in cluster numbers compared to control values for both inhibitors (Chapter 3.1.6, Figures 3.9 and 3.10), suggesting that the proposed changes in cluster size after GSK3β inhibition with lithium chloride might not influence the quantification results significantly.

Other effects of GSK3β inhibition may point to a different explanation for the observed reduction in tomato-gephyrin distribution. It could be shown that blockade of GSK3β with the inhibitor SB216763 resulted in increased levels of microtubule acetylation, detyrosination and polyglutamylation (Hammond *et al.*, 2010). This led to the misdirection of a constitutively active form of the motor protein KIF5 into the dendrites of hippocampal neurons, rather than the axon where it is normally targeted to (Hammond *et al.*, 2010). Increased polyglutamylation and decreased tyrosination of tubulin are consequences of AMPA receptor activation, as could be shown in the current study (Chapter 3.1.2, Figure 3.2). If lithium chloride or GSK-IX elicited similar effects on tubulin modifications as SB216763, then these changes introduced to microtubules might underly the reduction of tomato-gephyrin targeting into the periphery. The tubulin PTMs might lead to a mistargeting of KIF5-mediated tomato-gephyrin transport by preventing the motor-cargo-complex from entering the dendrites. This would imply, that the mechanisms causing the reduction in tomato-gephyrin targeting might be similar for both GSK3β blockade and AMPA receptor activation. Further, this might signify that AMPA receptor activation actually leads to the phosphorylation of GSK3β, thereby deactivating the kinase. In line with this hypothesis, it was previously shown that LTP stimuli can inhibit GSK3β (Peineau *et al.*, 2007). This effect was mediated by an increase in AMPA receptor-associated phosphatidylinositide 3-kinase (PI3K) activity, an upstream regulator of GSK3β (Peineau *et al.*, 2007). In the case of AMPA receptor activation by AMPA as performed in this study, a similar mechanism might lead to the inhibition of GSK3β.

However, this hypothesis is not supported by the results obtained after combined treatment of cultured hippocampal neurons with AMPA and a GSK3β inhibitor. In that case, quantification revealed a reduction of tomato-gephyrin cluster numbers in the periphery when compared to control cells (Figures 3.9 and 3.10). However, this effect was not significant for GSK3β blockade with lithium chloride (P = 0.2) and compared to tomato-gephyrin distribution after AMPA receptor activation without GSK3β inhibition, the combined treatment actually resulted in an increase in peripheral cluster numbers. If AMPA receptor activation would indeed lead to the inhibition of GSK3β, one would assume a potentiation of this effect in the presence of a GSK3β inhibitor, causing an even stronger reduction of the number of tomato-gephyrin clusters in the cell periphery or at least the same level as upon AMPA receptor activation alone. However, this expectation is not met by the obtained results.

To investigate the connection between AMPA receptor activation and GSK3β inhibition in more detail, the use of a few molecular tools would be sensible. First of all, a constitutively active form of GSK3β could be used to directly examine the effect of AMPA receptor activation on the activity state of the kinase. If the distribution of gephyrin within the cell was dependent on GSK3β-mediated phosphorylation at S270, a constitutively active kinase should be able to fulfil this function even if AMPA receptor activation would lead to the inhibition of the endogenous kinase. Another option for testing this connection between AMPA receptor activation and GSK3β inhibition could be a selective blockade of PI3K activity. If the inhibition of GSK3β following LTP stimuli depended on PI3K activity, this signaling cascade could be circumvented and the results might be apparent in tomato-gephyrin distribution within the cell. A second molecular tool that might elucidate the function of GSK3β upon AMPA receptor activation would be a phospho-mimicking gephyrin mutant. Similarly to a constitutively active form of GSK3β, a phospho-mimicking gephyrin mutant should display no sensitivity towards regulatory mechanisms mediated by AMPA receptor activation, if these mechanisms ultimately involved the dephosphorylation of gephyrin. Another mutant, phosphorylation-defective gephyrin could be used to evaluate if, and to which extend, the distribution of tomato-gephyrin depends on the phosphorylation state of the protein.

Generally, the results obtained upon inhibition of GSK3β alone point towards a critical role of phosphorylation as a mechanisms to regulate the distribution of newly-

synthesized tomato-gephyrin within the cell. Protein phosphorylation is a posttranslational modification that can change a protein's physical and chemical properties, influencing its activity, localization or stability (Farley & Link, 2009). In the case of PSD95, the major scaffolding protein at excitatory synapses, phosphorylation has been shown to induce enhanced clustering of the protein at postsynaptic sites and promote its ability to recruit AMPA receptors to the cell surface (Kim *et al.*, 2007). For gephyrin, only a few studies have attempted to shed light on the effects of phosphorylation. In 1992, it was first reported that gephyrin is phosphorylated by an endogenous protein kinase (Langosch *et al.*, 1992). More recently, studies revealed that the phosphorylation state of gephyrin affects its ability to form clusters at postsynaptic sites (Bausen *et al.*, 2010; Tyagarajan *et al.*, 2010; Kuhse *et al.*, 2012). Inhibition of cyclin-dependent kinases (CDKs) was shown to lead to a reduction in the amount of phosphorylated gephyrin within postsynpatic clusters, an effect that was detected with the phospho-specific gephyrin antibody mAb7a (Kuhse *et al.*, 2012). That would be consistent with findings that suggest that the dephosphorylation of gephyrin leads to the formation of larger postsynaptic clusters, as was proposed by two different studies (Tyagarajan *et al.*, 2010; Bausen *et al.*, 2010). One study showed that the dephosphorylation of gephyrin by inhibition of GSK3β led to an increase in cluster size (Tyagarajan *et al.*, 2010), while inhibition of protein phosphatase 1 (PP1), leading to increased levels of gephyrin phosphorylation caused a reduction in gephyrin cluster size (Bausen *et al.*, 2010). Tyagarajan and colleagues also provide an explanation for the decrease in gephyrin cluster size with increasing phosphorylation of gephyrin. The group could show, that the residue modified by GSK3β-dependent phosphorylation, S270, is part of a PEST sequence within gephyrin (PEST = rich in proline [S], glutamate [E], serine [S] and threonine [T]). This PEST sequence is a target for the Ca^{2+}-dependent cystein protease calpain-1, of which gephyrin is a known subtrate (Kawasaki et al., 1997). Upon phosphorylation of S270 by GSK3β a conformational change might expose the PEST sequence, thereby making gephyrin a substrate for calpain-1-mediated degredation (Tyagarajan et al., 2010). Furthermore, the Ca^{2+}-dependency of calpain-1 offers a mechanistic connection between activity-induced increases in Ca^{2+} concentrations and the subsequent down-regulation of inhibitory input by degradation of inhibitory postsynaptic scaffolds (Tyagarajan et al., 2010). In this context, the consequences of AMPA receptor activation become even more complex: On the one hand, the results of the current study led to the hypothesis

that AMPA receptor activation might trigger the inhibition of GSK3β, causing reduced targeting of tomato-gephyrin to the cell periphery. On the other hand, increases in intracellular Ca^{2+} concentrations as measured after AMPA receptor activation (Chapter 4.1.4) can induce calpain-1 activity, leading to the degradation of gephyrin clusters. Both mechanisms offer a reasonable explanation for the absence of large numbers of tomato-gepyhrin clusters from the dendrites of cultured hippocampal neurons. Moreover, the increase in gephyrin cluster size that was observed as a result of GSK3β inhibtion by Tyagarajan et al. (2010) may be reflected in the formation of elongated clusters in the cell soma that was observed upon AMPA receptor activation in this study.

However, despite the insights on phosphorylation-dependent clustering of gephyrin, the regulation of long-distance transport has not yet been connected to the phosphorylation state of the protein. The results obtained in the current study point towards a critical role of this type of modification as a regulator for intracellular transport processes and the molecular tools mentioned above might help to further elucidate this role.

4.1.6 Tomato-gephyrin distribution after recovery from AMPA receptor activation

The prolonged exposure of hippocampal neurons to the glutamate receptor agonist AMPA is a non-physiological condition. Excessive activation of neurons can lead to a phenomenon termed excitotoxicity, which is characterized by deleterious intracellular processes such as the impairment of Ca2+ buffering, generation of free radicals and mitochondrial dysfuntion (Dong *et al.*, 2009). Therefore, it had to be investigated if the effects that were observed regarding tomato-gephyrin distribution within the cell upon AMPA receptor activation, were the result of changes in cellular functions or a result of excitotoxicity. It was found, that the reduction in tomato-gephyrin targeting upon AMPA receptor activation normalizes after recovery from AMPA receptor stimulation for a sufficient amount of time. After incubation of cultured hippocampal neurons over night in fresh culture medium not containing AMPA, the distribution of tomato-gephyrin clusters recovered entirely to the level of untreated control cells (Chapter 3.1.7, Figure 3.11).

This finding suggests that the accumulation of tomato-gephyrin in the cell soma and the reduction of cluster numbers in the cell periphery are effects induced by AMPA receptor activation rather than consequences of excitotoxicity. Also, recovery from these effects suggests that the regulatory mechanisms underlying the distribution of tomato-gephyrin are transient in their nature and can react to extracellular stimuli.

4.2 PROTEIN REDISTRIBUTION FOLLOWING AMPA RECEPTOR ACTIVATION

While the first part of this study focused on the mechanisms underlying the regulation of intracellular protein transport upon AMPA receptor activation, the second part deals with further consequences of AMPA receptor activation on protein targeting such as changes in tomato-gephyrin cluster shape and an observed redistribution of tomato-gephyrin and other inhibitory synapse components into the axon.

4.2.1 Accumulation of tomato-gephyrin in the cell soma upon AMPA receptor activation

AMPA receptor activation in hippocampal neurons led to a reduction of tomato-gephyrin targeting into the cell periphery. Moreover, activation of the AMPA receptor caused a change in the shape of gephyrin clusters that accumulated in the cell soma. Instead of having a circular shape, tomato-gephyrin clusters took on an elongated, rod-like shape upon AMPA receptor activation. This effect had not been observed in the study conducted by Maas *et al.* (2009), which investigated the effects of glycine receptor blockade on the distribution of mRFP-gephyrin. The elongated shape of tomato-gephyrin clusters upon AMPA receptor activation showed similarities in appearance to F-actin bundles that line the extended peripheries of cell bodies (Kessels *et al.*, 2001). It had been shown previously, that an interaction between gephyrin and the actin cytoskeleton is mediated by adaptors from the Mena/VASP family (mammalian enabled/vasodilator stimulated phosphoprotein) and profilin (Giesemann *et al.*, 2003). Due to this known interaction, it was hypothesized that in

this study AMPA receptor activation caused enhanced colocalization of tomato-gephyrin with F-actin bundles, accounting for the elongated shape of tomato-gephyrin clusters. However, the results obtained from experiments in which the actin cytoskeleton was immunolabelled, did not suggest that such an interaction underlies the rod-like shape of tomato-gephyrin clusters upon AMPA receptor activation since very little colocalization was observed (Chapter 3.2.4, Figure 3.16).

Another reason for the reduced number of tomato-gephyrin clusters in the cell periphery upon AMPA receptor activation might be that the protein was retained in somatic compartments. This would not only offer a possible explanation for the change in tomato-gephyrin cluster shape, but also for the reduced number of tomato-gephyrin clusters in the cell periphery, as the protein would not be available to intracellular transport machinery. Since gephyrin is not synthesized at the endoplasmatic reticulum (ER) and subsequently passed through the Golgi network, a retention of gephyrin at these structures would require the interaction with a membrane protein associated with these compartments. Such an interaction partner could hypothetically be the glycine receptor (GlyR), as it is synthesized and assembled within the ER and then directed to the Golgi apparatus (Kneussel & Loebrich, 2007). At the *trans*-Golgi network (TGN) the GlyR is sorted into transport vesicles before it is actively transported towards the plasma membrane. This transport to the plasma membrane is mediated by the motor protein KIF5 and gephyrin, which serves as an adaptor protein (Chapter 1.1.3; Maas *et al.*, 2009). Binding of gephyrin to the GlyR is therefore likely to occur at the TGN, from where the transport complex is directed towards the cell periphery (Hanus *et al.*, 2004).

To investigate if tomato-gephyrin was indeed retained at the Golgi apparatus upon AMPA receptor activation, immunostainings were performed. The results showed that although colocalization of the two signals occurred to a certain degree, the characteristic unilateral distribution of Golgi cisternae was not mirrowed in the arrangement of tomato-gephyrin clusters around the nucleus (Chapter 3.2.4, Figure 3.16).

If accumulation of tomato-gephyrin in the cell soma would have been caused by a retention at the Golgi apparatus that was mediated by the binding of gephyrin to the GlyR, this would imply that a retention of the GlyR within the Golgi network is the underlying reason for the accumulation of gephyrin at this compartment. Immunostaining against the Golgi apparatus did not suggest a retention of tomato-

gephyrin at this structure and hence no retention of the GlyR either, but the effects of AMPA receptor activation on the distribution of inhibitory neurotransmitter receptors were investigated in more detail in subsequent experiments and are discussed in a later Chapter (4.2.3). Interestingly, studies on the distribution of the GlyR in response to continuous GlyR blockade by strychnine, revealed the accumulation of newly-synthesized receptor molecules in the perinuclear region, but no colocalization with the Golgi apparatus or the ER could be shown. Furthermore, the receptor was found to neither accumulate in the endocytic pathway leading to degradation in lysosomes, nor endosomal routes leading to the recycling of membrane proteins (Lévi *et al.*, 1998; Rasmussen *et al.*, 2002). Rasmussen *et al.* therefore concluded that the GlyR might accumulate in a yet unidentified compartment (Rasmussen *et al.*, 2002). Although a similar form of retention is possible for newly-synthesized tomato-gephyrin, it was found in the current study that tomato-gephyrin colocalizes with early endosomal vesicles upon AMPA receptor activation, as is discussed in detail in Chapter 4.2.3. The reason for the lack of colocalization of the GlyR with markers for the endocytic pathway in the studies mentioned above (Rasmussen *et al.*, 2002), might point towards differential consequences following GlyR blockade and AMPA receptor activation. For instance, the signaling cascades following GlyR blockade might involve the activation of other protein kinases, than those activated upon AMPA receptor stimulation.

4.2.2 Redistribution of tomato-gephyrin clusters into the axon upon AMPA receptor activation

Another aspect discovered in this study was that AMPA receptor activation led to a redistribution of tomato-gephyrin clusters into the axon of hippocampal neurons (Chapter 3.2.2; Figures 3.13 and 3.14).

Since gephyrin is a postsynaptic protein located at inhibitory synaptic sites within the dendritic tree, it was hypothesized that the redistribution of tomato-gephyrin upon AMPA receptor activation was the result of incorrect sorting following protein synthesis. After biosynthesis of proteins in the cell soma, the sorting process determines the destination of a certain protein, before it is transported into either the somato-dendritic or the axonal compartment. It is not yet fully understood which

components are involved in this sorting process and which mechanisms lead to the specific delivery of proteins to their final localization in either compartment (Burack *et al.*, 2000; Sampo *et al.*, 2003). The first decisive step towards the correct targeting of proteins is thought to be their packaging into specific carrier vesicles (Craig and Banker, 1994). Following the correct assembly of transport vesicles, several factors appear to influence the subsequent distribution: (1) the primary amino acid sequence of proteins can contain signals that determine their ultimate subcellular localization (Gu *et al.*, 2003; Rivera *et al.*, 2003; Kanaani *et al.*, 2002), (2) the binding to motor proteins via adaptor molecules can mediate transport specifically into one compartment rather than the other (Setou *et al.*, 2000; Saito *et al.*, 1997; Hirokawa & Takemura, 2005) or (3) the microtubule network underlying long-distance transport provides directional cues leading to polarized transport, for example in the form of PTMs on tubulin (Nakata & Hirokawa, 2003; Hammond *et al.*, 2010; Dunn *et al.*, 2008). Also, other hypotheses have been proposed such as the existence of a molecular "sieve" within the axon initial segment that prevents the entering of dendritically targeted motor-cargo-complexes into the axon (Song *et al.*, 2009). The actin cytoskeleton and myosin-based transport is supposed to contribute significantly to the function of this molecular filter, as it could be shown that an interaction with myosin Va is both necessary and sufficient to mediate targeting of proteins to dendrites (Song *et al.*, 2009; Lewis *et al.*, 2009).

As mentioned before, differences in microtubule orientation between axons and dendrites and the resulting implications on dynein movement also provide a model that aims to delineate the sorting process (Chapter 1.2.4.2; Kapitein & Hoogenraad, 2010). The current study investigated whether or not the dynein motor specifically contributes to the accumulation of tomato-gephyrin clusters within the axon upon AMPA receptor activation. It was hypothesized that AMPA receptor activation might lead to a functional modification of dynein that would prevent the motor from fulfilling its putative role in the sorting process of tomato-gephyrin to the somato-dendritic compartment. To investigate this, experiments were performed in which the distribution of tomato-gephyrin was evaluated after over-expression of GFP-dynamitin, which leads to the functional inhibtion of the dynein motor (Burkhardt *et al.*, 1997). It could be shown that dynein inhibition could neither prevent tomato-gephyrin to be targeted into the dendrites under control conditions, nor account for the accumulation

of tomato-gephyrin clusters within the axon after AMPA receptor activation (Chater 3.2.3, Figure 3.15).

Although these results suggested that tomato-gephyrin distribution into either cellular compartment is not dependent on dynein function, it could not be determined if the accumulation of newly-synthesized tomato-gephyrin is the consequence of a disrupted sorting process following AMPA receptor activation. Furthermore, technical limitations might have prevented GFP-dynamitin to be expressed in sufficient amounts at the time point at which tomato-gephyrin became available to the intracellular transport machinery. This limitation of co-expression of two fluorescently-labelled fusion proteins was discussed in detail in Chapter 4.1.3. However, results from following experiments showed that the redistribtion of tomato-gephyrin clusters into the axon could be induced even if a distribution of tomato-gephyrin throughout the cell was established previous to AMPA receptor activation (Chapter 3.2.7, Figure 3.22). This could suggest, that not only newly-synthesized protein was distributed into the axon due to possible defects in sorting mechanisms, but also tomato-gephyrin clusters that had previously been correctly targeted to the somato-dendritic compartment. Furthermore, additional experiments revealed that the redistribution of tomato-gephyrin clusters is reversible, as the removal of AMPA from the neuronal culture medium and subsequent recovery from AMPA receptor activation led to the complete normalization of tomato-gephyrin cluster numbers within the axon (Chapter 3.2.7, Figure 3.23).

Taken together, the obtained results point towards a model that includes the targeted redistribution of tomato-gephyrin clusters into the axon upon AMPA receptor activation, irrespective of the initial subcellular localization of the protein but transient in nature as it is reversed once pharmacological AMPA receptor activation is stopped.

4.2.3 Gephyrin immunoreactivity within the axon

Two studies conducted in 1994 and 1999 have previously described the presence of gephyrin immunoreactivity in the axons of neuronal cells (Craig *et al.*, 1994; Fallah *et al.*, 1999). While Craig *et al.* (1994) investigated the distribution of gephyrin within cultured hippocampal neurons from neonatal rats, Fallah *et al.* (1999) focused on sections of the corticospinal tract during development of young rats. Craig and

colleagues found that gephyrin immunoreativity is strong in axons of young cultured neurons (DIV 2 - 10), but significantly decreases within maturation and being almost completely absent from axons of cells DIV 16 and older. Furthermore, axonal gephyrin seemed to be distributed randomly, not displaying colocalization with excitatory synapses, as marked by GluR1 stainings, or with GABAergic postsynaptic sites. Immunostaining of the presynaptic marker protein synaptophysin did not reveal significant colocalization with gephyrin immunoreactivity either, leading to the conclusion that gephyrin must exist at extrasynaptic sites independend of inhibitory neurotransmitter receptors (Craig et al., 1994). Fallah and colleagues discovered gephyrin immunoreactivity in the corticoapinal tract in developing, unmyelinated axons. With increasing age and myelination of the axons, gephyrin immunoreactivity disappeared entirely, so that it was hypothesized that the tubulin-binding ability of gephyrin might contribute to the stabilization of microtubules in developing axons (Fallah *et al.*, 1999).

In this study it was attempted to investigate the distribution of endogenous gephyrin upon AMPA receptor activation. However, the low quality of the obtained data prevented a reliable analysis and evaluation of the results (data not shown). Furthermore, tomato-gephyrin was never expressed in young cultured hippocampal neurons (DIV 2 - 10), so that no evidence exists for a possible presence of tomato-gephyrin clusters within the axons of developing neurons, as observed by Craig *et al.* (1994) and Fallah *et al.* (1999). Therefore, the data obtained in this study does not permit an evaluation of endogenous gephyrin or differences in tomato-gephyrin distribution during development.

In more recent studies, gephyrin has been described to be present within the axon initial segment (AIS) of pyramidal cells in the monkey prefrontal cortex (Cruz *et al.*, 2009). It is located there together with α_2-containing $GABA_A$ receptors opposed to GABAergic presynaptic terminals from chandelier neurons that form axo-axonal synapses but the incidence of these synapses declines rapidly with increasing age of the monkeys (Cruz *et al.*, 2009). Evidence for the presence of GABAergic synapses and gephyrin within the AIS of cultured hippocampal neurons was presented by Burkarth *et al.*, (2007) who investigated the development of these synapses and the supporting role of the cell adhesion molecule neurofascin in this context (Burkarth *et al.*, 2007).

The significant increase of tomato-gephyrin clusters in axons upon AMPA receptor activation as found in the current study does not seem to correlate with the presence

of gephyrin within the AIS during development as described by Cruz *et al*. (2009) or the establishment of GABAergic synapses in the AIS (Burkarth *et al.*, 2007), since increasing numbers of gephyrin clusters were not only found in the AIS but also in the distal axon upon AMPA receptor stimulation (Chapter 3.2.2, Figure 3.14).

4.2.4 Additional components of inhibitory postsynaptic sites are also redistributed into the axon upon AMPA receptor activation

In a next step it was investigated if the protein redistribution into the axon upon AMPA receptor activation also applied to two types of inhibitory neurotransmitter receptors – γ_2-containing $GABA_A$ and glycine receptors – by immunolabelling the respective endogenous proteins. The experiments revealed that GlyRs, but not γ_2-containing $GABA_A$ receptors are redistributed into the axon upon AMPA receptor activation similar to tomato-gephyrin (Chapter 3.2.5, Figure 3.17 and Figure 3.18). Furthermore, GlyRs were shown to be present at the surface of the axonal membrane in AMPA-treated hippocampal neurons (Chapter 3.2.5, Figure 3.19). In additional experiments a marker of the endocytic pathway – early endosome antigen 1 (EEA1) – was employed to evaluate the possible involvement of this pathway in the redistributional process of tomato-gephyrin into the axon upon AMPA receptor activation. It was revealed that the majority of tomato-gephyrin clusters that were relocated to the axon after AMPA receptor stimulation colocalized with EEA1 (Chapter 3.2.6, Figure 3.20). Moreover, the cell adhesion molecule neuroligin-2, which is a component of inhibitory synapses and involved in the formation of these (Patrizi *et al.*, 2008; Varoqueaux *et al.*, 2004), also colocalized with tomato-gephyrin clusters within the axons of AMPA-treated neurons (Chapter 3.2.6, Figure 3.21).

GlyRs within the axon have so far only been described to fulfil a role as presynaptic receptors (Deleuze *et al.*, 2005; Turecek & Trusell, 2001; Kubota *et al.*, 2010). In hippocampal mossy fiber boutons and at calyceal synapses in the medial nucleus of the trapezoid body (MNTB), presynaptic glycine receptors were found to elicit an inhibitory effect on the release of excitatory neurotransmitter (Kubota *et al.*, 2010; Turecek & Trusell, 2001). Their incidence reduces dramatically with developmental age, but is still at high levels 12 days after birth (Kubota *et al.*, 2010). GlyRs have also been

described to be present in axon terminals of supraoptic nucleus neurons which project into the neurohypophysis (Deleuze *et al.*, 2005). In this type of cells, GlyRs are present postsynaptically within the dendrites and in the cell soma and presynaptically at axonal terminals. It could be shown that the subunit composition between postsynaptic and presynaptic receptors differs in that the postsynaptic receptors are heteromeric assemblies of α and β subunits, while the presynaptic receptors contain exclusively α subunits (Deleuze *et al.*, 2005). Interestingly, presynaptic GlyRs are distributed diffusely at axonal terminals which is thought to be due to the complete absence of gephyrin from these sites (Deleuze *et al.*, 2005).

The results obtained in this study showed a significant redistribution of α_1-containing GlyRs into the axon upon AMPA receptor activation, and it is possible that their ultimate destination was the axonal terminal, although this was not investigated in more detail. It was also not determined, if β subunit containing GlyRs are present within the axon upon AMPA receptor activation. If it was the case that β subunit-containing GlyRs were also redistributed, these results would oppose the findings of Deleuze et al. (2005) which described the presence of homomeric GlyRs in the axons of supraoptic nucleus neurons. Heteromeric GlyRs within the axon might be distributed along the axonoal shaft rather than fulfilling a regulatory role at the presynaptic bouton.

It can only be speculated on the reasons for the redistribution of inhibitory synapse components into the axon upon AMPA receptor activation. Hypothetically, the overall increase in excitation might create a requirement for presynaptic GlyRs at axon terminals for the regulation of neurotransmitter release, possibly to reduce excitotoxicity in target neurons. Individual neurons as well as entire neuronal circuits have the need to maintain stable function irrespective of destabilizing effects such as strong increases in synaptic activity (Turrigiano, 2011). The mechanism by which stability is achieved is called homeostatic plasticity and it aims to maintain an overall balance between excitation and inhibition (Turrigiano, 2011). The activity-dependent redistribution of GlyRs to the axon discovered in this study might point towards a mechanism to counterbalance excessive activity as induced by AMPA receptor activation by a shift of inhibitory synapse components to the axon. If the GlyRs found within the axon become part of postsynaptic sites or if they regulate glutamate release as presynaptic receptors can not be concluded at this point.

The mechanism by which GlyRs are relocated into the axon upon AMPA receptor activation might involve endocytic events followed by active transport. Although no direct colocalization of GlyRs and EEA1-positive vesicles was shown, it might be a possibility that GlyRs were removed from postsynaptic sites in the somato-dendritic compartment on an endocytic pathway in order to be relocated into the axon. In accordance with this, neuroligin-2 could also be a part of these endocytic vesicles, internalized together with GlyRs from inhibitory postsynaptic sites. Although most aspects of this hypothesis lack supporting experimental data, it could offer a coherent explanation for the obtained results and was so far not refuted. The absence of gephyrin from presynaptic GlyR-containing sites in supraoptic nucleus neurons (Deleuze *et al.*, 2005) however, is not in line with this hypothesis, but was also found independent of changes in activity.

4.2.5 PSD95 is not redistributed into the axon upon AMPA receptor activation

To exclude the possibility that protein redistribution into the axon upon AMPA receptor activation is a general mechanism, the subcellular distribution of an additional cytosolic protein had to be evaluate under the same conditions. GFP-PSD95 was chosen for this purpose as it is – like gephyrin – a postsynaptic scaffold protein that anchors neurotransmitter receptors at postsynaptic sites (Kornau *et al.*, 1995; Kornau *et al.*, 1997). However, in the case of PSD95 the neurotransmitter receptors and the postsynaptic specializations are of excitatory nature (Chapter 1.1.2.1). It was found that the redistributional process leading to the enrichment of inhibitory postsynaptic components within the axon upon AMPA receptor stimulation, did not apply to GFP-PSD95 (Chapter 3.2.8, Figure 3.24). These results suggests a specificity of the processes that underly the observed redistribution of proteins upon AMPA receptor activation. Also, they are in line with the hypothesis that GlyRs are targeted to axon terminals to regulate presynaptic neurotransmitter release, as they point towards the specific relocation of inhibitory synaptic components rather than constituents of excitatory synapses.

4.3 CONCLUSIONS AND FUTURE DIRECTIONS

The current study aimed at elucidating mechanisms that govern intracellular transport processes in response to synaptic activity. The results obtained shed some light on the role of tubulin modifications and the relevance of protein phosphorylation as regulators of intracellular transport, but much work remains to be done to confirm the presented results and to define more clearly the functions of each of the involved processes.

It is assumed that the increase in polyglutamylation upon AMPA receptor activation contributes significantly to the observed reduction on tomato-gephyrin targeting. It will need to be determined which polyglutamylating enzymes respond to the intracellular signaling cascades after AMPA receptor stimulation, by selective over-expression of different glutamylases individually before evaluating protein distribution. Furthermore, the combinatorial effects of several enzymes with different specificity need to be described and by over-expressing cytosolic carboxypeptidases (CCPs) the effects of AMPA receptor activation on protein targeting might be reversed, underlining the importance of this modification.

Tubulin tyrosination and its effects on targeted protein transport, especially in connection with the molecular motors KIF5 and cytoplasmic dynein will need to be evaluated, since these motors provide for the transport of gephyrin. Furthermore, changes in more than one modification of tubulin needs to be investigated, as the synergistic effects might be the relevant factor for transport regulation. Tubulin polyglutamylation and tubulin tyrosination could be increased by co-expression of TTL and TTLL enzymes and the effects on protein targeting could be evaluated.

The used of cell culture techniques that allow the seperation of neuronal somata from axons, might allow analysis of tubulin modifications after AMPA receptor activation for each compartment seperately, which might provide information on why tomato-gephyrin is increasingly targeted into axons.

The importance of phosphorylation as a modification on gephyrin can be evaluated with the use of gephyrin mutants with phophorylation mimicking or phosphorylation defective properties. Furthermore, several options exist to unravel the signaling cascades following AMPA receptor activation. It is necessary to determine whether or not AMPA receptor activation leads to the inhibtion of GSK3β. This could be achieved

by over-expression of a constitutively-active form of the kinase which is resistant to AMPA-receptor-mediated blockade.

The second part of the project described the redistribution of inhibitory synapse components into the axon upon AMPA receptor activation but the underlying mechansims could not be unraveled so far, resulting in a myriad of possibilities for future investigation.
Insights might be gained from a functional knock-down of gephyrin, by RNA interference or with the use of a dominant negative mutant which could serve as a model to detemine if gephyrin is the critical component driving the relocation of GlyRs and neuroligin-2 molecules. The colocalization of neuroligin-2 and GlyRs within the axon needs to be confirmed with immunostainings against both components at once. To unravel the redistributional process, live-imaging techniques could be applied to monitor the redistribution of gephyrin into the axon upon AMPA receptor activation. Ideally, the relocation of the GlyR could also be shown in live imaging experiments and possibly a co-tranport of gephyrin and the GlyR can be monitored within the axon.
The subunit composition of axonal GlyRs could be determined with the use of antibodies recognizing specifically the β subunit of the GlyR. To establish whether GlyRs are relocated into the axon to become integrated into presynaptic terminals, it would be necessary to continue AMPA receptor activation for longer periods of time, allowing the transit through the entire axon until fluorescence accumulates in axon terminals. If this is not the case, GlyRs within the axon might be located to postsynaptic sites, an aspect that could be investigated with immunostainings against presynaptic marker proteins.

It can generally be concluded that this study led to the discovery of new aspects regarding activity-dependent protein targeting, providing a basis for several lines of investigations that can be conducted in the future.

5 References

Alberts, B, Johnson, A, Lewis, J, Raff, M, Roberts, K, Walter P (2008) Molecular Biology of the Cell, 5th Edition Garland Science, Abingdon, UK

Amadio M, Battaini F, Pascale A (2006) The different facets of protein kinases C : old and new players in neuronal signal transduction pathways. Pharmacological Research 54:317–325

Armstrong CM, Hille B (1998) Voltage-gated ion channels and electrical excitability. Neuron 20:371–380

Baas PW, Black MM, Banker G (1989) Changes in microtubule polarity orientation during the development of hippocampal neurons in culture. The Journal of cell biology 109:3085–3094

Baas PW, Deitch JS, Black MM, Banker G (1988) Polarity orientation of microtubules in hippocampal neurons: uniformity in the axon and nonuniformity in the dendrite. Proceedings of the National Academy of Sciences of the United States of America 85:8335–8339

Baas PW, Lin S (2011) Hooks and comets: The story of microtubule polarity orientation in the neuron. Developmental neurobiology 71:403–418

Barra, HS, Rodriguez, JA, Arce, CA, Caputto R (1973) A soluble preparation from rat brain that incorporates into its own proteins (14C)arginine by a ribonuclease-sensitive system and (14C)tyrosine by a ribonuclease-insensitive system. Journal of neurochemistry 20(1):97–108

Bausen M, Weltzien F, Betz H, O'Sullivan G (2010) Regulation of postsynaptic gephyrin cluster size by protein phosphatase 1. Molecular and cellular neurosciences 44:201–209

Belelli D, Harrison NL, Maguire J, Macdonald RL, Walker MC, Cope DW (2009) Extrasynaptic GABAA receptors: form, pharmacology, and function. The Journal of Neuroscience 29:12757–12763

Bellinger FP, Fox BK, Chan WY, Davis LK, Andres M a, Hirano T, Grau EG, Cooke IM (2006) Ionotropic glutamate receptor activation increases intracellular calcium in prolactin-releasing cells of the adenohypophysis. American journal of physiology Endocrinology and metabolism 291:E1188–E1196

Birnboim, HC, Doly J (1979) A rapid alkaline extraction procedure for screening recombinant plasmid DNA. Nucleic acids Res 7:1513–1523

Bliss, TV, Lomo T (1973) Long-lasting potentiation of synaptic transmission in the dentate area of the anaesthetized rabbit following stimulation of the perforant path. Journal of Physiology 232(2):331–356

Bloodgood BL, Sabatini BL (2007) Ca(2+) signaling in dendritic spines. Current opinion in neurobiology 17:345–351.

Bloodgood BL, Sabatini BL (2008) Regulation of synaptic signalling by postsynaptic, non-glutamate receptor ion channels. The Journal of physiology 586:1475–1480

Bonnet C, Boucher D, Lazereg S, Pedrotti B, Islam K, Denoulet P, Larcher JC (2001) Differential binding regulation of microtubule-associated proteins MAP1A, MAP1B, and MAP2 by tubulin polyglutamylation. The Journal of biological chemistry 276:12839–12848

Boucher D, Larcher, JC, Gros, F, Denoulet P (1994) Polyglutamylationof tubulin as a progressive regulator of in vitro interactions between the microtubule-associated protein tau and tubulin. Biochemistry 33(41):12471–12477

Boyer C, Schikorski T, Stevens CF (1998) Comparison of hippocampal dendritic spines in culture and in brain. The Journal of neuroscience : the official journal of the Society for Neuroscience 18:5294–5300

Brodal P (2004) The central Nervous System: Structure and function, 3rd ed. Oxford University Press, New York

Brünig I, Kaech S, Brinkhaus H, Oertner TG, Matus A (2004) Influx of extracellular calcium regulates actin-dependent morphological plasticity in dendritic spines. Neuropharmacology 47:669–676

Burack M a, Silverman M a, Banker G (2000) The role of selective transport in neuronal protein sorting. Neuron 26:465–472

Burkarth N, Kriebel M, Kranz EU, Volkmer H (2007) Neurofascin regulates the formation of gephyrin clusters and their subsequent translocation to the axon hillock of hippocampal neurons. Molecular and cellular neurosciences 36:59–70

Burkhardt JK, Echeverri CJ, Nilsson T, Vallee RB (1997) Overexpression of the dynamitin (p50) subunit of the dynactin complex disrupts dynein-dependent maintenance of membrane organelle distribution. The Journal of cell biology 139:469–484

Cai D, McEwen DP, Martens JR, Meyhofer E, Verhey KJ (2009) Single molecule imaging reveals differences in microtubule track selection between Kinesin motors. PLoS biology 7:e1000216

Campbell PK, Waymire KG, Heier RL, Sharer C, Day DE, Reimann H, Jaje JM, Friedrich G a, Burmeister M, Bartness TJ, Russell LD, Young LJ, Zimmer M, Jenne DE, MacGregor GR (2002) Mutation of a novel gene results in abnormal development of spermatid flagella, loss of intermale aggression and reduced body fat in mice. Genetics 162:307–320

Chebib M, Johnston GAR (1999) Proceedings of the Australian Neuroscience Society Symposium GABA and Glycine Receptors: From Neurochemistry to Neural Networks The "ABC" of GABA receptors: a brief review. Clinical and Experimental Pharmacology and Physiology:937–940

Chen C, Okayama H (1987) High-efficiency transformation of mammalian cells by plasmid DNA. Molecular and cellular biology 7:2745–2752

Chen X, Vinade L, Leapman RD, Petersen JD, Nakagawa T, Phillips TM, Sheng M, Reese TS (2005) Mass of the postsynaptic density and enumeration of three key molecules. Proceedings of the National Academy of Sciences of the United States of America 102:11551–11556

Choquet D (2010) Fast AMPAR trafficking for a high-frequency synaptic transmission. The European journal of neuroscience 32:250–260

Cipolotti L, Shallice T, Chan D, Fox N, Scahill R, Harrison G, Stevens J, Rudge P (2001) Long-term retrograde amnesia...the crucial role of the hippocampus. Neuropsychologia 39:151–172

Citri A, Malenka RC (2008) Synaptic plasticity: multiple forms, functions, and mechanisms. Neuropsychopharmacology : official publication of the American College of Neuropsychopharmacology 33:18–41

Cohen S, Greenberg ME (2008) Communication between the synapse and the nucleus in neuronal development, plasticity, and disease. Annual review of cell and developmental biology 24:183–209

Collingridge GL, Isaac JTR, Wang YT (2004) Receptor trafficking and synaptic plasticity. Nature reviews Neuroscience 5:952–962

Coy DL, Hancock WO, Wagenbach M, Howard J (1999) Kinesin's tail domain is an inhibitory regulator of the motor domain. Nature cell biology 1:288–292

Craig AM, Banker G (1994) Neuronal polarity. Annual review of neuroscience 17:267–310

Craig AM, Banker G, Chang W, McGrath ME, Serpinskaya a S (1996) Clustering of gephyrin at GABAergic but not glutamatergic synapses in cultured rat hippocampal neurons. The Journal of neuroscience : the official journal of the Society for Neuroscience 16:3166–3177

Cruz D a, Lovallo EM, Stockton S, Rasband M, Lewis D a (2009) Postnatal development of synaptic structure proteins in pyramidal neuron axon initial segments in monkey prefrontal cortex. The Journal of comparative neurology 514:353–367

Danglot L, Rostaing P, Triller A, Bessis A (2004) Morphologically identified glycinergic synapses in the hippocampus. 27:394–403

Deleuze, C, Runquist, M, Orcel, H, Rabié, A, Dayanithi, G, Alonso, G, Hussy N (2005) Structural difference between heteromeric and homomeric axonal glycine receptors in the hypothalamo-neurohypophysial system. Neuroscience 135(2):475–483

Dent EW, Gertler FB (2003) Cytoskeletal dynamics and transport in growth cone motility and axon guidance. Neuron 40:209–227

Derkach V a, Oh MC, Guire ES, Soderling TR (2007) Regulatory mechanisms of AMPA receptors in synaptic plasticity. Nature reviews Neuroscience 8:101–113

Dijk JV, Rogowski K, Miro J, Lacroix B, Edde B, Janke C (2007) Article A Targeted Multienzyme Mechanism for Selective Microtubule Polyglutamylation. Molecular Cell:437–448

Dingledine R, Borges K, Bowie D, Traynelis SF (1999) The glutamate receptor ion channels. Pharmacological reviews 51:7–61

Dompierre JP, Godin JD, Charrin BC, Cordelières FP, King SJ, Humbert S, Saudou F (2007) Histone deacetylase 6 inhibition compensates for the transport deficit in Huntington's disease by increasing tubulin acetylation. The Journal of neuroscience : the official journal of the Society for Neuroscience 27:3571–3583

Dong X-xia, Wang Y, Qin Z-hong (2009) Molecular mechanisms of excitotoxicity and their relevance to pathogenesis of neurodegenerative diseases. Acta pharmacologica Sinica 30:379–387

Dresbach T, Nawrotzki R, Kremer T, Schumacher S, Quinones D, Kluska M, Kuhse J, Kirsch J (2008) Molecular architecture of glycinergic synapses. Histochemistry and cell biology 130:617–633

Du J, Wei Y, Liu L, Wang Y, Khairova R, Blumenthal R, Tragon T, Hunsberger JG, Machado-Vieira R, Drevets W, Wang YT, Manji HK (2010) A kinesin signaling complex mediates the ability of GSK-3beta to affect mood-associated behaviors. Proceedings of the National Academy of Sciences of the United States of America 107:11573–11578

Dudek SM, Bear MF (1992) Homosynaptic long-term depression in area CA1 of hippocampus and effects of N-methyl-D-aspartate receptor blockade. Proceedings of the National Academy of Sciences of the United States of America 89:4363–4367

Dunn S, Morrison EE, Liverpool TB, Molina-París C, Cross R a, Alonso MC, Peckham M (2008) Differential trafficking of Kif5c on tyrosinated and detyrosinated microtubules in live cells. Journal of cell science 121:1085–1095

Ersfeld K, Wehland J, Plessmann U, Dodemont H, Gerke V, Weber K (1993) Characterization of the tubulin-tyrosine ligase. The Journal of cell biology 120:725–732

Esteban J (2003) AMPA receptor trafficking: a road map for synaptic plasticity. Molecular interventions 3(7):375–385

Fallah Z, Clowry GJ (1999) Gephyrin-like immunoreactivity is a marker for growing axons in the central nervous system of the immature rat. Developmental neuroscience 21:50–57

Farley AR, Link AJ (2009) Identification and quantification of protein posttranslational modifications., 1st ed. Elsevier Inc

Farrant M, Nusser Z (2005) Variations on an inhibitory theme: phasic and tonic activation of GABA(A) receptors. Nature reviews Neuroscience 6:215–229

Favata MF, Horiuchi KY, Manos EJ, Daulerio a J, Stradley D a, Feeser WS, Van Dyk DE, Pitts WJ, Earl R a, Hobbs F, Copeland R a, Magolda RL, Scherle P a, Trzaskos JM (1998) Identification of a novel inhibitor of mitogen-activated protein kinase kinase. The Journal of biological chemistry 273:18623–18632

Feng G (1998) Dual Requirement for Gephyrin in Glycine Receptor Clustering and Molybdoenzyme Activity. Science 282:1321–1324

Fischer F, Kneussel M, Tintrup H, Haverkamp S, Rauen T, Betz H, Wässle H (2000) Reduced synaptic clustering of GABA and glycine receptors in the retina of the gephyrin null mutant mouse. The Journal of comparative neurology 427:634–648

Foth BJ, Goedecke MC, Soldati D (2006) New insights into myosin evolution and classification. Proceedings of the National Academy of Sciences of the United States of America 103:3681–3686

Fritschy J-M, Harvey RJ, Schwarz G (2008) Gephyrin: where do we stand, where do we go? Trends in neurosciences 31:257–264

Fuhrmann JC, Kins S, Rostaing P, El Far O, Kirsch J, Sheng M, Triller A, Betz H, Kneussel M (2002) Gephyrin interacts with Dynein light chains 1 and 2, components of motor protein complexes. The Journal of neuroscience : the official journal of the Society for Neuroscience 22:5393–5402

Giesemann T, Schwarz G, Nawrotzki R, Berhörster K, Rothkegel M, Schlüter K, Schrader N, Schindelin H, Mendel RR, Kirsch J, Jockusch BM (2003) Complex formation between the postsynaptic scaffolding protein gephyrin, profilin, and Mena: a possible link to the microfilament system. The Journal of neuroscience : the official journal of the Society for Neuroscience 23:8330–8339

Gill SR, Schroer T a, Szilak I, Steuer ER, Sheetz MP, Cleveland DW (1991) Dynactin, a conserved, ubiquitously expressed component of an activator of vesicle motility mediated by cytoplasmic dynein. The Journal of cell biology 115:1639–1650

Glater EE, Megeath LJ, Stowers RS, Schwarz TL (2006) Axonal transport of mitochondria requires milton to recruit kinesin heavy chain and is light chain independent. The Journal of cell biology 173:545–557

Gray EG (1969) Electron microscopy of excitatory and inhibitory synapses: a brief review. Progress in brain research 31:141–155

Grimes C a, Jope RS (2001) The multifaceted roles of glycogen synthase kinase 3beta in cellular signaling. Progress in neurobiology 65:391–426

Grosskreutz, Y, Betz, H, Kneussel M (2003) Rescue of molybdenum cofactor biosynthesis in gephyrin-deficient mice by a Cnx1 transgene. Biochemical and biophysical research communications 301(2):450–455

Gu C, Jan YN, Jan LY (2003) A conserved domain in axonal targeting of Kv1 (Shaker) voltage-gated potassium channels. Science (New York, NY) 301:646–649

Hammond JW, Huang C-fang, Kaech S, Jacobson C, Banker G, Verhey KJ (2010) Posttranslational Modifications of Tubulin and the Polarized Transport of Kinesin-1 in Neurons. Molecular Biology of the Cell 21:572–583

Hansen KB, Yuan H, Traynelis SF (2007) Structural aspects of AMPA receptor activation, desensitization and deactivation. Current opinion in neurobiology 17:281–288

Hanus C, Vannier C, Triller A (2004) Intracellular association of glycine receptor with gephyrin increases its plasma membrane accumulation rate. The Journal of Neuroscience 24:1119–1128

Hartman MA, Finan D, Sivaramakrishnan S, Spudich J a (2011) Principles of unconventional myosin function and targeting. Annual review of cell and developmental biology 27:133–155

Heidemann, SR, McIntosh J (1980) Visualization of the structural polarity of microtubules. Nature 286(5772):517–519

Hirokawa N (2011) From electron microscopy to molecular cell biology, molecular genetics and structural biology: intracellular transport and kinesin superfamily proteins, KIFs: genes, structure, dynamics and functions. Journal of electron microscopy 60 Suppl 1:S63–S92

Hirokawa N, Niwa S, Tanaka Y (2010) Molecular motors in neurons: transport mechanisms and roles in brain function, development, and disease. Neuron 68:610–638

Hirokawa N, Takemura R (2005) Molecular motors and mechanisms of directional transport in neurons. Nature reviews Neuroscience 6:201–214

Hirokawa, N, Noda Y (2008) Intracellular Transport and Kinesin Superfamily Proteins, KIFs: Structure, Function, and Dynamics. Molecular Cell 88(3):1089–1118

Hubbert C, Guardiola A, Shao R, Kawaguchi Y, Ito A, Nixon A, Yoshida M, Wang X-F, Yao T-P (2002) HDAC6 is a microtubule-associated deacetylase. Nature 417:455–458

Hudmon A, Schulman H (2002) Neuronal CA2+/calmodulin-dependent protein kinase II: the role of structure and autoregulation in cellular function. Annual review of biochemistry 71:473–510

Ikegami K, Heier RL, Taruishi M, Takagi H, Mukai M, Shimma S, Taira S, Hatanaka K, Morone N, Yao I, Campbell PK, Yuasa S, Janke C, Macgregor GR, Setou M (2007) Loss of alpha-tubulin polyglutamylation in ROSA22 mice is associated with abnormal targeting of KIF1A and modulated synaptic function. Proceedings of the National Academy of Sciences of the United States of America 104:3213–3218

Inoue, H, Nojima, H, Okayama H (1990) High efficiency transformation of Escherichia coli with plasmids. Gene 96:23–28

Janke C, Kneussel M (2010) Tubulin post-translational modifications: encoding functions on the neuronal microtubule cytoskeleton. Trends in neurosciences 33:362–372

Janke C, Rogowski K, Wloga D, Regnard C, Kajava AV, Strub J-M, Temurak N, van Dijk J, Boucher D, van Dorsselaer A, Suryavanshi S, Gaertig J, Eddé B (2005) Tubulin polyglutamylase enzymes are members of the TTL domain protein family. Science (New York, NY) 308:1758–1762

Janke C, Rogowski K, van Dijk J (2008) Polyglutamylation: a fine-regulator of protein function? "Protein Modifications: beyond the usual suspects" review series. EMBO reports 9:636–641

Jonas P, Racca C, Sakmann B, Seeburg PH, Monyer H (1994) Differences in Ca2+ permeability of AMPA-type glutamate receptor channels in neocortical neurons caused by differential GluR-B subunit expression. Neuron 12:1281–1289

Kanaani J (2002) A combination of three distinct trafficking signals mediates axonal targeting and presynaptic clustering of GAD65. The Journal of Cell Biology 158:1229–1238

Kanai Y, Dohmae N, Hirokawa N (2004) Kinesin transports RNA: isolation and characterization of an RNA-transporting granule. Neuron 43:513–525

Kandel, E, Schwartz, JH, Jessel T (2000) Principles in Neuroscience. In, 4th ed. McGraw-Hill, Columbus, USA

Kapitein LC, Schlager M a, Kuijpers M, Wulf PS, van Spronsen M, MacKintosh FC, Hoogenraad CC (2010) Mixed microtubules steer dynein-driven cargo transport into dendrites. Current biology 20:290–299

Karcher RL, Deacon SW, Gelfand VI (2002) Motor-cargo interactions: the key to transport specificity. Trends in cell biology 12:21–27

Kardon JR, Vale RD (2009) Regulators of the cytoplasmic dynein motor. Nature reviews Molecular cell biology 10:854–865

Karki S, Holzbaur EL (1999) Cytoplasmic dynein and dynactin in cell division and intracellular transport. Current opinion in cell biology 11:45–53

Kawasaki BT, Hoffman KB, Yamamoto RS, Bahr BA (1997) Rapid Communication Variants of the Receptor / Channel Clustering Molecule Gephyrin in Brain : Distinct Distribution Patterns , Developmental Profiles , and Proteolytic Cleavage by Calpain. 388:381–388

Kennedy MB, Bennett MK, Erondu NE (1983) Biochemical and immunochemical evidence that the "major postsynaptic density protein" is a subunit of a calmodulin-dependent protein kinase. Proceedings of the National Academy of Sciences of the United States of America 80:7357–7361

Kennedy MJ, Ehlers MD (2006) Organelles and trafficking machinery for postsynaptic plasticity. Annual review of neuroscience 29:325–362

Kessels MM, Engqvist-Goldstein a E, Drubin DG, Qualmann B (2001) Mammalian Abp1, a signal-responsive F-actin-binding protein, links the actin cytoskeleton to endocytosis via the GTPase dynamin. The Journal of cell biology 153:351–366

Kim MJ, Futai K, Jo J, Hayashi Y, Cho K, Sheng M (2007) Synaptic accumulation of PSD-95 and synaptic function regulated by phosphorylation of serine-295 of PSD-95. Neuron 56:488–502

Kimura Y, Kurabe N, Ikegami K, Tsutsumi K, Konishi Y, Kaplan OI, Kunitomo H, Iino Y, Blacque OE, Setou M (2010) Identification of tubulin deglutamylase among Caenorhabditis elegans and mammalian cytosolic carboxypeptidases (CCPs). The Journal of biological chemistry 285:22936–22941

King, SJ, Schroer T (2000) Dynactin increases the processivity of the cytoplasmic dynein motor. Nature cell biology 2(1):20–24

Kingston R (1999) Transfection and expression of cloned DNA. Current Protocols in Immunology:1–9

Kins S, Kuhse J, Laube B, Betz H, Kirsch J (1999) SHORT COMMUNICATION Incorporation of a gephyrin-binding motif targets NMDA receptors to gephyrin-rich domains in HEK 293 cells. Neuroscience 11:740–744

Kirsch J (2006) Glycinergic transmission. Cell and tissue research 326:535–540

Kirsch J, Betz H (1993) Widespread expression of gephyrin, a putative glycine receptor-tubulin linker protein, in rat brain. Brain research 621:301–310

Kirsch J, Langosch D, Prior P, Littauer UZ, Schmitt B, Betz H (1991) The 93-kDa glycine receptor-associated protein binds to tubulin. The Journal of biological chemistry 266:22242–22245

Kirsch, J, Betz H (1995) The Postsynaptic Protein Gephyrin Localization Is Regulated of the Glycine Receptor-Associated by the Cytoskeleton. Journal of Neuroscience 75:4148–4156

Klein PS, Melton D a (1996) A molecular mechanism for the effect of lithium on development. Proceedings of the National Academy of Sciences of the United States of America 93:8455–8459

Kneussel M, Betz H (2013) Topical Review Receptors , gephyrin and gephyrin-associated proteins : novel insights into the assembly of inhibitory postsynaptic membrane specializations. The Journal of Physiology:1–9

Kneussel M, Brandstätter JH, Laube B, Stahl S, Müller U, Betz H (1999) Loss of postsynaptic GABA(A) receptor clustering in gephyrin-deficient mice. The Journal of neuroscience : the official journal of the Society for Neuroscience 19:9289–9297

Kneussel M, Hermann a, Kirsch J, Betz H (1999) Hydrophobic interactions mediate binding of the glycine receptor beta-subunit to gephyrin. Journal of neurochemistry 72:1323–1326

Kneussel M, Loebrich S (2007) Trafficking and synaptic anchoring of ionotropic inhibitory neurotransmitter receptors. Biology of the cell / under the auspices of the European Cell Biology Organization 99:297–309

Kondo S, Sato-Yoshitake R, Noda Y, Aizawa H, Nakata T, Matsuura Y, Hirokawa N (1994) KIF3A is a new microtubule-based anterograde motor in the nerve axon. The Journal of cell biology 125:1095–1107

Konishi Y, Setou M (2009) Tubulin tyrosination navigates the kinesin-1 motor domain to axons. Nature neuroscience 12:559–567

Kordeli E, Lambert, S, Bennett V (1995) Ankyrin G. The Journal of biological chemistry 270 (5):2352–2359

Kornau HC, Schenker LT, Kennedy MB, Seeburg PH (1995) Domain interaction between NMDA receptor subunits and the postsynaptic density protein PSD-95. Science (New York, NY) 269:1737–1740

Kornau HC, Seeburg PH, Kennedy MB (1997) Interaction of ion channels and receptors with PDZ domain proteins. Current opinion in neurobiology 7:368–373

Kubota H, Alle H, Betz H, Geiger JRP (2010) Presynaptic glycine receptors on hippocampal mossy fibers. Biochemical and biophysical research communications 393:587–591

Kuhse J, Kalbouneh H, Schlicksupp A, Mükusch S, Nawrotzki R, Kirsch J (2012) Phosphorylation of gephyrin in hippocampal neurons by cyclin-dependent kinase CDK5 at Ser-270 is dependent on collybistin. The Journal of biological chemistry 287:30952–30966

Langosch D, Hoch W, Betz H (1992) The 93 kDa protein gephyrin and tubulin associated with the inhibitory glycine receptor are phosphorylated by an endogenous protein kinase. FEBS letters 298:113–117

Laube B, Maksay G, Schemm R, Betz H (2002) Modulation of glycine receptor function: a novel approach for therapeutic intervention at inhibitory synapses? Trends in pharmacological sciences 23:519–527

Lee HK, Barbarosie M, Kameyama K, Bear MF, Huganir RL (2000) Regulation of distinct AMPA receptor phosphorylation sites during bidirectional synaptic plasticity. Nature 405:955–959

Lehman I (1974) DNA Ligase: structure, mechanism, and function. Science 186(4166):790–797

Lester, RA, Clements, JD, Westbrook, GL, Jahr C (1990) Channel kinetics determine the time course of NMDA receptor mediated synaptic currents. Nature:565–567

Levitan, IB, Kazcmarek L (1997) The Neuron: Cell and Molecular Biology. 3rd Edition (Oxford University Press NY)

Lewis TL, Mao T, Svoboda K, Arnold DB (2009) Myosin-dependent targeting of transmembrane proteins to neuronal dendrites. Nature neuroscience 12:568–576

Lin MT, Lujan R, Watanabe M, Frerking M, Maylie J, Adelman JP (2011) Coupled activity-dependent trafficking of synaptic SK2 Channels and AMPA receptors. Journal of Neuroscience 30:11726–11734

Lisman J (1994) The CaM kinase II hypothesis for the storage of synaptic memory. Trends in neurosciences 17(10):406–412

Lisman J, Yasuda R, Raghavachari S (2012) Mechanisms of CaMKII action in long-term potentiation. Nature reviews Neuroscience 13:169–182

Lopez-Corcuera, B, Geerlings, A, Aragon C (2001) Glycine neurotransmitter transporters: an update. Molecular Membrane Biology 18:13–20

Ludueñna R (1998) Multiple forms of tubulin: different gene products and covalent modifications. Interational Review of Cytology 178:207–275

Lynch JW (2004) Molecular structure and function of the glycine receptor chloride channel. Physiological reviews 84:1051–1095

Lévi S, Vannier C, Triller a (1998) Strychnine-sensitive stabilization of postsynaptic glycine receptor clusters. Journal of cell science (111)Pt 3:335–345

Maas C, Belgardt D, Lee HK, Heisler FF, Lappe-Siefke C, Magiera MM, van Dijk J, Hausrat TJ, Janke C, Kneussel M (2009) Synaptic activation modifies microtubules underlying transport of postsynaptic cargo. Proceedings of the National Academy of Sciences of the United States of America 106:8731–8736

Maas C, Tagnaouti N, Loebrich S, Behrend B, Lappe-Siefke C, Kneussel M (2006) Neuronal cotransport of glycine receptor and the scaffold protein gephyrin. The Journal of cell biology 172:441–451

MacDermott, Amy, Mayer, Mark, Westbrook, Gary, Smith, Steven, Barker J (1986) © 1986 Nature Publishing Group. Nature 329:519–522

Malenka RC, Bear MF (2004) LTP and LTD: an embarrassment of riches. Neuron 44:5–21

Mao L, Takamiya K, Thomas G, Lin D-ting, Huganir RL (2010) receptor recycling via exocyst complex interactions. PNAS 2010:1–6

Martin KC, Kosik KS (2002) Synaptic tagging - who's it? Nature reviews Neuroscience 3:813–820

Mayer BYML, Westbrook GL (1987) Permeation and block of N-methyl-D-aspartic acid receptor channels by divalent cations in mouse cultured central neurons. Journal of Physiology:501–527

Mayer, ML, Westbrook, GL, Guthrie P (1984) Voltage-dependent block by Mg2+ of NMDA responses in spinal cord neurons. Nature 309:261–263

Mayford M (2007) Protein kinase signaling in synaptic plasticity and memory. Current opinion in neurobiology 17:313–317

Meijer L, Skaltsounis A-leandros, Magiatis P, Polychronopoulos P, Knockaert M, Leost M, Ryan XP, Vonica CA, Brivanlou A, Dajani R, Crovace C, Tarricone C, Musacchio A, Roe SM, Pearl L, Greengard P, Ripamonti V (2003) GSK-3-Selective Inhibitors Derived from Tyrian Purple Indirubins. Proteins 10:1255–1266

Meyer G, Kirsch J, Betz H, Langosch D (1995) Identification of a gephyrin binding motif on the glycine receptor beta subunit. Neuron 15:563–572

Miki H, Setou M, Kaneshiro K, Hirokawa N (2001) All kinesin superfamily protein, KIF, genes in mouse and human. Proceedings of the National Academy of Sciences of the United States of America 98:7004–7011

Miller SG, Kennedy MB (1986) Regulation of brain type II Ca2+/Calmodulin-dependent protein kinase by autophosphorylation: a Ca2+-triggered molecular switch. Cell 44:861–870

Milner B (1970) Memory in the medial and temporal lobe regions of the brain. In: In K.H. Primbram & D.E. Broadbent (Eds.), Biology of Memory, pp. 29-50. New York: Academic Press, USA

Mosbacher J, Schoepfer R, Monyer H, Burnashev N, Seeburg PH, Ruppersberg JP (1994) A molecular determinant for submillisecond desensitization in glutamate receptors. Science (New York, NY) 266:1059–1062

Moss SJ, Smart TG (2001) Constructing inhibitory synapses. Nature reviews Neuroscience 2:240–250

Nakata T, Hirokawa N (2003) Microtubules provide directional cues for polarized axonal transport through interaction with kinesin motor head. The Journal of cell biology 162:1045–1055

Niswender CM, Conn PJ (2010) Metabotropic glutamate receptors: physiology, pharmacology, and disease. Annual review of pharmacology and toxicology 50:295–322

Nägerl UV, Eberhorn N, Cambridge SB, Bonhoeffer T (2004) Bidirectional activity-dependent morphological plasticity in hippocampal neurons. Neuron 44:759–767

Oakley, BR, Akkari Y (1999) gamma-tubulin at ten: Progress and Prospects. Cell structure and function 24:365–372

Ozawa S, Kamiya H, Tsuzuki K (1998) Glutamate receptors in the mammalian central nervous system. Progress in neurobiology 54:581–618

O'Brien WT, Klein PS (2009) Validating GSK3 as an in vivo target of lithium action. Biochemical Society transactions 37:1133–1138

Palazzo a F, Joseph HL, Chen YJ, Dujardin DL, Alberts a S, Pfister KK, Vallee RB, Gundersen GG (2001) Cdc42, dynein, and dynactin regulate MTOC reorientation independent of Rho-regulated microtubule stabilization. Current biology 11:1536–1541

Park C, Szostak JW (1992) ARD1 and NAT1 proteins form a complex that has N-terminal acetyltransferase activity. EMBO Journal 1:2087–2093

Park M, Penick EC, Edwards JG, Kauer J a, Ehlers MD (2004) Recycling endosomes supply AMPA receptors for LTP. Science (New York, NY) 305:1972–1975

Partin KM, Fleck MW, Mayer ML (1996) AMPA receptor flip/flop mutants affecting deactivation, desensitization, and modulation by cyclothiazide, aniracetam, and thiocyanate. The Journal of Neuroscience 16:6634–6647

Paturle, L, Wehland, J, Margolis, RL, Job D (1989) Complete seperation of tyrosinated, detyrosinated, and non-tyrosinatable brain tubulin subpopulations using affinity chromatography. Biochemistry 28(6):2698–2704

Paturle-Lafanechere, L, Eddée, B, Denoulet, P, Van Dorsselaer, A, Mazarguil, H, LeCaer, JP, Wehland, J, Job D (1991) Characterization of a major brain tubulin variant which cannot be tyrosinated. Biochemistry 30(43):10523–10528

Peineau S, Taghibiglou C, Bradley C, Wong TP, Liu L, Lu J, Lo E, Wu D, Saule E, Bouschet T, Matthews P, Isaac JTR, Bortolotto Z a, Wang YT, Collingridge GL (2007) LTP inhibits LTD in the hippocampus via regulation of GSK3beta. Neuron 53:703–717

Peris L, Wagenbach M, Lafanechère L, Brocard J, Moore AT, Kozielski F, Job D, Wordeman L, Andrieux A (2009) Motor-dependent microtubule disassembly driven by tubulin tyrosination. The Journal of cell biology 185:1159–1166

Perrot R, Berges R, Bocquet A, Eyer J (2008) Review of the multiple aspects of neurofilament functions, and their possible contribution to neurodegeneration. Molecular neurobiology 38:27–65

Pfeiffer BE, Huber KM (2006) Current advances in local protein synthesis and synaptic plasticity. The Journal of Neuroscience 26:7147–7150

Pfister KK, Fisher EMC, Gibbons IR, Hays TS, Holzbaur ELF, McIntosh JR, Porter ME, Schroer T a, Vaughan KT, Witman GB, King SM, Vallee RB (2005) Cytoplasmic dynein nomenclature. The Journal of cell biology 171:411–413

Prior P, Schmitt B, Werner P, Betz H (1992) Primary Structure and Alternative Splice Variants of Gephyrin , a Putative Clycine Receptor-Tubulin Linker Protein. Cell 8:1161–1170

Qian N, Sejnowski TJ (1990) When is an inhibitory synapse effective? Proceedings of the National Academy of Sciences of the United States of America 87:8145–8149

Quirk, J. C., Siuda, E.R., Nisenbaum ES (2004) Molecular Determinants Responsible for Differences in Desensitization Kinetics of AMPA Receptor Splice Variants. Journal of Neuroscience 24:11416–11420

Rasmussen H, Rasmussen T, Triller A, Vannier C (2002) Strychnine-blocked glycine receptor is removed from synapses by a shift in insertion/degradation equilibrium. Molecular and cellular neurosciences 19:201–215

Redmond L (2008) Translating neuronal activity into dendrite elaboration: signaling to the nucleus. Neuro-Signals 16:194–208

Redondo RL, Morris RGM (2011) Making memories last: the synaptic tagging and capture hypothesis. Nature reviews Neuroscience 12:17–30

Reid C a, Fabian-Fine R, Fine a (2001) Postsynaptic calcium transients evoked by activation of individual hippocampal mossy fiber synapses. The Journal of Neuroscience 21:2206–2214

Rivera JF, Ahmad S, Quick MW, Liman ER, Arnold DB (2003) An evolutionarily conserved dileucine motif in Shal K+ channels mediates dendritic targeting. Nature neuroscience 6:243–250

Rizzuto, R, Pozzan T (2006) Microdomains of Intracellular Ca^{2+} : Molecular Determinants and Functional Consequences. Physiological Reviews:369–408

Rodríguez-Moreno a, Lerma J (1998) Kainate receptor modulation of GABA release involves a metabotropic function. Neuron 20:1211–1218

Rongo C (2002) A fresh look at the role of CaMKII in hippocampal synaptic plasticity and memory. BioEssays : news and reviews in molecular, cellular and developmental biology 24:223–233

Ross JL, Ali MY, Warshaw DM (2008) Cargo transport: molecular motors navigate a complex cytoskeleton. Current opinion in cell biology 20:41–47

Rudy J (2008) The Neurobiology of Learning and Memory, First Edit. Sinauer Associates, Inc. Sunderland, USA

Saiki, RK, Gelfand, DH, Stoffel, S, Scharf, SJ, Higuchi, R, Horn, GT, Mullis, KB, Erlich H (1988) Primer-directed enzymatic amplification of DNA with a thermostable DNA polymerase. Science 239(4839):487–491

Saito N, Okada Y, Noda Y, Kinoshita Y, Kondo S, Hirokawa N (1997) KIFC2 is a novel neuron-specific C-terminal type kinesin superfamily motor for dendritic transport of multivesicular body-like organelles. Neuron 18:425–438

Sambrook, J, Fritsch, EF, Maniatis T (1989) Molecular Cloning I/II/III. Al Laboratory Manual, Second Edition. Cold Spring Harbor Laboratory Press, New York, USA

Sampo B, Kaech S, Kunz S, Banker G (2003) Membrane Proteins to the Axonal Surface. 37:611–624

Sanger F, Nicklen S (1977) DNA sequencing with chain-terminating. Biochemistry 74:5463–5467

Sassoe-Pognetto, M, Kirsch, J, Grünert, U, Fritschy, JM, Möhler, H, Betz, H, Wässle H (1995) Colocalization of gephyrin and GABAA-receptor subunits in the rat retina. Journal of Comp Neurology:1–14

Schlager M a, Hoogenraad CC (2009) Basic mechanisms for recognition and transport of synaptic cargos. Molecular brain 2:25

Schliwa M, Woehlke G (2003) Molecular motors. Nature 422:759–765

Schmitt, B, Knaus, P, Becker, CM, Betz H (1987) The Mr 93,000 polypeptide of the postsynaptic glycine receptor complex is a peripheral membrane protein. Biochemistry 10:805–811

Schröder HC, Wehland J, Weber K (1985) Purification of brain tubulin-tyrosine ligase by biochemical and immunological methods. The Journal of cell biology 100:276–281

Schulze E, Asai DJ, Bulinski JC, Kirschner M (1987) Posttranslational modification and microtubule stability. The Journal of cell biology 105:2167–2177

Setou M (2000) Kinesin Superfamily Motor Protein KIF17 and mLin-10 in NMDA Receptor-Containing Vesicle Transport. Science 288:1796–1802

Setou M, Seog D-H, Tanaka Y, Kanai Y, Takei Y, Kawagishi M, Hirokawa N (2002) Glutamate-receptor-interacting protein GRIP1 directly steers kinesin to dendrites. Nature 417:83–87

Sheng M, Hoogenraad CC (2007) The postsynaptic architecture of excitatory synapses: a more quantitative view. Annual review of biochemistry 76:823–847

Smith BK (n.d.) Settling the great glia debate. Science:8–10

Soderling TR, Derkach V a (2000) Postsynaptic protein phosphorylation and LTP. Trends in neurosciences 23:75–80

Sola M, Bavro VN, Timmins J, Franz T, Ricard-Blum S, Schoehn G, Ruigrok RWH, Paarmann I, Saiyed T, O'Sullivan G a, Schmitt B, Betz H, Weissenhorn W (2004) Structural basis of dynamic glycine receptor clustering by gephyrin. The EMBO journal 23:2510–2519

Sola M, Kneussel M, Heck IS, Betz H, Weissenhorn W (2001) X-ray crystal structure of the trimeric N-terminal domain of gephyrin. The Journal of biological chemistry 276:25294–25301

Song A-H, Wang D, Chen G, Li Y, Luo J, Duan S, Poo M-M (2009) A selective filter for cytoplasmic transport at the axon initial segment. Cell 136:1148–1160

Spruston N, Schiller Y, Stuart G, Sakmann B (1995) Activity-dependent action potential invasion and calcium influx into hippocampal CA1 dendrites. Science (New York, NY) 268:297–300

Swanson GT, Kamboj SK, Cull-candy SG (1997) Single-Channel Properties of Recombinant AMPA Receptors Depend on RNA Editing , Splice Variation , and Subunit Composition. Molecular Neurobiology 17:58–69

Tada T, Sheng M (2006) Molecular mechanisms of dendritic spine morphogenesis. Current opinion in neurobiology 16:95–101

Takahashi Y, Hsü CS, Suzuki Y (1969) Analytical studies on brain polysomal RNA using polyacrylamide and agarose-polyacrylamide gel electrophoresis. Brain research 13:397–401

Takeda S, Yamazaki H, Seog DH, Kanai Y, Terada S, Hirokawa N (2000) Kinesin superfamily protein 3 (KIF3) motor transports fodrin-associating vesicles important for neurite building. The Journal of cell biology 148:1255–1265

Tan SC, Scherer J, Vallee RB (2011) Recruitment of dynein to late endosomes and lysosomes through light intermediate chains. Molecular biology of the cell 22:467–477

Thaler, CD, Haimo L (1996) Microtubules and microtubule motors: mechanisms of regulation. Interational Review of Cytology 164::269–327

Thirumurugan K, Sakamoto T, Hammer J a, Sellers JR, Knight PJ (2006) The cargo-binding domain regulates structure and activity of myosin 5. Nature 442:212–215

Tokumitsu, H, Chijiwa, T, Hagiwara, M, Mizutani, A, Terasawa, M, Hidaka H (1990) KN-62, a Specific Inhibitor of Ca^{2+}/Calmodulin-dependent Protein Kinase II. Journal of Biological Chemistry 265:4315–4320

Toullecs D, Pianettis P, Belleverguel P, Grand-perrets T, Ajakanee M, Baudets V, Boissinb P, Boursiers E, Loriolles F, Duhamelll L, Charon D, Kirilovskysii J (1991) The bisindolylmaleimide GF109203X is a potent inhibitor of protein kinase C. Journal of Biological Chemitry (266):15771

Traynelis SF, Wollmuth LP, Mcbain CJ, Menniti FS, Vance KM, Ogden KK, Hansen KB, Yuan H, Myers SJ, Dingledine R (2010) Glutamate Receptor Ion Channels : Structure , Regulation , and Function. Structure 62:405–496

Trepel M (2004) Neuroanatomie - Struktur und Funktion, Dritte Edition. Urban & Fischer Verlag, München

Tretter V, Jacob TC, Mukherjee J, Fritschy J-M, Pangalos MN, Moss SJ (2008) The clustering of GABA(A) receptor subtypes at inhibitory synapses is facilitated via the direct binding of receptor alpha 2 subunits to gephyrin. The Journal of Neuroscience 28:1356–1365

Tsien RY, Rink, TJ, Poenie M (1985) Measurement of cytosolic free Ca2+ in individual small cells using fluorescence microscopy with dual excitation wavelengths. Cell calcium 6(1-2):145–157

Turecek R, Trussell LO (2001) Presynaptic glycine receptors enhance transmitter release at a mammalian central synapse. Nature 411:587–590

Turrigiano G (2012) Homeostatic synaptic plasticity: local and glabal mechanisms for stbilizing neuronal function. Cold Spring Harbor Perspectives in Biology 4(1):a0057

Tyagarajan SK, Ghosh H, Yévenes GE, Nikonenko I, Ebeling C, Schwerdel C, Sidler C, Zeilhofer HU, Gerrits B, Muller D, Fritschy J-M (2011) Regulation of GABAergic synapse formation and plasticity by GSK3beta-dependent phosphorylation of gephyrin. Proceedings of the National Academy of Sciences of the United States of America 108:379–384

Vale RD, Reese TS, Sheetz MP (1985) Identification of a novel force-generating protein, kinesin, involved in microtubule-based motility. Cell 42:39–50

Varoqueaux, F, Jamain, S, Brose N (2004) Neuroligin 2 is exclusively localized to inhibitory synapses. European Journal of Cell Biology 83(9):449–456

Verhey KJ, Gaertig J (2007) The Tubulin Code. Cell Cycle:2152–2160

Vicini S, Wang JF, Li JH, Zhu WJ, Wang YH, Hong J, Wolfe BB, Grayson DR, Li JINH, Zhu WEIJ, Wang YUEHUA, Luo JH (2013) Functional and Pharmacological Differences Between Recombinant N-Methyl-D-Aspartate Receptors Journal of Neurophysiology:555–566

Waters, J, Schaefer, A, Sakmann B (2005) Backpropagating action potentials in neurons: measurement, mechanisms and potential functions. Progress in Biophysics 87(1):145–170

Welte MA (2004) Bidirectional transport along microtubules. Current biology : CB 14:R525–R537

Westermann S, Weber K (2003) Post-translational modifications regulate microtubule function. Nature reviews Molecular cell biology 4:938–947

Wiegert JS, Bading H (2011) Activity-dependent calcium signaling and ERK-MAP kinases in neurons: a link to structural plasticity of the nucleus and gene transcription regulation. Cell calcium 49:296–305

Wolff, A, Néchaud, B, Chillet, D, Mazarguil, H, Desbruyeres, E, Audebert, S, Eddé, B, Gros, F, Denoulet P (1992) Distribution of glutamylated alpha and beta-tubulin in mouse tissues using a specific monoclonal antibody, GT335. European Journal of Cell Biology 59(2):425–432

Yuste R, Majewska a, Cash SS, Denk W (1999) Mechanisms of calcium influx into hippocampal spines: heterogeneity among spines, coincidence detection by NMDA receptors, and optical quantal analysis. The Journal of Neuroscience 19:1976–1987

Yuste R, Majewska a. (2001) Book Review: On the Function of Dendritic Spines. The Neuroscientist 7:387–395

Zola-Morgan S, Squire LR, Amaral DG, Suzuki W a (1989) Lesions of perirhinal and parahippocampal cortex that spare the amygdala and hippocampal formation produce severe memory impairment. The Journal of neuroscience : the official journal of the Society for Neuroscience 9:4355–4370

6 Appendix

6.1 Figures

6.2 Tables

6.3 Abbreviations

α	anti/alpha
AMPA	a-amino-3-hydroxy-5-methyl-4-isoxazole
AraC	b-D-arabinofuraosyl-cytosine
ATP	adenosine triphosphate
BCA	bicinchoninic acid
BDNF	brain derived neurotrophic factor
bidest.	distilled twice
bp	base pairs
BSA	bovine serum albumin
CaMKII	Ca^{2+}/Calmodulin-dependent protein kinase II
CCD	charged-coupled device
CNS	central nervous system
C-terminal	carboxy terminal
Cy3	Indocarbocyanine
Cy5	Indodicarbocyanine
DIV	days *in vitro*
DMEM	Dulbecco's modified eagle medium
DMSO	dimethylsulfoxide
DNA	desoxyribonucleic acid
DNase	desoxyribonuclease
dpi	dots per inch
dNTP	desoxyribonucleoside triphosphate
DTT	dithiothreitol
E. coli	*Escherichia coli*
EDTA	Ethylenediamin tetraacetate
EGFP	enhanced green fluorescent protein
ER	endoplasmatic reticulum
et al..	and others
FBS	fetal bovine serum
f.c.	final concentration
FCS	fetal calf serum
g	gravity
GABA	γ-aminobutyric acid
GFP	green fluorecent protein
GluR	glutamate receptor
G-protein	GTP-binding protein
GRIP1	glutamatereceptor
GTP	guanosine triphosphate
HBS	HEPES-buffered saline
HEK	human embryonic kidney
HEPES	hydroxyethylpiperazine
HRP	horseraddish peroxidase
ICC	Immunocytochemistry
JSAP1	Jun N-terminal protein kinase/ stress-activated protein 1
kDa	kilo Dalton
KIF	Kinesin super family
LTD	long-term depression
LTP	long-term potentiation
MAP	microtubule-associated protein
mRFP	monomerir red fluorescent protein
mRNA	messenger RNA
n	number of experiments
NLG	neuroligin
NMDA	N-methyl-D-aspartate
NR	NMDA receptor subunit

NSE	neuron specific enolase
N-terminal	amino terminal
OD	optical density
ORF	open reading frame
Px	postnatal day x
PAGE	polyacrylamide gelelectrophoresis
PBS	Phosphate buffered saline
PCR	polymerase chain reaction
pH	-log [H+]
PMSF	Phenylmethyl-sulfonylfluoride
PNS	peripheral nervous system
PP1	protein phosphatase 1
PSD95	postsynaptic density 95
PTM	posttranslational modification
PVDF	Polyvinylidene fluoride
Ras	rat sarcoma
RNA	ribonucleic acid
RNAi	RNA interference
RNase	ribonuclease
rpm	rounds per minute
RT	room temperature
SDS	sodium dodecyle sufate
SEM	standard error of the mean
TAE	Tris acetate EDTA buffer
TB	terrific broth
TBS	tris buffered saline
TBST	tris buffered saline Tween-20
TE	tris EDTA buffer
U	unit
UV	ultraviolet
v/v	volume/volume
WB	western blot
w/v	weight/volume

Units

%	Percent
°C	degree Celcius
Da	Dalton
g	gram
h	hour
l	liter
m	meter
min	minute
mol	Mol
s	second
V	Volt

Prefixes

n	nano (10^{-9})
µ	micro (10^{-6})
m	milli (10^{-3})
c	centi (10^{-2})
k	kilo (10^{3})
M	mega (10^{6})
G	giga (10^{9})

7 Acknowledgements

I thank Prof. Matthias Kneussel for giving me the opportunity to work in his laboratory and his continuous support.

Prof. Christian Lohr has been an integral part of this project and has inspired, supported and motivated me many times. Thank you.

I would also like to thank PD Dr. Sabine Hoffmeister-Ullerich and Prof. Alexander Haas for taking the time to evaluate my work as parts of the examination board.

Many thanks go to the colleagues at the Institute for Molecular Neurogenetics for creating such a good working atmosphere. Kira has been of great help with this project, continuously providing input and motivation. I especially want to thank Edda, Yvonne and Petra for outstanding technical support and Dorthe for everything she did to help me and for being a friend.

My parents and my brother have been very close for the entire time of my PhD and I am incredibly happy to have them by my side.

Most of all I thank Daniel for repeatingly showing me what really matters in life.